論文 / 著書情報
Article / Book Information

題目(和文)	
Title(English)	Fully exfoliated epoxy/organoclay nanocomposites: process development, properties and those mechanisms
著者(和文)	KEYOONWONGWIWAT
Author(English)	KEYOONWONGWIWAT
出典(和文)	学位:博士(工学), 学位授与機関:東京工業大学, 報告番号:甲第9442号, 授与年月日:2014年3月26日, 学位の種別:課程博士, 審査員:久保内　昌敏,太田口　和久,Wiwut Tanthapanichakoon,吉川　史郎,森　伸介,青木　才子,塩谷　正俊
Citation(English)	Degree:Doctor (Engineering), Conferring organization: Tokyo Institute of Technology, Report number:甲第9442号, Conferred date:2014/3/26, Degree Type:Course doctor, Examiner:,,,,,,
学位種別(和文)	博士論文
Type(English)	Doctoral Thesis

Fully exfoliated epoxy/organoclay nanocomposites: process development, properties and those mechanisms

by

Wiwat Keyoonwong

for

Degree of Doctor of Engineering

Thesis supervisor

Professor Masatoshi Kubouchi

Associate Professor Saiko Aoki

Department of Chemical Engineering

Tokyo Institute of Technology

Table of Contents

Chapter 1

Introduction

1.1 Nanocomposites

1.1.1 Definition of nanocomposites

According to the American Heritage Dictionary [1], a composite material is "a complex material in which two or more distinct, structurally complementary substances, especially metals, ceramics, glasses, and polymers, are combined to produce structural or functional properties not present in any individual component". A **nanocomposite** [2] is a multiphase solid material where one of the phases has one, two or three dimensions of less than 100 nanometers (nm), or structures having nano-scale repeat distances between the different phases that make up the material.

1.1.2 Nature of nanocomposites

Over the last decade, the area of nanocomposite materials has gained much attention, both in the academic fields as well as industry and government. The overall properties of nanocomposites are not only determined by their parent components, but also by the composites phase morphology and interfacial properties. Nanocomposites are commonly base on polymer matrices reinforced by nanofillers such as precipitated silica and layered silicate (clays) synthesized by several methods i.e. in-situ polymerization, solvent method, polymer melt intercalation and shear mixing method.

Layered materials are potentially well suited for the design of nanocomposites because their lamellar elements have high strength, stiffness and aspect ratios [3]. In layered

solids, smectic clays (e.g montmorillonite) are more popularly used because they exhibit a very rich intercalation chemistry which allows them to be chemically modified and made compatible with organic polymers for dispersion. Montmorillonite is a nanoparticle, which has a plate-like shape with high aspect ratio. The typical structure of smectic clays is showed in Fig. 1.1.

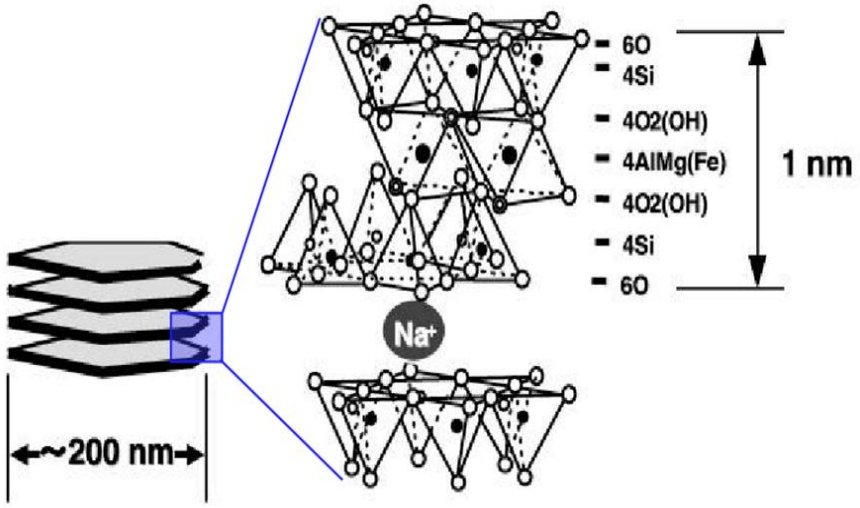

Fig.1.1 Structuture of montmorrillonite clay [4]

With the same loading, nanoparticle can lead to a better performance than other large size particles at low cost. In the early 1990s, Toyota researchers [5-6] discovered that treatment of montmorillonite clay (MMT) with amino acids in-situ polymerization allowed dispersion of the individual 1 nm thick silicate layers of the clay in the polymer. Their hybrid material showed major improvements in heat resistance and mechanical properties even at very low clay content (1.6 vol.%). Since this opportunity, many researchers have performed investigations in the new field of polymer nanocomposites.

1.2 Types of polymer-clay nanocomposites

From a structural point of view, polymer – clay composites can be generally classified into "conventional composites" and "nanocomposites". In a conventional composite, the clay nanolayers are retained when mixed with the polymer without intercalation of the polymer into the clay structure (see Fig. 1.2a). Consequently, the clay fraction in conventional clay composites play little or no functional role and acts mainly as filling agent for economic considerations. An improvement in dimensional stability is normally achieved by reduction of thermal expansion in conventional clay composite, but this reinforcement benefit is usually accompanied with a sacrifice in other properties, such as strength and ductility [7].

Two types of polymer-clay nanocomposite are possible [8]. Intercalated nanocomposites (Fig. 1.2b) are formed when a few molecular of polymers are inserted into the clay galleries with keeping layered structure. Exfoliated nanocomposites (Fig. 1.2c) are formed when the silicate nanolayers are individually dispersed in the polymer matrix, and the average distance between the segregated layers being dependent on the clay loading. The separation between the exfoliated nanolayers may be uniform (regular) or variable (disordered). Exfoliated nanocomposites show greater phase homogeneity than intercalated nanocomposites. More importantly, each nanolayer in an exfoliated nanocomposite contributes fully to interfacial interactions with the matrix. This structural distinction is the primary reason why the exfoliated clay state is especially effective in improving the reinforcement and other performance properties of clay composite materials.

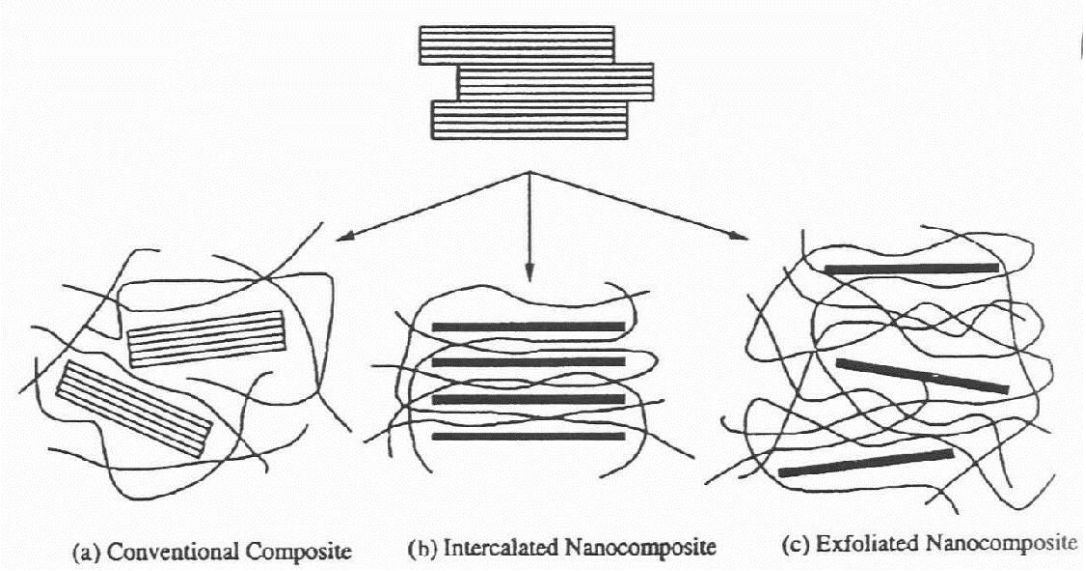

Fig. 1.2 Schematic illustrations of the structures of (a) conventional composite, (b) intercalated and (c) exfoliated polymer clay nanocomposites [8]

R. A. Vaia [9] classified structural characterization of polymer-layered silicate nanocomposites (PLSNs) in more details. The previous discussion indicates that a simple description of PLSN morphology as intercalated or exfoliated is far from adequate. Additional descriptors, such as ordered, disordered or partial, are helpful for accurate description of nanoscale morphologies. An expanded classification scheme is summarized in Figure 1.5. Disordered intercalated structures are characterized by weaker interlayer correlations sufficient to disrupt strong basal reflections observed in conventional wide-angle X-ray diffraction (discussed below).

Furthermore, a minor fraction of smaller layers near the surface of the crystallites may be dispersed (e.g. Figure 1.3). On the other hand, PLSNs containing highly swollen interlayers still exhibiting registry associated with the original crystallitie (e.g. Figure 1.4) or small stacks of 2-4 layers are partially exfoliated. Here, the layer correlation is

Fig. 1.3 Bright-field TEM of poly(3-bromostyrene)-F12 (dodecylammonium-exchanged fluorohectorite) [10]

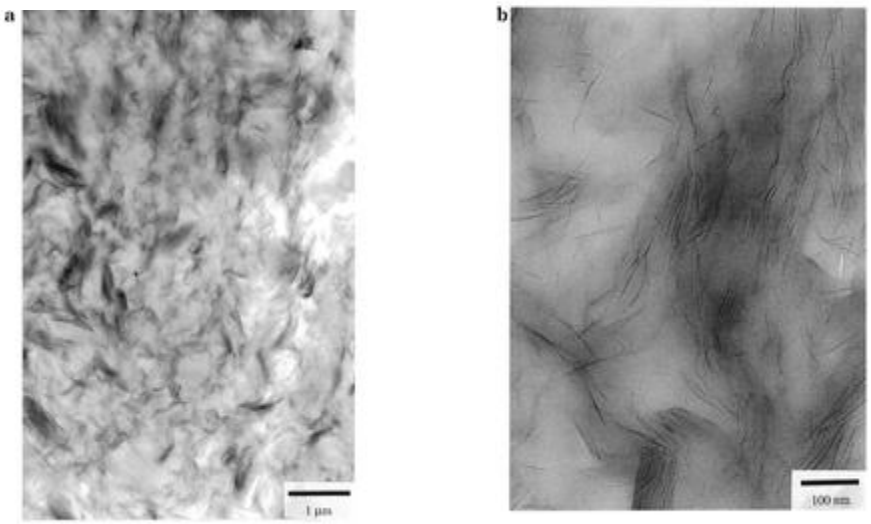

Fig. 1.4 Bright-field TEM images of 10 mass% Closite 30A (Southern clay Products, Inc.) in a diamine-cured (Jeffamine D-2000, Huntsman) epoxy (EPON 828, Shell) [11]: a) submicron variation in silicate content as well as packets of parallel layers with various degree of swelling; b) regions with stacks of 25 layers with spacing about 5 nm to regions with 3-5 layers separated by 10-20 nm

not detectable by WAXD, and correct characterization requires microscopy. Finally, for true exfoliated layers, processing history and intermolecular interactions will make ultralong-range (>10 nm) ordering of the layers. Maximum layer separation will depend on the volume friction of silicate. Thus, depending on the degree of orientation (and translational) order and volume fraction, exfoliated PLSNs can further be described as ordered or disordered.

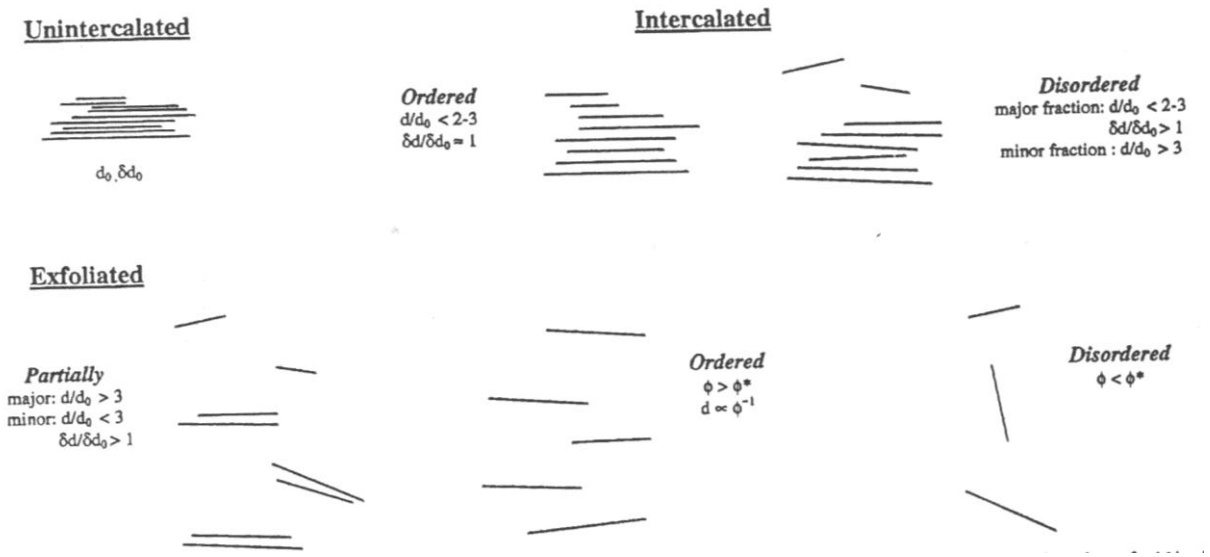

Fig. 1.5 Nanoscale arrangements of layered silicate in PLSN that can be differentiated on the basis of: (1) the relative change in layer spacing and correlation (d and δd); (2) the relative volume fraction of single layers and layer stacks; (3) the dependence of single-layer separation on silicate volume fraction, ϕ, above a critical volume fraction for ordering, ϕ*. Differentiation of morphologies based on d/d0 >3 is qualitatively associatied with common lower-angle resolution in powder diffraction [9]

Overall, the morphologies indicate that the formation of intercalation and exfoliated PLSNs occurs by a more complex process than simple sequential swelling and

separation of individual layers starting from the surface of the primary particle and crystallite [12-14]. Defect structures, local chemical inhomogeneities, electrostatic forces, viscoelastic properties of the polymer and stress fields arising from interlayer swelling will all contribute to mediate polymer transport and layer mobility and thus final morphology. These effects coupled with processing factors such as shear flows lead to more complex morphologies than those theoretically discussed to date. It is important to note that descriptors in Figure 1.5 only account for nanoscopic morphology, whereas the microscale arrangement of the crystallites or individual layers must also be determined and considered when establishing structure-property relationships.

1.3 Layered Silicate: Schematic Structure & Chemical Compound

Among the large number of inorganic layered materials which exhibit intercalation capabilities, layered silicates are one of the most typical because of the versatility of the reaction. In particular, the smectite group minerals such as montmorillonite, saponite and hectorite have mainly been used because they have excellent intercalation capabilities. Several reviews have recently discussed polymer nanocomposites based on smectites [15-16]. Studies on other types of layered silicate-polymer intercalation compounds have been conducted to a much lesser degree because of the relative difficulties in the preparation of polymer-intercalated compounds. Y. Komori, *et al.* [17] believe, however, that extension of the kind of host materials leads to various layered silicate-based nanocomposites with compositional and structural variations that can be directed towards new applications.

In that review, they presented intercalation compounds composed of layered polysilicates, kaolinite and layered double hydroxide as the hosts. Although layered double hydroxides are not silicates, they are often regarded as “anionic clay” and can be treated in a manner similar to layered silicates. The structures of these layered materials are illustrated in Fig. 1.6.

The framework of layered polysilicates consists of SiO_4 tetrahedra with some silanol groups in the interlayer region, and exchangeable cations are present in the interlayer region. Kaolinite consists of SiO_4 tetrahedral sheets and $AlO_2(OH)_4$ octahedral sheet. Neither cation nor anions are present between the layers, and the layers are linked to each other by hydrogen bonding between hydroxyl groups on the octahedral sheets and the oxide arrangement of the tetrahedral sheet. The structure of layered double hydroxide (LDH) consists of mainly brucite-like sheet. Anions are present between the layers of LDH. All these materials can be synthesized artificially, meaning that the composites are free from impurities. Their intercalation properties and the formation of intercalation compounds with polymers are quite different from those of smectites.

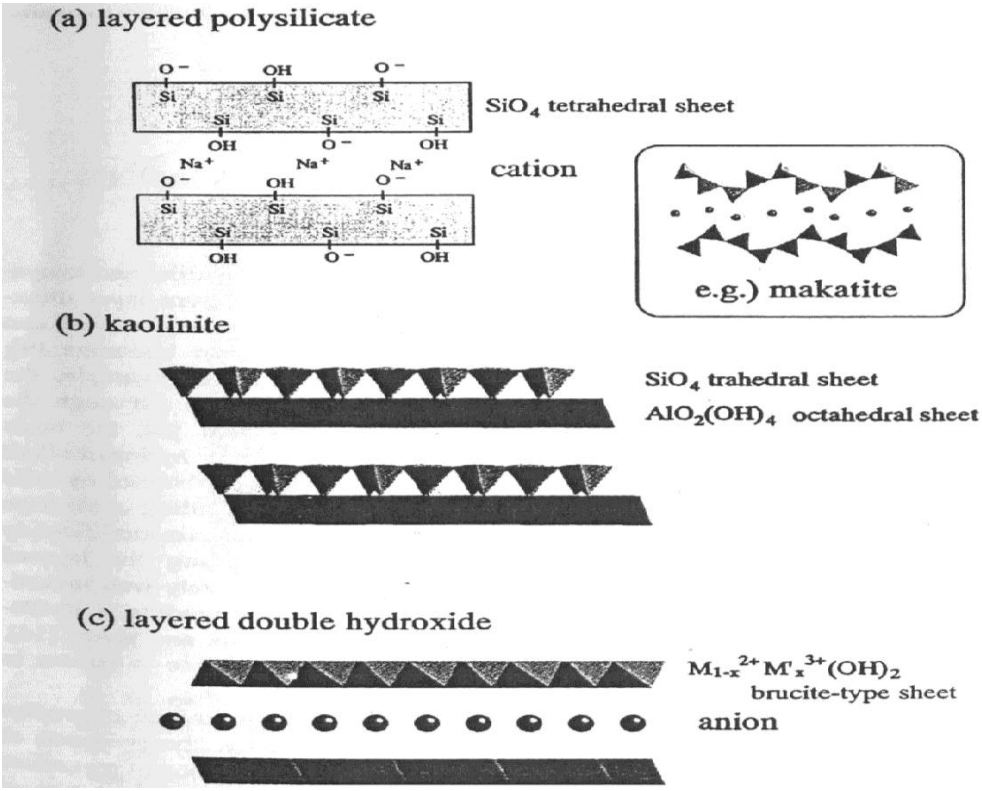

Fig. 1.6 Schematic structures of layered materials - some ions, water molecules or hydrogen atoms are omitted for clarity [17]

1.4 Polymer-layered silicate nanocomposties

1.4.1 Synthesis

1.4.1.1 In situ polymerization

Toyota Motor Company (Japan) filed the first US patent (#4739007) [18] for the development of nylon-clay nanocomposites by *in situ* polymerization route [19-20]. This route starts intercalation of monomers between the clay galleries and then polymerizing it *in situ*. To facilitate the intercalation and polymerization reaction catalysts are supported on the clay surfaces. By replacing the hydrophilic Na^+ and Ca^+ exchange cations of the native clay with a more hydrophobic organic onium ion, they

were able to intercalate and polymerize ε-caprolactam in the interlayer (gallery) space of the clay to form a nylon-exfoliated clay hybrid composite (Fig. 1.7).

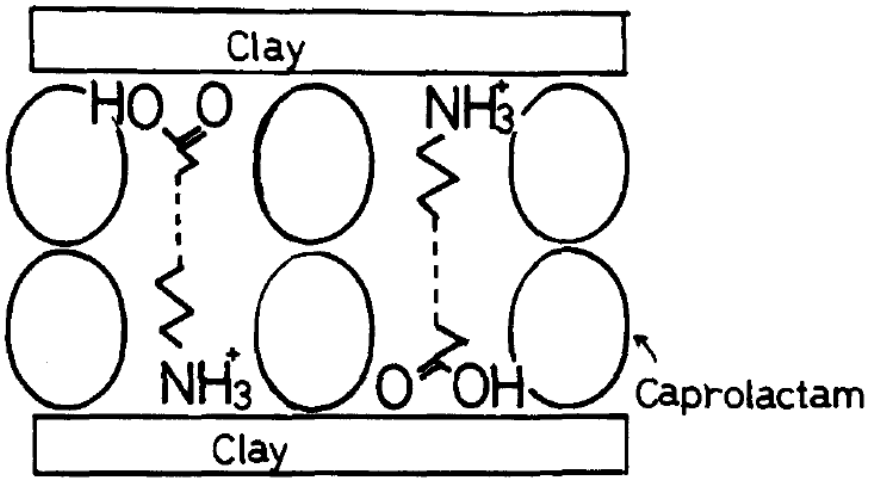

Fig. 1.7 Model of the n-montmorillonite swollen by ε-caprolactam [20]

The solution containing catalyst supported on the clay is then introduced into a high-pressure polymerization reactor along with the monomer. Reaction is carried out at high temperature and pressure to obtain a polymer nanocomposite. The key to this extraordinary performance of nylon 6-clay hybrids is the complete dispersal (exfoliation) of the clay nanolayers in the polymer matrix (Fig. 1.8).

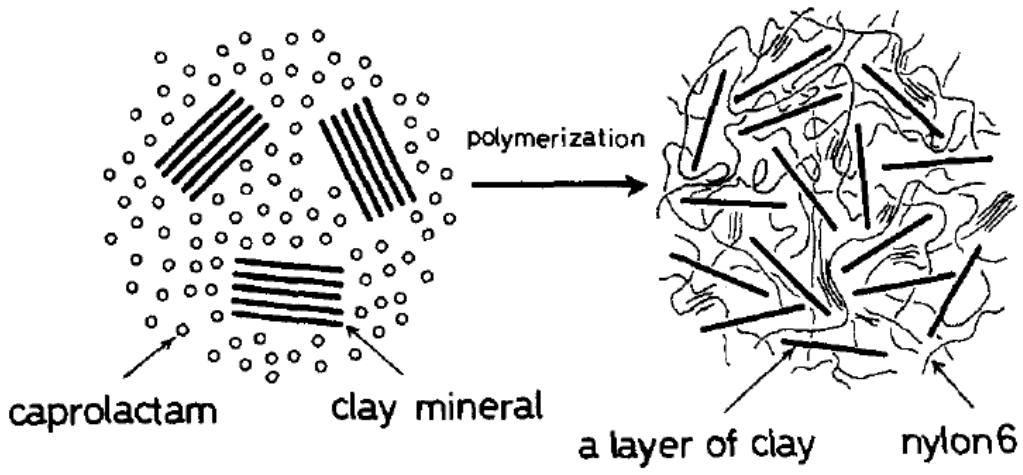

Fig. 1.8 A conceptual of figure of nylon 6-clay hybrid (NCH) [20]

Various polymer-clay nanocomposites, using polymers like polystyrene [21], epoxy [22], poly (ethylene terepthalate) [23], polyethylene [24-25], poly (methyl methacrylate) (PMMA) [26] etc., have been synthesized by this route.

Although nanocomposites prepared by this route have promisingly showed improved properties, the batch size achieved by this route in a laboratory is limited as small reactors due to followed reason. From an industrial point of view, presence of additives in the system lead to reaction conditions making the production of these materials very complicated in the large reactors used in an industry [27]. These are some of the reasons that have made the bulk production of the nanocomposites by this route very unlikely in the industry.

1.4.2 Melt blending

Polymer-clay nanocomposites could be developed by melt blending, the polymer and

an organophilic clay are mixed in a twin-screw extruder. In this route both polymer and clay are either simultaneously fed, or separately premixed and then fed, to the twin-screw extruder [28]. The heat and shear generated by the screw in the barrel of the extruder facilitates the intercalation/exfoliation of clay in the polymer matrix. Various polymer-clay nanocomposites, using thermoplastic polymers like nylons [29] , PET [30], PP [31] etc., have been synthesized by this route. Being comparatively easier than the *in situ* route, the development of the melt blending route brought polymer-clay nanocomposites closer to commercialization.

1.4.3 Solution synthesis

Aranda and Ruiz (1992) [32] reported poly (ethylene oxide) /montmorillonite nanocomposites can be prepared by dissolving, PEO in a suitable solvent which also swells the montmorillonite. In this method for synthesizing polymer-clay nanocomposites, the polymer is first dissolved in a solvent and then modified clay is added to it. The solvent used in this technique should dissolve the polymer and also swell the clay layers. The mechanism for the formation of nanocomposites by this technique involves two steps. 1) Swelling of the clay layers by the solvent and then 2) intercalation of the polymer chains into the expanded clay galleries by displacing the solvent molecules out of the gallery.

After the solvent is penetrated into the clay galleries, the system is heated till all the solvent evaporates. On removal of all the solvent it has been observed that the intercalated clay remains, resulting in polymer-clay nanocomposite. Various

polymer-clay nanocomposites, using polymers like poly-vinyl acetate [33], PE [34] and PEO [35], have been synthesized using this route.

Although few studies involving measurements of this route of nanocomposite properties after a certain period of time (in order to study the proterties of the nanocomposite) has been reported, it was believed that once the clay is dispersed by a certain distance from the neighboring platelet since no Van Der Waals interactions are present, the clay layers would not swing back and increase the properties.

Although this route can be used to synthesize nanocomposites from polymers with little or no polarity, from a commercial point of view, this route involves use of organic solvents in a large amount, which is environmentally unfriendly and economically prohibitive. Also it is believed that a small amount of solvent remains in the final product at the polymer-clay interface thus weaker interfacial interaction between the polymer and the clay surfaces is formed [36].

1.4.4 Shear mixing

Vaia, *et al*. [37] implied that the degree of exfoliation would be improved through the aid of conventional shear devices. T. D. Ngo, *et al*. [38] studied the effects of temperature, speed, and time at the pre-mixing step on the dispersion and intercalation/exfoliation of clay in epoxy resin. Pre-mixing temperature, speed and time do not significantly affect the intercalation of organoclay at the pre-mixing step. However they have a positive effect on the dispersion of nanoclay into smaller aggregates. In addition, speed shows more powerful than temperature in terms of clay

dispersion. Fine dispersion and distribution was achieved with pre-mixing at 120 °C and 24,000 rpm.

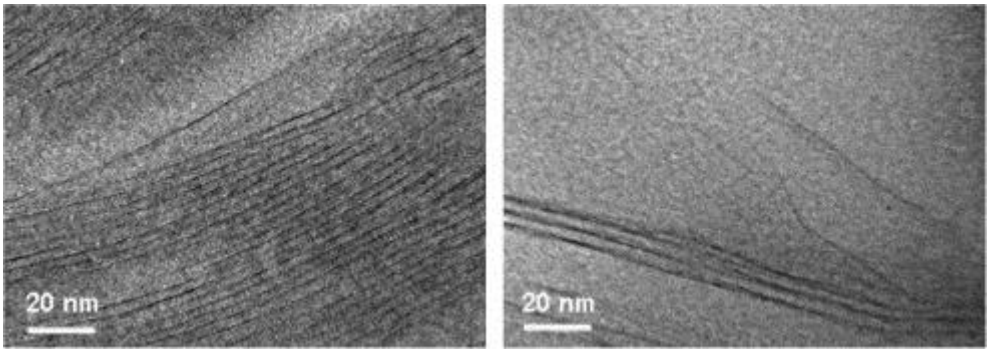

Fig. 1.9 TEM photos of nanocomposites: Pre-mixed at 120 °C for: (a) 0 min with 0 rpm and (b) 60 min with 24,000 rpm. [38]

1.4.2 Properties and applications

Toyota researchers [20] reported that, as mentioned before, by replacing the hydrophilic Na^+ and Ca^+ exchange cations, they were able to obtain the intercalated clay composite. At a loading of only 4.7 mass% of clay, the modulus is raised by 40%, the strength is increased by 50% and the heat distortion temperature is increased by 80 °C compared with the pristine polymer as shown in Table 1.1.

Unitika Ltd. of Japan [39] developed polyamine 6 nanocomposite (Nylon M2350) using synthetic clay as reinforcement during polymerization. Nylon M2350 has been used by Mitsubishi Motors for an engine cover on its GDI models, where the nanocomposite is said to offer a 20% weight reduction and excellent surface finish. Kojima, *et al*. [40] studied the mechanical properties of polyamine 6-clay nanocomposites prepared using organically modified montmorillonite and synthetic clays. TEM showed that both

Table 1.1 Mechanical and thermal properties of nylon 6-clay composites [20]

Material	Clay (mass %)	Tensile Strength (MPa)	Tensile Modulus (GPa)	HDT at 1.82 MPa (°C)
Nylon 6-clay Nanocomposite (exfoliated)	4.7	97.2	1.87	152
Nylon 6 (pristine polymer)	0	68.6	1.11	65

nanocomposites were exfoliated. The polyamine 6-clay composite (PACC) was superior in strength and modulus to nylon 6. The flexural strength of PACH at 120 °C was double than that of polyamine 6. The flexural and tensile modulus was 4 times and 3 times that of polyamine 6 respectively.

The enhancement of barrier properties is believed to depend on the degree of exfoliation of the clay platelets. In the fully exfoliated state, individual clay platelets have the highest aspect ratio possible and thus the highest barrier improvement is expected. Kojima, *et al.* [41] studied the barrier of polyamine-montmorillonite and polyamine-saponite (syntheticclay) nanocomposites to water. Both polyamine-montmorillonite and polyamine-saponite nanocomposites had better barrier to water than nylon homopolymer. The higher aspect ratio of montmorillonite compared to saponite, it clearly that polyamine-montmorillonite nanocomposites were better barrier property to water than polyamine-saponite nanocomposites.

1.5 Epoxy/clay nanocomposties

1.5.1 Synthesis

Epoxy resins are characterized by the presence of epoxide rings which can be reacted with curing agents or catalytically to form a crosslinked polymeric structure. Crosslinked epoxies exhibit outstanding properties such as good adhesion to a variety of surfaces, low shrinkage during curing, no emission of volatile products, resistant to thermal and chemical attack, high glass temperature, electrical proterty and high mechanical modulus. Montmorillonite is one of the most common inorganic filler. MMT, which has an alumino-silicate structure, consists of two tetrahedral layers sandwiching an octahedral layer with Na^+ or Ca^+ ions residing in the layer resistant to thermal and chemical attack, high glass temperature, and high mechanical modulus.

In the past decades, mechanism of clay dispersion into the epoxy matrix has been one of the most interesting issues of polymer research. Sancaktar, *et al.* [42] proposed stages of dispersing nanoparticles in polymeric matrices: (1) intercalation into particles by polymer chains; (2) shear force-induced exfoliation of individual particles, and (3) homogeneous dispersion of exfoliated particles into the matrix. The first stage is governed by clay pre-treatment. The last two stages are controlled by mixing. Wang, *et al.* [43] studied organo-intercalates, interlayered by various onium ions, to form epoxy-layered silicate nanocomposites. After treatment, the nanolayers were spaced over long distances at 80 Å Bragg spacing. According to the ref. [44], polymerization of monomers in the galleries of protonated onium ion exchanged form of smectic clays during intercalation stage is necessary for synthesis of amine-cured epoxy nanocomposites.

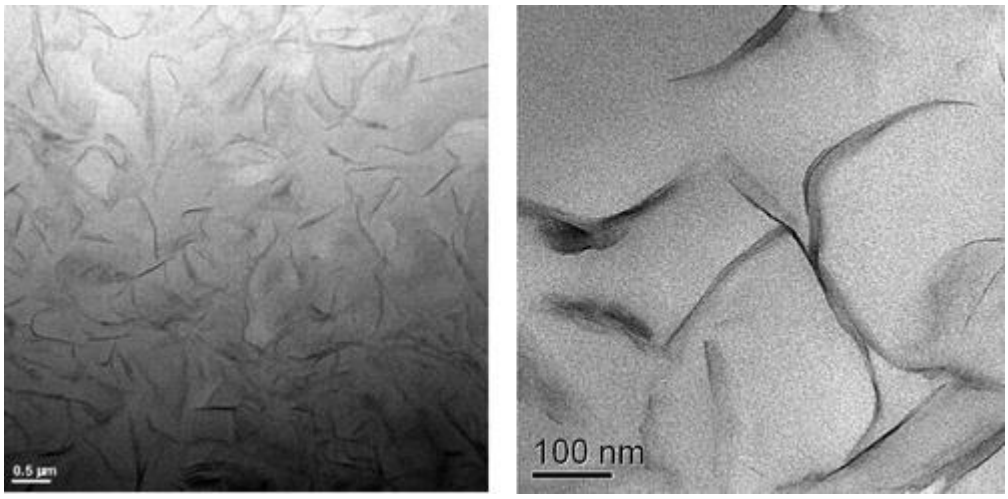

Fig. 1.10 TEM micrographs of the epoxy/clay Nanocomposite containing 2.5 mass% of clay [44]

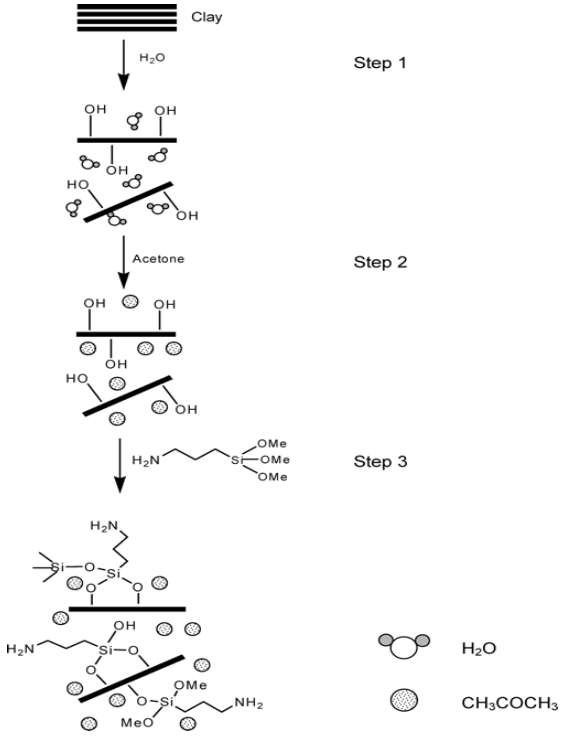

Fig. 1.11 Schematic representation of clay modification [44]

Ke, *et al.* [44] reported that clay modification using chemical treatment – "slurry-compounding process" had significantly enlarged the d-spacing and assisted the pristine clay to exfoliated structure in epoxy matrix. The dispersion state of clay in water has been transferred into the epoxy matrix by a solvent exchange step and a modification step. The critical step is the replacement of water with organic solvent, which facilitates the surface modification and dispersion of modified clay in the epoxy matrix (Fig. 1.11). Fig 1.10 presented TEM micrographs shows clay was exfoliated. Clay dispersion is uniform and random in the matrix.

Messersmith and Giannelis [45] prepared organoclay/epoxy composites using diglycidyl ether of bisphenol-A (DGEBA), and a layered silicate treated with alkylammonium ions containing primarily octadecylamine and hydroxyethyl group, obtain commercially from Southern Clay Products. The hydroxyethyl group appears to participate in curing of the epoxy resin, directly attaching the polymer network to the nearly exfoliated clay layers.

Another study by Jiankun, *et al.* [46] showed that organoclays were easily intercalated by epoxy oligomer to form stable composites. They treated sodium montimorillionite with $CH_3(CH_2)_{17}N(CH_3)_3$. Their work shows that prior intercalation of clay galleries before the polymerization reaction takes place promotes clay exfoliation. While exfoliation is difficult to achieve in the thermoset system, well-intercalated clay structure are produced with d-spacing of clays from 2-4 nm, as measured by XRD. They showed that it is necessary for the clay to undergo exfoliation due to high

polymerization rate of intra-gallery crosslinking before the surrounding resin reaches it gel point.

Pinnavaia, *et al.* [47] found that the extent of exfoliation depends on the accessibility of the epoxy to the clay galleries as well as the relative rates of intra-and extragallery network formation as shown in Fig 1.12. Their work also showed that intercalated/exfoliated epoxy/clay nanocomposites have higher moduli than intercalated clay composites as shown in Fig 1.13. Thus exfoliation before curing is a desired state.

In order to achieve this, a driving force for exfoliation must overcome the attractive forces between the silicate layers and interlayer cations holding the clays together. This can be achieved by engineering the polymerization rate inside the galleries to be higher than that outside of the clay tactoid. A minimum difference in these polymerization rates is required to achieve clay exfoliation. However, if the difference in the intra- vs. extra-gallery materials is large, they may make phase separation, which would negative modified composite properties. Therefore, this difference in polymerization rate is difficult to balance at the proper level to attain both clay intercalation/exfoliation and good properties.

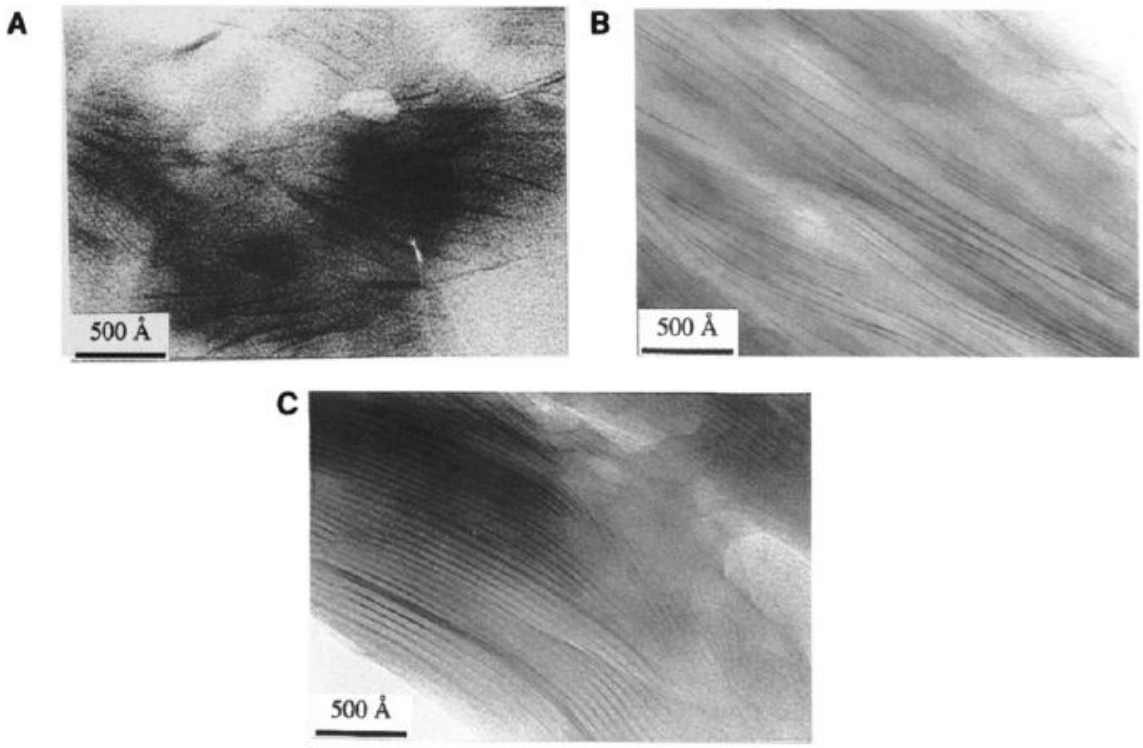

Fig. 1.12 TEM images of amine-cured epoxy-clay nanocomposite with a clay content of 5 mass %. Epoxy exfoliated clay nanocomposite architecture obtained with (A) $CH_3(CH_2)_{15}NH^{3+}$. Intercalated epoxy-clay nanmmposite structures obtained with (B) $CH(CH_2)_{15}NH^{+}$ and (C) $CH_3(CH_2)_{15}NH^{3+}$ [47]

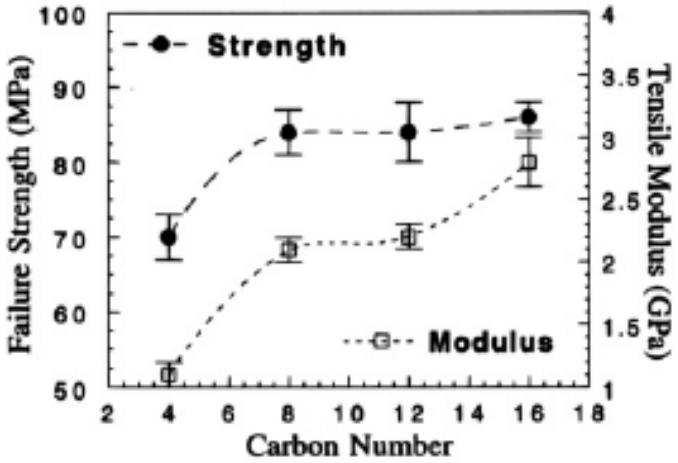

Fig. 1.13 Dependence of tensile strength and modulus of amine-cured epoxy-clay nanocomposites on onium ion carbon number at clay loadings of 2 mass % [47]

This challenge was addressed in epoxy/clay research by Park and Jana [48-50]. These authors studied the role of speed of epoxy curing, intra- vs. extra-gallery polymerization rates, and the use of polar solvents. In their work, they started with clay tactoids intercalated with epoxy molecules. As the epoxy cross-linked, the outwardly exerted elastic forces that resulted inside the clay galleries was found to be responsible for exfoliation.

These experiments used clays containing hydroxylated quaternary ammonium ions and organic ammonium ions with no polar functional groups. It was found that both types of clay produced exfoliated structures equally easily. It was also noted that higher curing temperature and the use of organically modified clay accelerated gel formation. The gel time was found to be the upper bound of time available for exfoliation. Intercalation and exfoliation appear to be influenced by the catalytic activity of the organic modifier, speed of diffusion of curing agents, and curing temperatures. Intra- vs. extra-gallery polymerization rates can be changed by altering the ratio of amine to epoxy.

1.5.1 Mechanical properties

Erol Sancaktan and Jason Kuznicki [51] reported that intercalated organoclay/epoxy nanocomposites show improved properties including enhanced mechanical properties at low nanofillers loading. The optimal level of nanoclay loading seems to be around 0.5-2% mass for mechanical properties i.e. maximum stress, elastic modulus, and yield stress.

Messersmith and Giannelis [45] prepared organoclay/epoxy composites using DGEBA and the treated layered silicate. Those composites showed an increase in dynamic storage modulus with only 4% addition of organoclay by volume.

Pinnavaia, et al. [47] presented TEM micrographs that clay was exfoliated. Clay dispersion is uniform and random in the matrix. Storage modulus at 240 °C of 5 mass% of clay in the epoxy matrixis increased by about 150% compared to the neat epoxy

Park and Jana [48-50] reported that the combination of a slow increase of complex viscosity (|η*|) outside the clay tactoids and fast increase of storage modulus (G′) inside the clay galleries during the crosslinking reaction, resulted in complete exfoliation of the clay layers. It was also observed that faster intragallery polymerization expedited the exfoliation process, but was not necessary for complete exfoliation.

1.5.2 Corrosion behavior

Focusing on corrosion studies, Rana et al. [51] studied moisture diffusion through neat vinyl ester resin containing nanoclay and illustrated that "montmorillonite clay was effective in reducing the diffusion coefficient of water through the vinyl ester resin". Their diffusion experiments revealed that advantage in incorporating the clay was dramatic for diffusion at elevated temperatures as for the diffusion of distilled water at 42.5 °C, with D going down from 16.43×10^{-13} to 0.93×10^{-13} m^2/s.

Abacha, et al. [52] studied diffusion behavior of water and sulfuric acid in

epoxy/organoclay nanocomposites. They reported that under their processing conditions, the penetration depth and diffusivity of the nanocomposites were reduced and additions of nanoclay would be improved barrier properties against corrosive acid.

Chenggang, et al. [53] reposted that the improvement in the corrosion-resistance behavior of epoxies by the introduction of a small volume fraction (0.5–3.0%) of a layered silicate. The panels were immersed in a dilute Harrison's solution (a mixture of 0.05% sodium chloride and 0.35% ammonium sulphate). The solvent uptake for the nanocomposites is significantly low compared with the pristine polymer and the weight saturation was observed to be reduced.

1.6 Characterizations

There are several methods to characterize the structure and properties of polymer/clay nanocomposites. To evaluate clay dispersion in the epoxy/clay suspension, viscosity is used. The most straightforward to monitor the structure of epoxy/clay nanocomposites is X-ray diffraction (XRD) because it is a good way to evaluate the spacing between the clay layers. Lack of sensitivity of the analysis and limits of the equipment can lead to wrong conclusions about the nanocomposite structure. Therefore, transmission electron microscopy (TEM) is a necessary complement to XRD. TEM gives a direct measure of the clay distribution but it requires substantial skills in specimen preparation and analysis. The mechanical property and corrosion behavior of nanocomposites are necessary to evaluate. Flexural property using 3-point bending and immersion test are employed to investigate.

1.6.1 Viscosity Analysis

In order to calculate the viscosity of pristine epoxy prepolymer and clay dispersed epoxy prepolymer Anton Paar – Physica MCR 100 viscometer using cone and plate geometry was used. Constant temperature water was circulated around the container by temperature controlled water bath. The viscosity readings at constant temperature of 25°C were recorded for each set of samples.

1.6.2 X-Ray Diffraction (XRD) Analysis

Interlayer distance (d-spacing) of organoclay (montmorillonite) was measured using a Philips MRD X'Pert with a rotation anode and CuKα radiation (λ = 1.5418 Å). The scanning range was from 1.05° to 9.95°, 0.02° step size and 3sec step time for the measurement of the d-spacing. The d-spacing was investigated at different mixing conditions. For the analysis of the clay powder, particles were mounted on a sample holder with a large cavity and a smooth surface was obtained by passing the particles with a glass plate. Analysis of organoclay swollen in the epoxy resin with the curing agent was performed by spreading the sample composites on the sample holder. The nanocomposite plates produced during the molding process had a fairly smooth surface which had been directly analyzed.

The organophilic nature of the clay allows the dispersion of organic solvent or monomer between the clay layers. XRD measurement can be used to characterize the interlayer distance. If diffraction peaks are observed in the low-angle region, such peaks indicate the d-spacing or the basal spacing of ordered-intercalated and ordered exfoliated

(delaminated) nanocomposites. The d-spacing was calculated according to Bragg's equation as following:

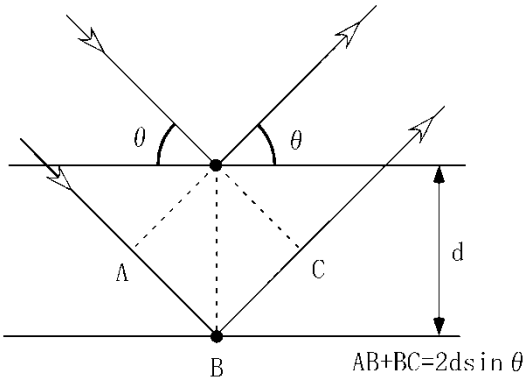

$$n\lambda = 2d\sin\theta \quad (1.1)$$

where λ is CuKα radiation (λ = 1.5418 Å) [Å]

d is interfacial distance or layer spacing(d-spacing) [Å]

θ is intensity [Counts]

1.6.3 Transmission Electron Microscopy (TEM)

Transmission electron microscopy (TEM) is a power technique to study structures at the nanoscale. The nanoclay composite structure and clay distribution were examined using TEM. It can be used to confirm results with XRD about the organization of the clay layers in the nanocomposites. It allows a precise observation of nanostructures with anxceptional high resolution (about 0.2 nm). Therefore, this technique is widely used to characterize polymer-nanocomposites.

Transmission Electron Microscopy (TEM) images in this study were obtained using a JEOL 2010F equipped with a field-emission gun operating at 200kV. TEM specimens

need to be sufficiently thin to allow the transmission of electrons. TEM samples were prepared by ultramicrotoming thin sections of the polymer nanocomposite with a diamond knife. These thin sections were then captured on coated Cu grids. The samples were tested at different magnifications from 0.2 μm to 50 nm.

1.6.4 Flexural Property

Three-point bending is a convenient way to determine flexural property. Flexural strength and modulus were evaluated by three-point bending test using a bending machine, Shimazu Autograph AGS-1KNJ. The bending test specimens of 60×25×2 mm^3 for flexural property according to ASTM D790 were tested at room temperature as shown in Fig. 1.14. Operating condition of the bending test was 40 mm span distance and 2 mm/min cross head speed. Flexural modulus is the ratio of stress to strain in flexural deformation, or the tendency for a material to bend. It is determined from the slope of a stress-strain curve produced by a flexural test and uses units of force per area. The flexural strength and modulus were calculated according to equation as following:

$$\sigma = \frac{3Pl}{2bh^2} \tag{1.2}$$

$$E = \frac{l^3}{4bh^3} \cdot \frac{P}{y} \tag{1.3}$$

where σ = flexural strength [MPa]

E = flexural modulus [GPa]

P = load at a given point on the load deflection curve [kg]

l = support span [mm]

b = width of specimen [mm]

h = thickness of specimen [mm]

y = deflection [mm]

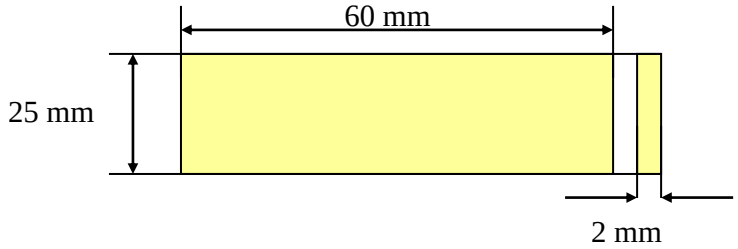

Fig.1.14 Size and shape of flexural tested specimen

1.6.5 Immersion test

The classic theory of diffusion has been derived from Fick's law, which considers that the driving force for diffusion through a thin film is a concentration gradient. When Fick's law of diffusion is combined with mass balance, Fick's second law of diffusion is obtained. Two basic assumptions are involved in the subsequent derivation as following:

1. Diffusivity, D, of the diffusing species is independent of the concentration.
2. Diffusion is unidirectional, normal to the plane of the film.

Fick's second law of diffusion is represented mathematically by:

$$\frac{\partial c}{\partial t} = D\frac{\partial^2 C}{\partial x^2} \tag{1.4}$$

Where c = concentration of diffusion species

t = time

D = diffusion coefficient

x = position

The solution of Eq. 1.4 gives mass uptake M_t of a thin polymer film in humid conditions. This is given by

$$\frac{M_t}{M_\infty} = \left[1 - \sum_0^\infty \frac{8}{(2n+1)^2 \pi^2} \exp\left[\frac{-D(2n+1)^2 \pi^2 t}{4l^2}\right]\right] \tag{1.5}$$

where M_t: mass uptake at time

M_∞: ultimate mass uptake

l : half the thickness of the sample

Eq 1.5 can be rewritten as,

$$\frac{M_t}{M_\infty} = 2\left(\frac{Dt}{l^2}\right)^{\frac{1}{2}} \left\{\pi^{-\frac{1}{2}} + 2\sum_0^\infty (-1)^n ierfc \frac{nl}{\sqrt{Dt}}\right\} \tag{1.6}$$

For short time, Eq. 1.6 can be simplified into the form:

$$\frac{M_t}{M_\infty} = \left(4\sqrt{\frac{D}{\pi}}\right) \cdot \frac{\sqrt{t}}{2 \cdot l} \tag{1.7}$$

A plot of $\frac{M_t}{M_\infty}$ VS. $\frac{\sqrt{t}}{2 \cdot l}$ is linear at the specimen to a penetrant and monitoring the change in specimen mass with time. For liquid uptake experiment, a "blot-and-weight" technique is often used. Mass uptake is referenced to the original mass of the specimen and is calculated by

$$M = \frac{M_t - M_0}{M_0} x100\% \tag{1.8}$$

Where M = moisture content (%)

M_t = mass uptake of water at time t

M_0 = dry weight of the initial sample

However for filler filled polymer, a common model [38, 39] describing the diffusion coefficient D of a small solute through continues partly filled with a suspension of impermeable spheres was established.

$$\frac{D}{D_0} = \frac{1-\varphi}{1+\frac{\varphi}{2}} \tag{1.9}$$

Where D_0 = diffusion coefficient in the absence of spheres

φ = volume fraction of spheres

The above equation is valid only for dilute solutions (φ <0.1). The equation is independent of the size of spheres but not valid when containing spheres of different sizes.

1.7 Objectives

Epoxy resin is a very attractive of polymer in terms of their high strength and stiffness, high temperature resistance, low shrinkage, good electrical property, good adhesion to metal and ceramic substrates, as well as their excellent processability. They find use in many engineering applications as adhesives, coating and matrices for composites as well as construction industries [54]. In corporation of organically modified layered silicate to form an epoxy-layered silicate nanocomposite is an attractive way to further enhance the performance of the epoxy matrix.

The main challenge in synthesis of organoclay nanocomposite is how to achieve fully exfoliated organoclay nanocomposite in the epoxy matrix. Viscosity, X-ray diffraction (XRD) and transmission electron microscopy (TEM) were employed to discuss on degree of clay exfoliation in the samples and nanocomposite morphology. Three-point bending tests according to ASTM standards were undertaken to evaluate flexural properties.

For these polymeric materials, one of the most common parameters in Chemical engineering fields and factories is corrosion performance of materials. However, less works have been done on the performance of epoxy/organoclay nanocomposites which would be applied on chemical environment i.e. coating and/or lining of storage tank, especially on the chemical corrosion behavior. To investigate anti-corrosion performance of the nanocomposites, immersion test was employed.

In Chapter 2, three physical nanoclay dispersion methods of epoxy/organoclay nanocomposites were select to study. After obtaining the suitable physical dispersion method, effect of mixing parameters and ultrasonic application on clay dispersion and their properties were investigated. Regarding to the appropriated mixing conditions, effect of clay loading on mechanical property was evaluated.

To combine physical and chemical clay dispersion methods, Chapter 3 studies effect of chemical nanoclay dispersion method using epoxy reactive dilutes and diamine curing agents as clay exfoliators via high speed mixing method for epoxy/organoclay

nanocomposites and their properties. The clay exfoliators were varied not only functional group, but also sizes of molecular chains of the compounds.

Amine exfoliators have more potential on increasing both clay exfoliation and nanocomposite properties. Chapter 4 focused on effect of monoamine, diamine and triamine exfoliators on organoclay dispersion for fully epoxy/organoclay nanocomposites and their properties. Regarding to the knowledge from Chapter 3, the amine clay exfoliators were varied sizes of molecular chains of the compounds.

Mechanisms of organoclay exfoliation as well as relationship between exfoliated clay structure and development of properties of nanocomposites are discussed in Chapter 5 based on the results from Chapter 2 to Chapter 4.

Chapter 2

Physical clay dispersion

2.1 Introduction

In the past decades, mechanism of clay dispersion into the epoxy matrix has been one of the most interesting issues of polymer research. Sancaktar, *et al*. [42] proposed stages of dispersing nanoparticles in polymeric matrices: (1) intercalation of organic compounds in layered clay; (2) shear force-induced exfoliation of individual particles, and (3) homogeneous dispersion of exfoliated particles into the matrix. The first stage is governed by clay pre-treatment. The last two stages are controlled by mechanical mixing. Wang, *et al*. [42] studied organo intercalates, interlayered by various onium ions, to form epoxy-layered silicate nanocomposites. After the treatment, the nanolayers were spaced over long distances at 80 Å Bragg spacing. According to this paper [42], polymerization of monomers in the galleries of protonated onium ion exchanged form of smectic clays during intercalation stage is necessary for synthesis of amine-cured epoxy nanocomposites. Vaia, *et al.* [37] implied that the degree of exfoliation would be improved through the aid of shear devices in the mixing process.

However, PLSN using MMT with epoxy resin as the matrix have not convincingly proved to be a complete exfoliation of the layered structure in the epoxy matrix. These intercalated organoclay/epoxy nanocomposites are expected to show improved properties including enhanced mechanical properties at low nanofillers loading [51], increased thermal property [18] and improved corrosion performance [53]. Ngo, *et al.* [38] reported that epoxy/clay nanocomposite via high speed mixing device showed

strain energy release rate was increased 130 times than original epoxy (about 100 J/m^2).

The main goal of this chapter is to obtain the suitable clay dispersion method into epoxy matrix via three different physical mixing methods and to evaluate mechanical property and corrosion behavior of epoxy/organoclay nanocomposites under immersion test, weight change and penetration behavior. After obtaining the suitable clay dispersion method, effect of mixing parameters - mixing speed, mixing duration and mixing procedure as well as effect of ultrasonic application were investigate. Finally, regarding to the appropriated mixing conditions, effect of clay loading on mechanical property was evaluated.

2.2 Experimental Method

2.2.1 Materials

Epoxy composite used in this study was synthesized witha bisphenol A type (Epomik R140) form Mitsui Chemical Co., Ltd; a diamine curing agent (Jeffamine D230) from Huntsman Corporation, and montmorillonite-based organoclay (Nanomer I.30E) from Nanocor Inc. Fig. 2.1 and 2.2 show chemical structure of bisphenol A type epoxy monomer - Epomik R 140 and diamine curing agent - Jeffamine D230, respectively.

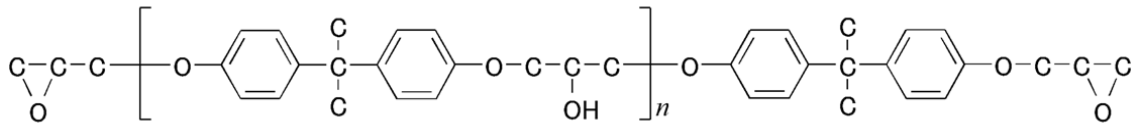

Fig. 2.1 Chemical structure of epoxy - Epomike R140 (n=0.13)

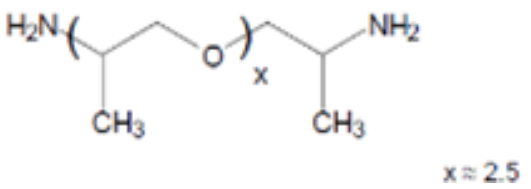

Fig. 2.2 Chemical structure of diamine curing agent - Jeffamine D230

Montmorillonite-based organoclay - Nanomer I.30E from Nanocor Inc. was used as a nanofiller. The clay used for synthesis of the nanocomposites was a commercial treated organoclay. It is basically *n*-octadecyl ammonium salt of montmorillonite clay. Schematic structure and Product data for I.30E montmorillonite are shown in Fig. 2.3 and Table 2.1, respectively.

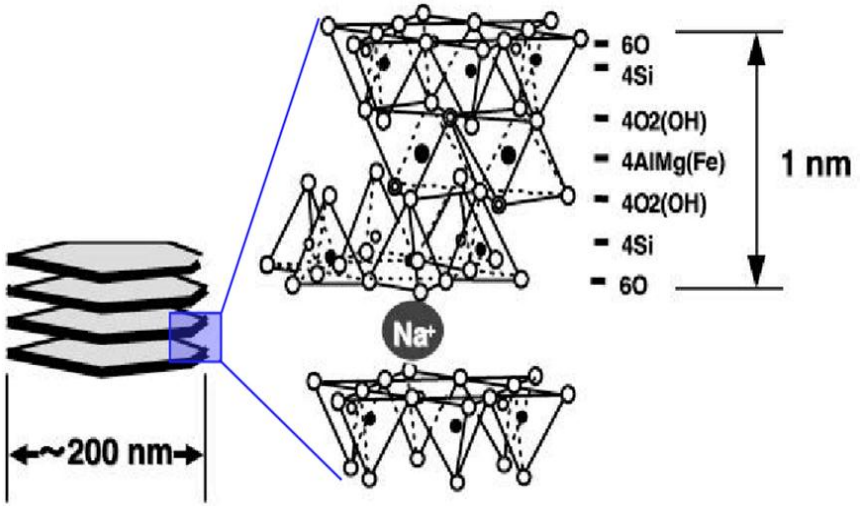

Fig. 2.3 Schematic structure of montmorillonite-based organoclay - I.30E

Table 2.1 Product data of I.30E

FORMULA :	Montmorillonite Clay	70～75wt%
	Octadecylamine	25～30wt%
Montmorillonite		
Sheet thickness	0.96 nm	
Platelet length	100～500nm	
Number of sheets	2～10	
Aspect ratio	100～500	

2.2.2 Method

Epoxy/organoclay nanocomposites were prepared at various conditions. Initially, epoxy and 1 part per hundred resin (phr) organoclay were mixed via three different mixing methods: 1) normal mixing at 1,000 rpm via propeller mixer for three hours as showed in Fig. 2.4) shear mixing via three-roll calendar (EXAKT 50, Exakt GmbH) for three times as showed in Fig. 2.5) high speed mixing at 20,000 rpm via homogenizer (Ultra-TURRAX T18, IKA.) for three hours as showed in Fig. 2.6.

To study effect of two mixing parameters, ultrasonic applications, and five concentrations of organoclay (0.5-5 phr), epoxy/organoclay nanocomposites were prepared at different conditions as shown in Table 2.2.

After mixing according to the conditions, the mixtures were degassed under vacuum for 10 minutes. Thereafter, cooling down to room temperature, and then the corresponding curing agent was added to the mixtures stirred with degassing again for 10 minutes

before casting. The mass ratio of resin to hardener is 100:30. Finally, the resin mixture of epoxy with diamine was cured at 80°C in oven for six hours and followed by post curing at 120°C in the oven for 12 hours.

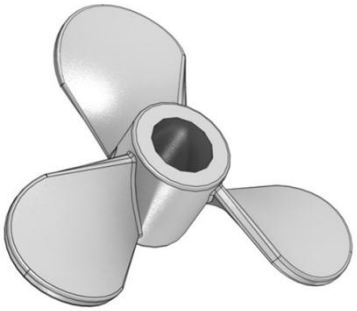

Fig. 2.4 Illustration of propeller mixer

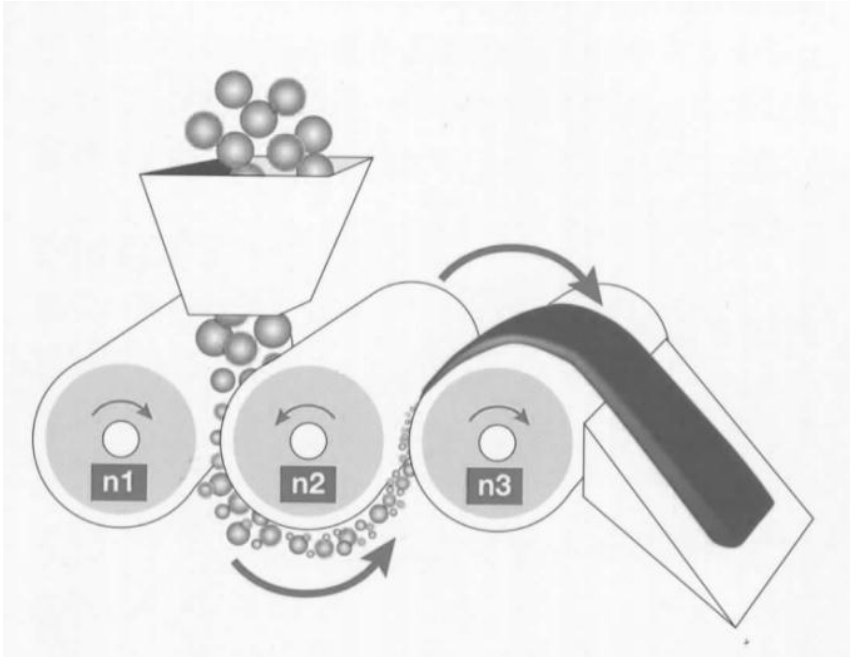

Fig. 2.5 Illustration of mixing mechanism by three-roll calendar.

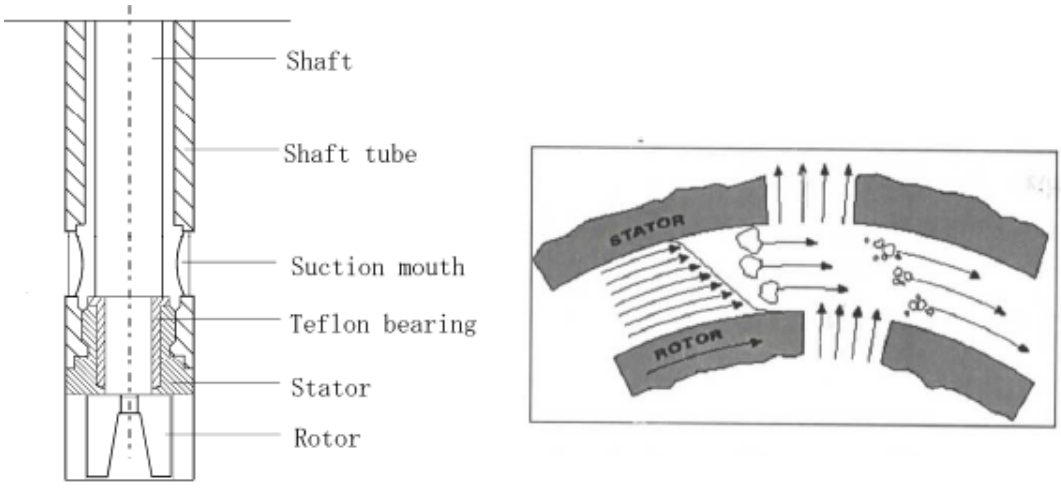

(left) (right)

Fig. 2.6 Cross-section of high speed homogenizer (left) and mechanism of rotor-stator (right).

Table 2.2 Parameters examined for the experiments

Experiment Name	**Parameter**	**Speed (rpm)**	**Mixing Duration (min)**	**Ultrasonic Application (min)**	**Concentration of Organoclay (phr)**
Effect of physical clay dispersion method	Propeller mixer	1000	180	-	1
	Three-roll calendar	(Shear force)	180	-	1
	high speed homogenizer	20,000	180	-	1
Effect of mixing parameter	Mixing speed	Hand mixing 60 rpm, 24,000	60	-	1
	Mixing duration	24,000	30, 60, 120, 180, 240	-	1
Effect of Ultrasonic Application	Ultrasonic bath	24,000	60	60,120	1
Effect of Clay Loading	Clay Loading	24,000	60		0.5, 1, 2, 3,5

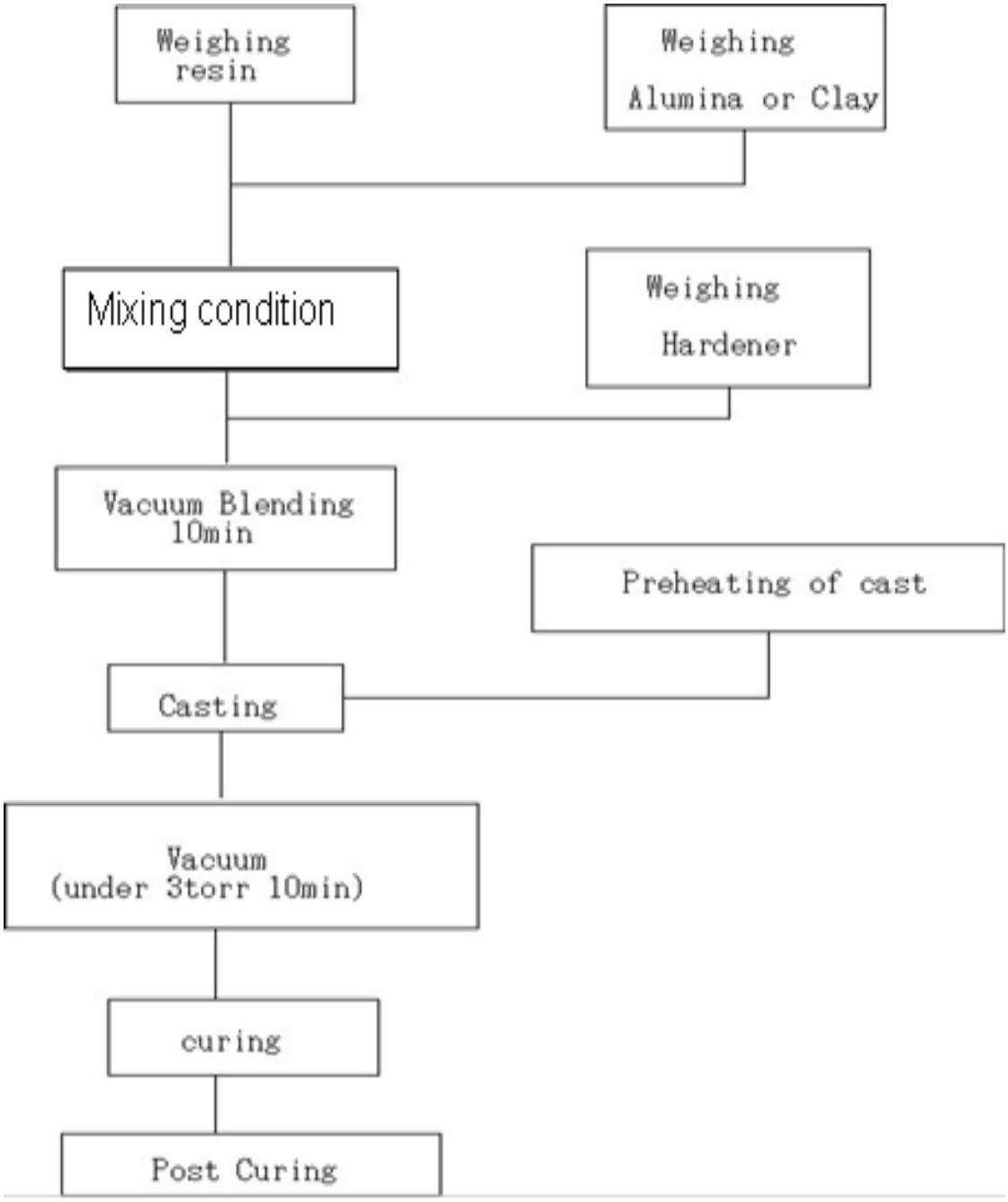

Fig. 2.7 Preparation procedure of epoxy/organoclay nanocomposites

2.2.3 Characterizations

2.2.3.1 Clay dispersion

2.2.3.1.1 Viscosity

To evaluate clay dispersion, viscosities of organoclay/pre-mixing substance suspensions after mixing process were measured at 25°C on Anton Paar – Physica MCR 100 viscometer using cone and plate geometry.

Fig. 2.8 Typical rheology machine in this study

2.2.3.1.2 Interlayer Distance (d-spacing)

Interlayer distance (d-spacing) of organoclay (montmorillonite) was measured using a XRD Philips MRD X'Pert with a rotation anode and CuKα radiation ($\lambda = 1.5418$ Å).

The scanning range was from 1.05° to 9.95°. The step size was 0.02° and the step time was 3 sec for the measurement of the d-spacing. The d-spacing of different mixing conditions were investigated. For the analysis of the clay powder, particles were mounted on a sample holder with a large cavity and a smooth surface was obtained by passing the particles with a glass plate. Analysis of organoclay swollen in the epoxy resin with the curing agent was performed by spreading the sample composites on the sample holder. The nanocomposite plates produced during the molding process had a fairly smooth surface which has been directly analyzed.

The organophilic nature of the clay allows the dispersion of organic solvent or monomer between the clay layers. XRD measurement can be used to characterize the interlayer distance. If diffraction peaks were observed to shift to in the low-angle region, such peaks indicate the d-spacing of ordered-intercalated and to fade away, then suggest exfoliated (delaminated) nanocomposites.

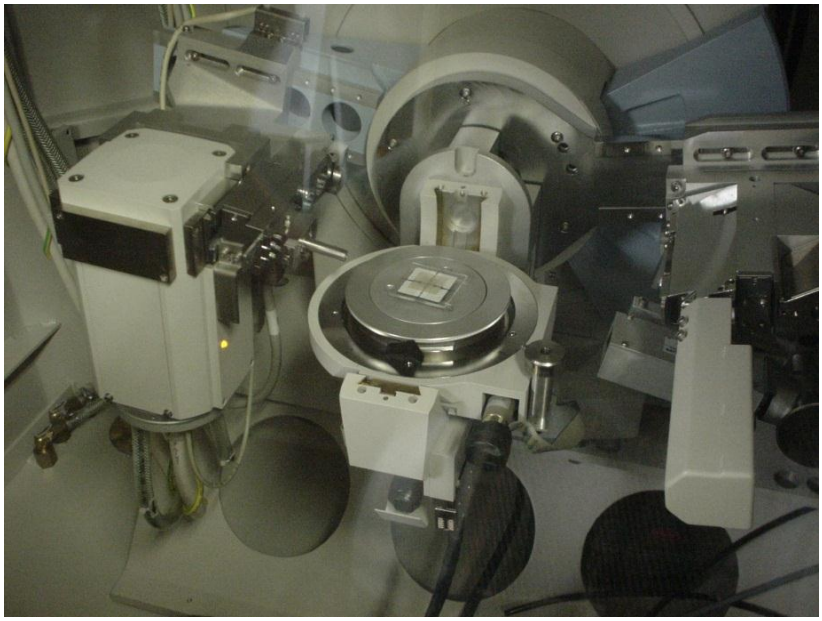

Fig. 2.9 XRD machine

2.2.3.2 Corrosion Behavior

2.2.3.2.1 Immersion test

The immersion test specimens of 60×25×2 mm^3 for measurement of initial mass were dried at 50°C in oven for more than 75 hours according to the previous study [23]. All specimens holding with a Teflon tube, in order to avoid sample overlapping, were tested in beaker containing 10% of sulfuric acid solution. The beakers were sealed with plastic film to avoid evaporation of the solution. The samples were performed in water bath controlled at 60°C as shown in Fig. 2.10.

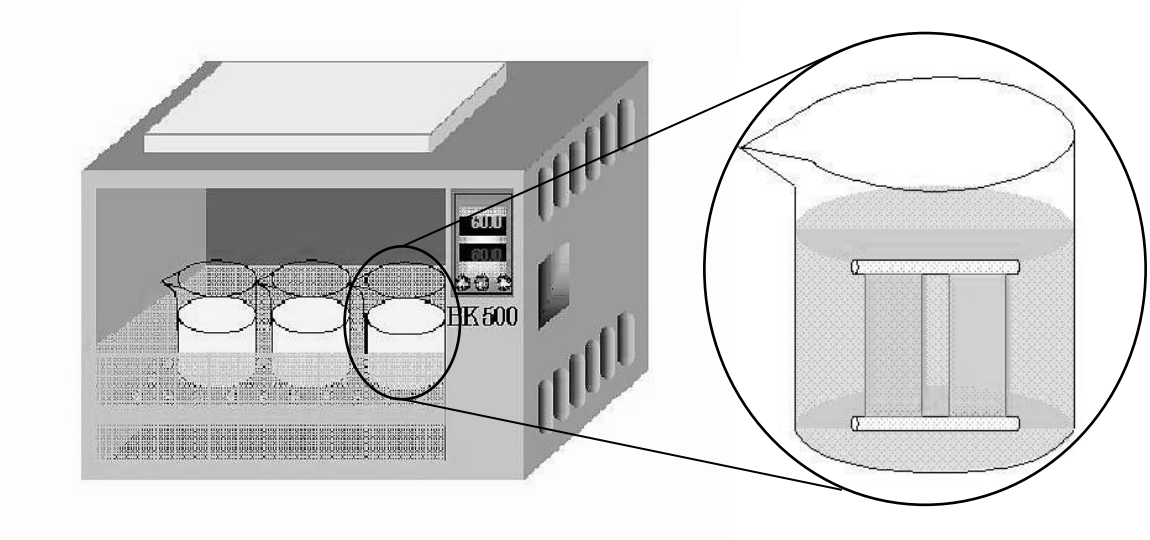

Fig. 2.10 Typical apparatus of immersion test.

2.2.3.2.2 Mass Change Measurement

Specimens were removed at regular time, washed by water and then carefully wiped to remove excess of acid on the specimens. A microbalance was used for measuring the

specimen weight. The weight change was determined by obtaining the change in mass of specimen in 10 different times from 0 hour up to 625 hours, relative to the initial weight and is calculated by,

$$M_t = \frac{W_t - W_0}{W_0} \times 100\% \quad \text{(Eq.2.1)}$$

Where M_t = Mass gain (%), W_0 = Initial mass of dry sample (g) and W_t = Mass of wet sample (g).

2.2.3.2.3 Penetration Behavior

To observe and measure penetration depth and penetration profile of sulfur (S) element of epoxy/organoclay nanocomposites, Energy Dispersive X-ray Spectroscopy (EDS) is used as an analytical technique for the elemental analysis of samples. Energy-dispersive X-ray spectroscopy JEOL JEM-5310LV was employed by investigating cross section of the immersed specimens as shown in Fig. 2.11 (above). Typical investigation of EDS micrograph is illustrated in Fig. 2.11 (below) where the line express the profile of the element S along to depth from surface. The penetration depth which is the distance from surface to level off the profile, is calculated by,

$$Pd = \frac{h_0 - h}{2} \quad \text{(Eq. 2.2)}$$

Where P_d = Penetration Depth (meter), h_0 = unpenetrated layer at initial time (meter) and h = penetrated layer at sampling time (meter)

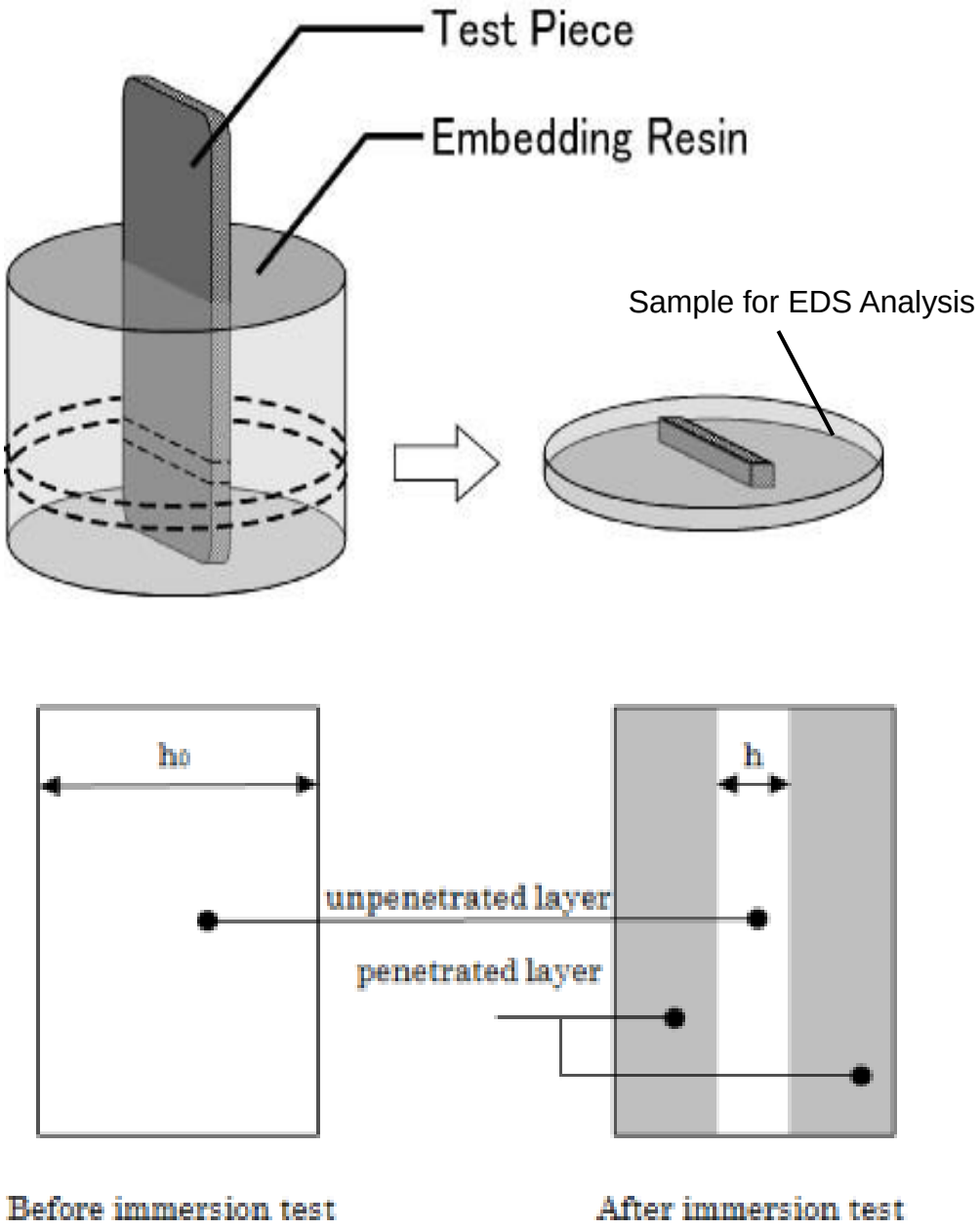

Fig. 2.11 Schematic diagrams of sample (above) and typical micrograph (below) of EDS analysis.

2.2.3.3 Flexural Property

Flexural strength and modulus were evaluated by three-point bending test using a bending machine, Shimazu Autograph AGS-1KNJ. The bending test specimens of 60×25×2 mm^3 for flexural property according to ASTM D790 were tested at room temperature.

Fig. 2.12 Three-point bending machine

2.2.3.4 Morphology

The nanoclay composite structure and clay distribution were examined using Transmission Electron Microscopy (TEM). TEM images were obtained by a JEOL 2010F equipped with a field-emission gun operating at 200kV. TEM samples were prepared by ultramicrotome to be thin sections of the polymer nanocomposite with a

diamond knife. These thin sections were then captured on coated Cu grids. The samples were tested at different magnifications from 0.5 µm to 20 nm scale bar.

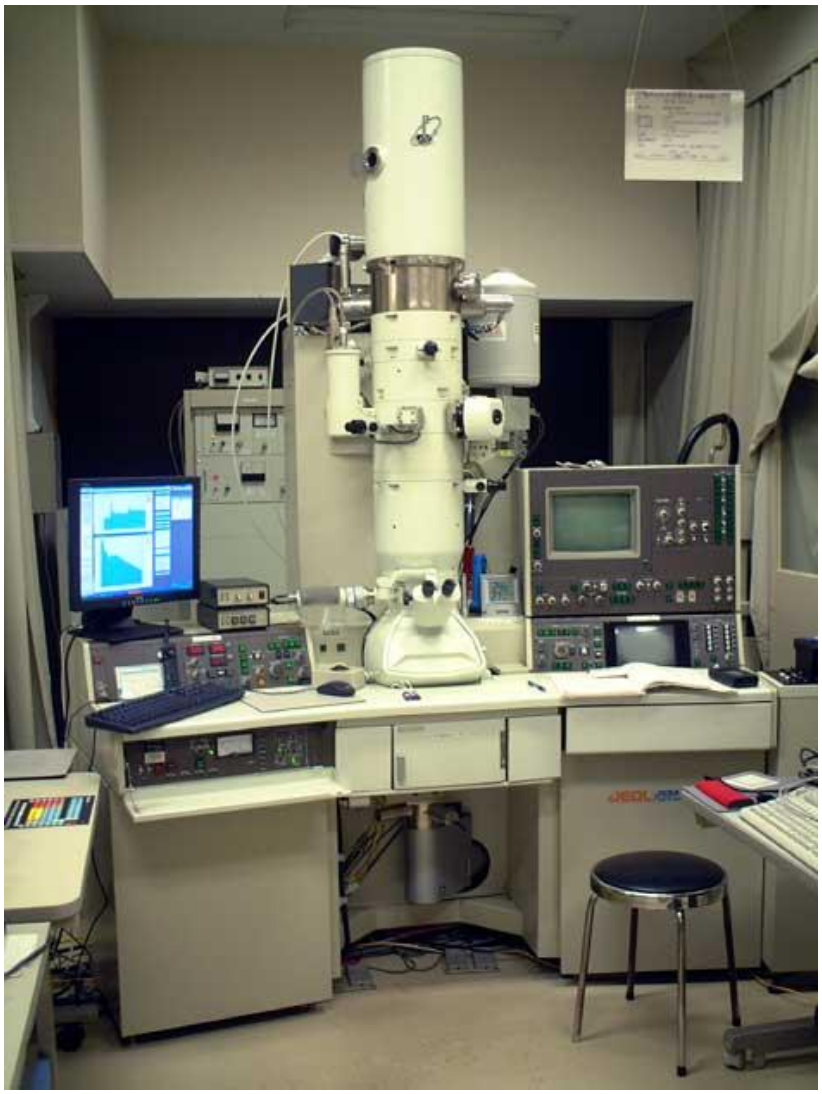

Fig. 2.13 TEM machine

2.3 Effect of physical clay dispersion method

2.3.1 Interlayer Distance (d-spacing)

X-ray diffraction curves of organoclay and 1 phr epoxy/organoclay nanocomposite are illustrated in Fig. 2.14 and 2.15. The interlayer distance (d-spacing) corresponding to the gap between clay layers is calculated according to Bragg's law: $n\lambda = 2d\sin\theta$. The supplied organoclay has a single sharp peak at 2θ = 3.9° as shown in Fig. 2.8, which corresponds to d-spacing of 22.6 Å. In the case of all nanocomposites, clear peaks were not detected except the nanocomposite under high speed mixing method (Fig. 2.9). Figure 2.15 shows the nanocomposite via high speed mixing was found to intercalate and increase the d-spacing to 33.9 Å. These results show two considering information: firstly, organoclay is significantly intercalated by epoxy resin and secondly, due to the high degree of shear involve the dispersion of large clay galleries into smaller ones took place and therefor increase clay interlayer distance.

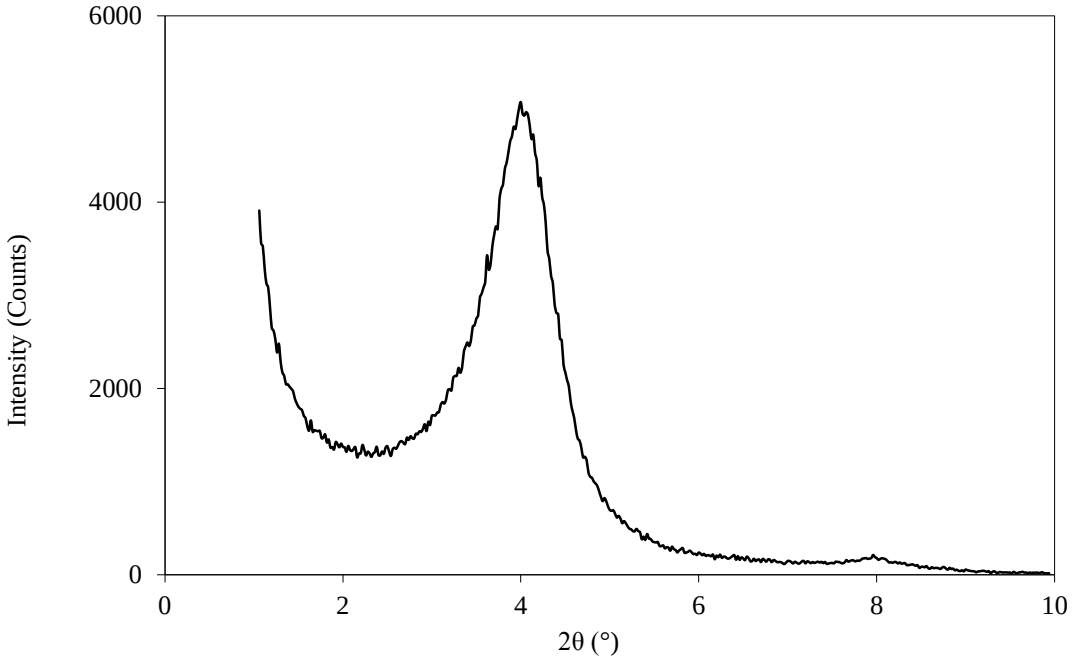

Fig. 2.14 X-ray diffraction curve of original organoclay (Nanomer I.30 E).

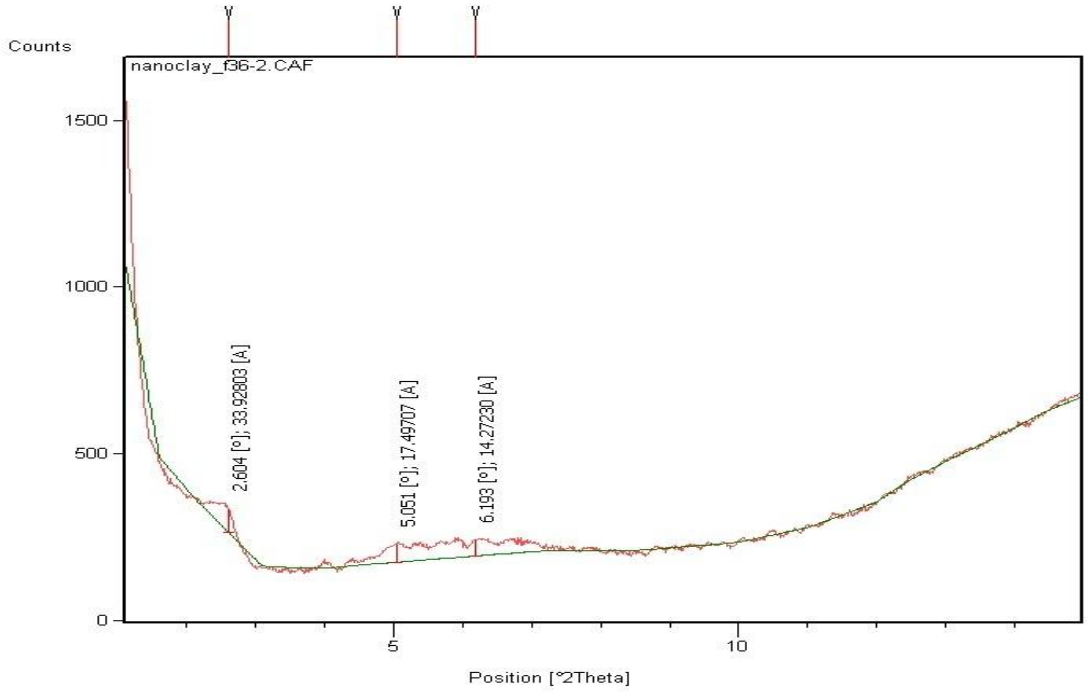

Fig. 2.15 X-ray diffraction curve of 1 phr epoxy/organoclay nanocomposite under high speed mixing method.

2.3.2 Corrosion Behavior

All specimens: neat resin (EP), normal mixing (NMA), shear mixing (RHA), and high speed mixing (DME) nanocomposite, were immersed in 10 % of sulfuric acid solution at fixed temperature, 60°C. The aim of this analysis is to determine whether diffusion of sulfuric acid through epoxy/organoclay nanocomposites following Fick's Law, and to investigate weight change of samples which immersed in 10 mass% sulfuric acid solution at 60°C as a function of square root of immersion time in Fig. 2.16.

In this report, corrosion in the composite is described by its weight change behavior and penetration depth in immersed corrosive environment. The diffusion behavior of sulfuric acid in both neat resin and nanocomposites follows Fick's Law in weight

change. As Figure 2.16 shows all the samples initially were linearly increased and after all the specimens fulfill with sulfuric acid solution, leading to equilibrium. The difference of weight saturation of high speed mixing method comparing to normal mixing and three-roll mill mixing is considerably large, more than 5%. It is considering that the enhancement of corrosion property has related to the degree of dispersion of the clay platelets.

In order to discuss the behavior in details, all samples have almost similar penetration rate, however, high speed mixing sample and neat epoxy resin reached equilibrium at similar time and earlier compared to normal mixing and shear mixing samples. It would be for the reason that layered clays themselves do not assist to improve anti-corrosion performance as labyrinth effect [55] in term of penetration rate, moreover, the conventional and intercalated clays act as a moisture scavenger by absorbing solution into themselves. As a result, both conventional and intercalated clay structures, which still remain layer-layer structure, in the epoxy matrix via normal and shear mixing.

Therefore, high degree of intercalation/exfoliation of high speed mixing specimen has the lowest weight saturation than low degree of intercalation/exfoliation of the other two methods. This suggests that mixing method of clay, especially via high speed mixing method, significantly affects to corrosion behavior in term of solution equilibrium. The behavior can be explained that the random orientation of clay plates in the bulk material, which is reasonably effective in improving property, especially corrosion resistance. As a result, it could be effectively against penetration and weight uptake.

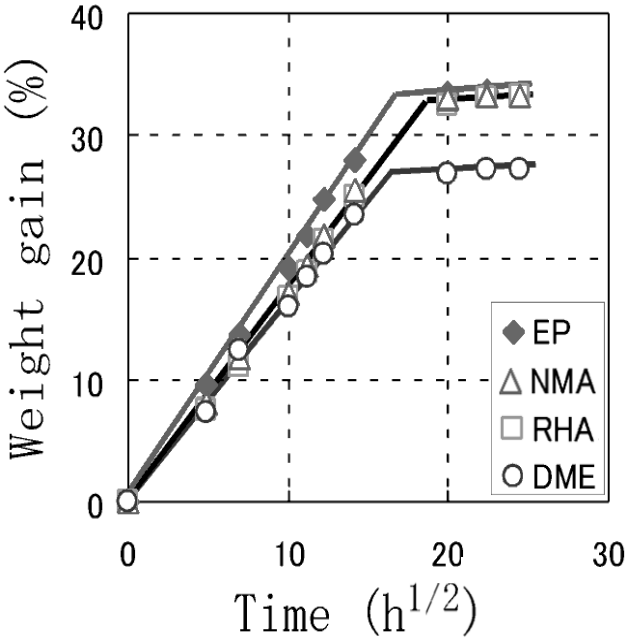

Fig. 2.16 Weight change of neat epoxy (EP), normal mixing (NMA), shear mixing (RHA) and high speed mixing (DME) nanocomposite in term of square root of time in 10 % sulfuric acid solution at 60°C.

Penetration profiles of sulfur in neat epoxy and one of three mixing methods: high speed mixing (DME) nanocomposite at different immersion time under 10 % of sulfuric acid solution using EDS analysis are shown in Fig.2.17. There are two areas from EDS micrograph: 1) unpenetrated layer and 2) penetrated layer. The lines in the Figure 2.17 expresses the penetration profile of element S along to depth from surface. For deeply analysis the penetration profiles of sulfur element, penetrated area in nanocomposite showed slightly less than neat epoxy resin for all immersion time, except after reaching saturation. The result implies that nanoclay particles improve barrier property by physically impeding the movement of penetrant molecules through the matrix.

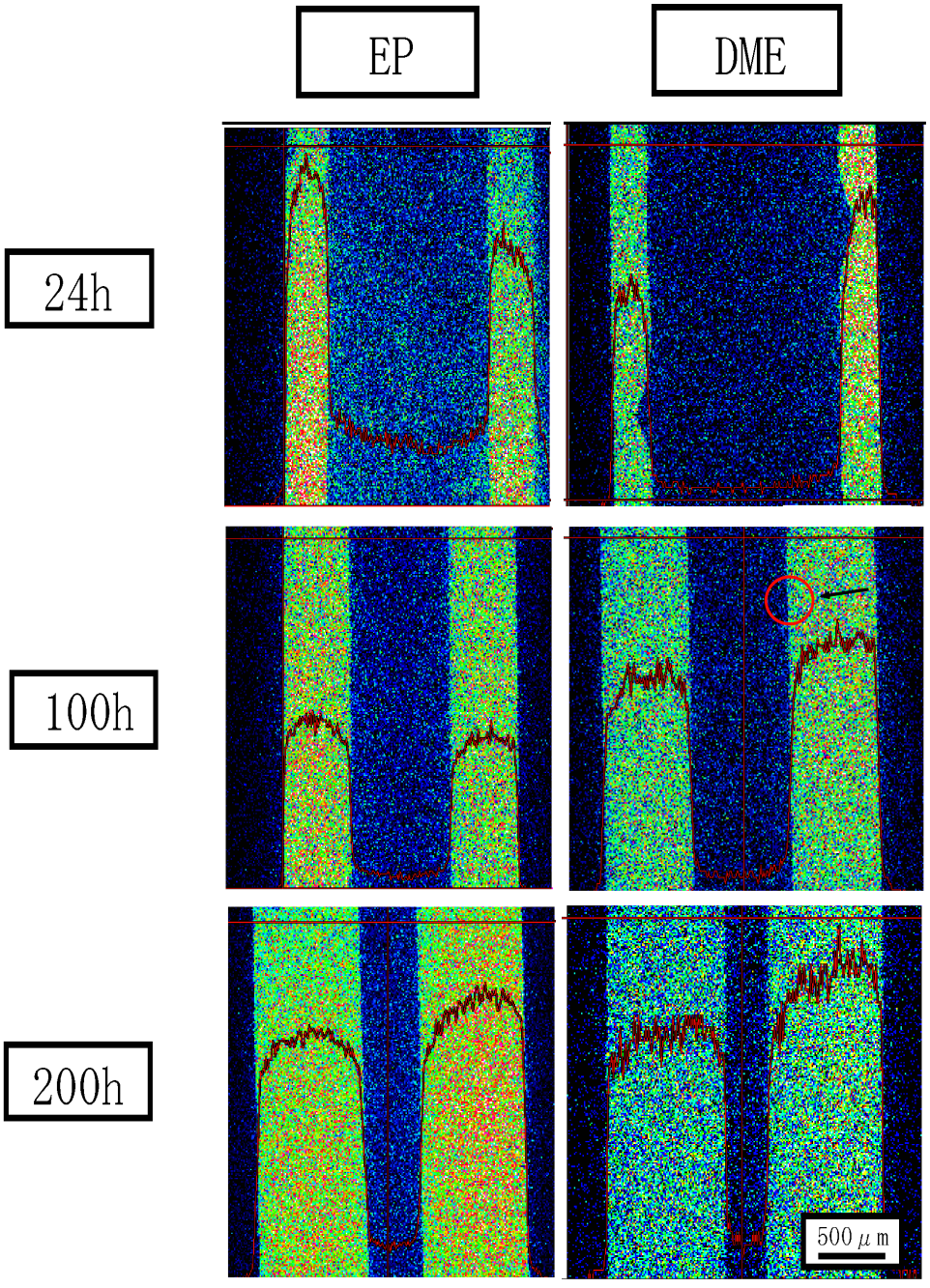

Fig.2.17 Penetration profiles of sulfur of neat epoxy and high speed mixing (DME) nanocomposite at different immersion time under 10 % of sulfuric acid solution.

Sulfur penetration depth of neat resin and epoxy/organoclay nanocomposite versus square root of time is shown in Fig. 2.18. The penetration depth which obtains from EDS analysis is calculated according to Eq. 2. It notices that nanocomposites have a lower penetration depth as compared to the neat resin. As we expected, the nanoclay would act as a barrier for the diffusion of acid solution in nanocomposite. Comparing three various mixing method, penetration depths of these nanocomposites were not expectedly different. It would be discussed that the equal nanofiller content for all nanocomposites and mixing method does not play an important role on penetration depth.

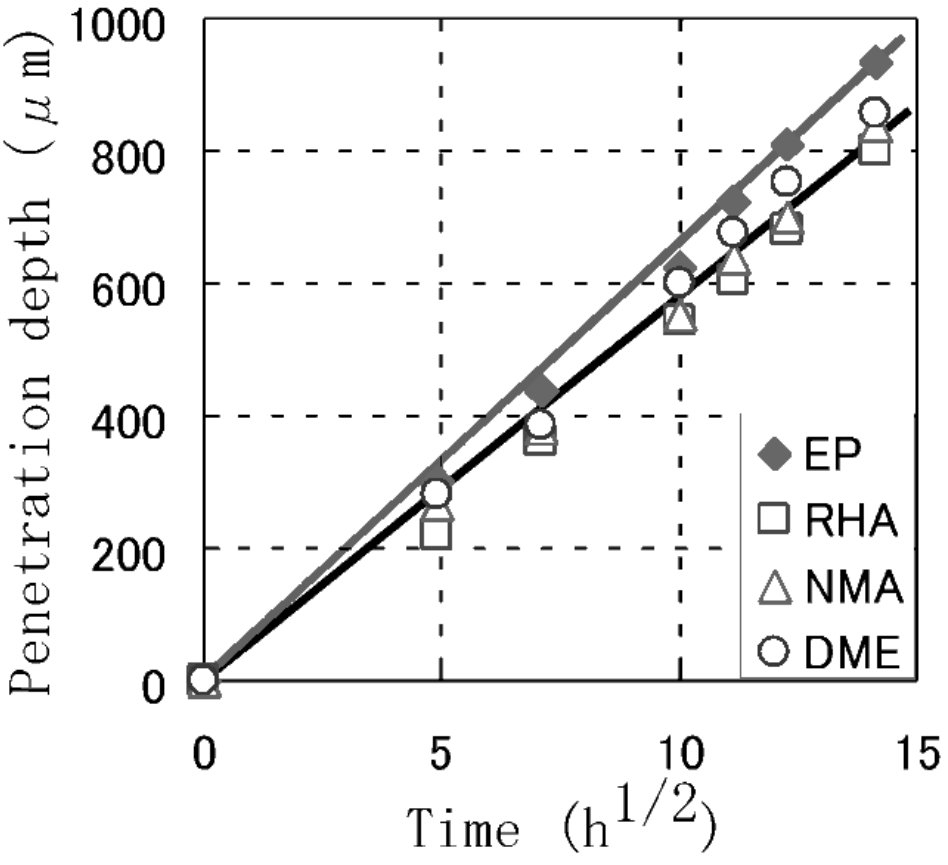

Fig. 2.18 Penetration depth of neat epoxy and epoxy/organoclay nanocomposite under different mixing method in term of square root of time.

2.3.3 Morphology

Fig. 2.19 shows TEM micrographs of epoxy/organoclay nanocomposite via normal propeller mixing method at different magnifications. As expected, normal mixing method has a small shear force for clay exfoliation and distribute uniformly in epoxy nanocomposite. The results show that layered clay visually agglomerate (left picture) and the gap between clay layers in the epoxy matrix keeps naturally tight (right picture). In order to intercalate/exfoliate, it requires energy to disperse large clay galleries into smaller ones and peel each platelet one after one. It is possible to notice that shear force from normal propeller mixing is not high enough to break up large clay stacks into smaller stacks of clay platelets

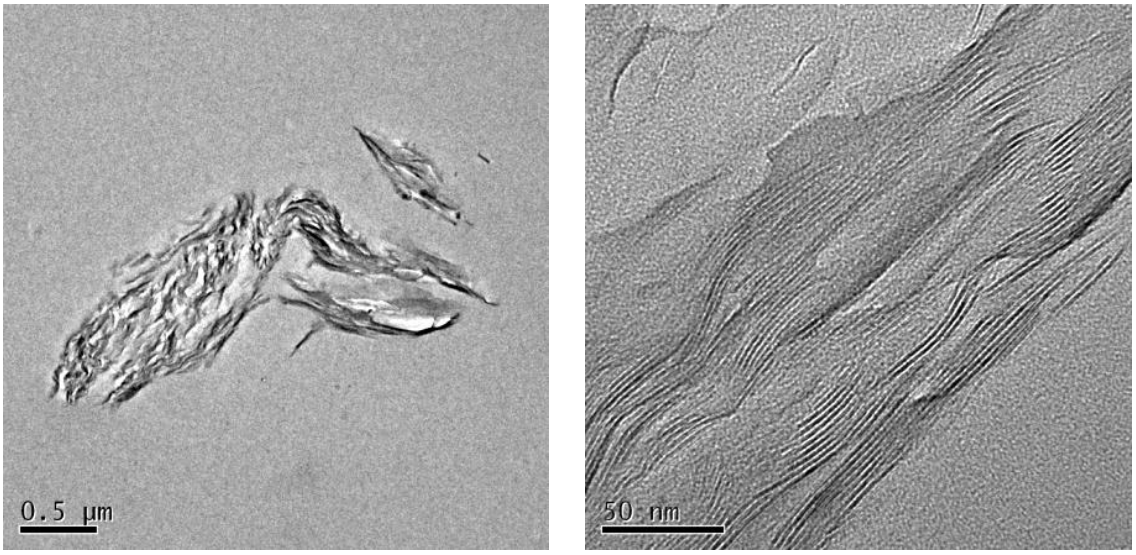

Fig. 2.19 TEM images of epoxy/clay nanocomposites via normal mixing method at different magnifications.

Fig. 2.20 shows TEM images of epoxy/clay nanocomposites via shear mixing method at different magnifications. The TEM micrographs show that clay galleries are less tight agglomeration comparing to normal mixing (upper left and right pictures). The clay interlayer distance is larger than normal mixing especially at the edge area (lower picture). It suggests that shear force affects to clay dispersion and further continuing apply the shear force to intercalated clay particle could be develop to clay exfoliation.

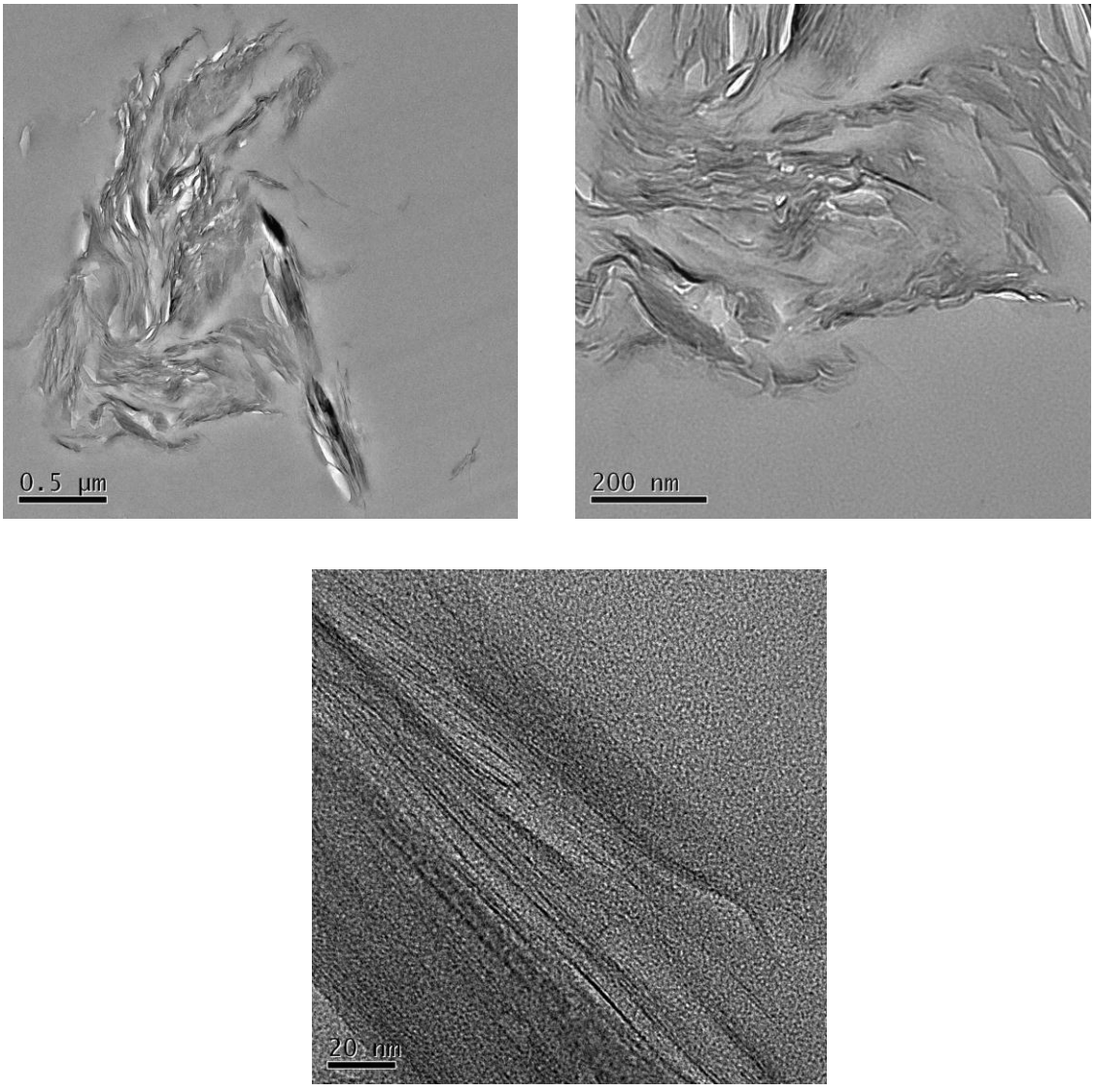

Fig. 2.20 TEM images of epoxy/clay nanocomposites via shear mixing method at different magnifications.

Fig. 2.21 shows TEM images of epoxy/clay nanocomposites via high speed mixing method at different magnifications. All TEM results shows well dispersion of clay layers with noticed large interlayer distance. The d-spacing of clay in the epoxy matrix via the high speed mixing method is larger and shows excellent exfoliation with the clay platelets parallel to each other, comparing to the other methods, because of the high speed homogenizer. The results obviously confirm that high speed mixing method leads to a clay exfoliation and mixing method has an effect on clay dispersion in epoxy resin.

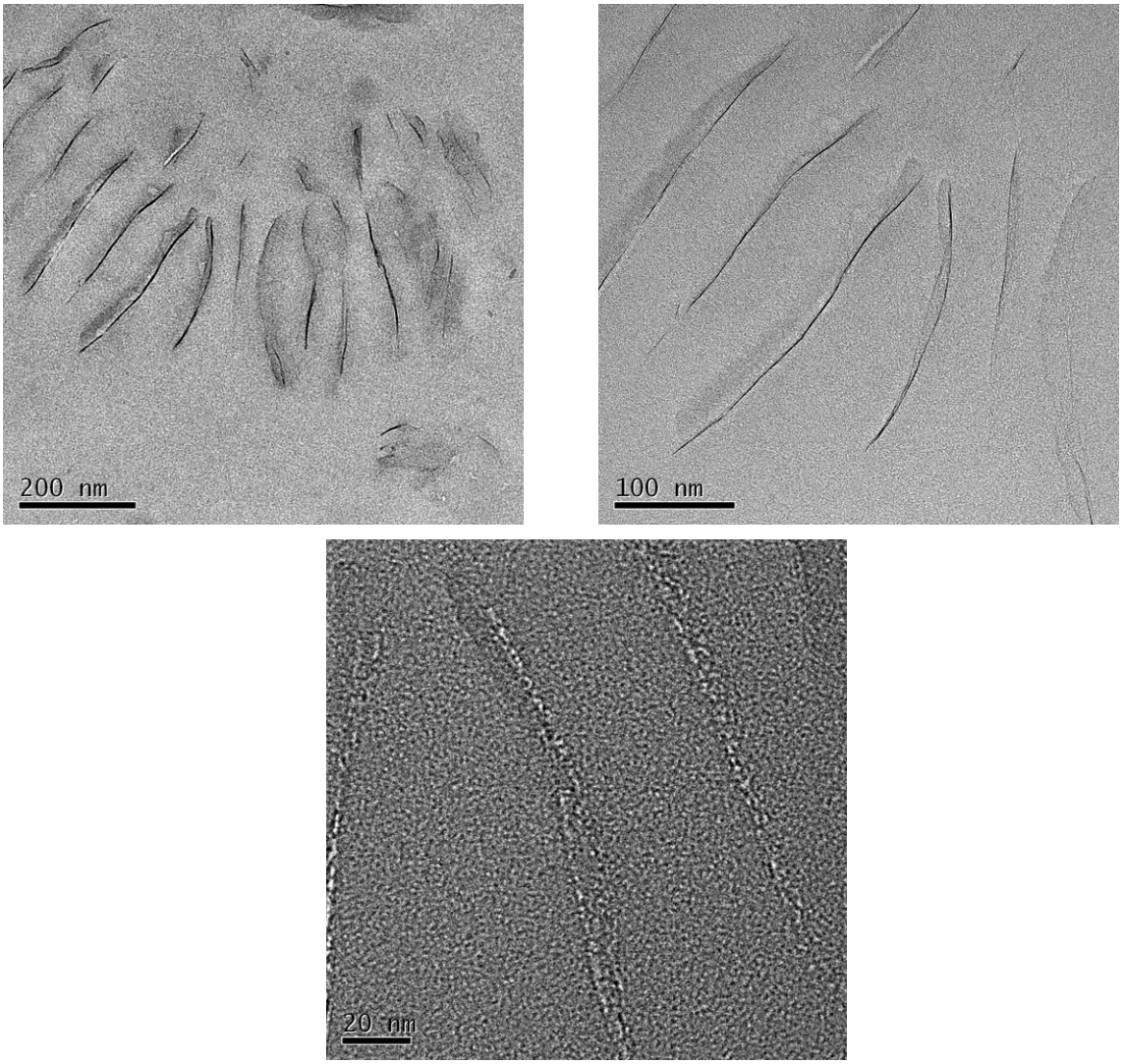

Fig.2.21 TEM images of epoxy/clay nanocomposites via high speed mixing method at different magnifications.

2.4 Effect of mixing parameters

From the result of effect of physical clay dispersion methods, high speed mixing showed good clay dispersion and obtained intercalated/exfoliated organoclay structure in the epoxy matrix. Then, effect of mixing speed and mixing duration were examied.

2.4.1 Mixing speed

The samples were prepared at 1 phr organoclay filler loading under different mixing speeds (hand mixing and 24,000 rpm) for 60 minutes.

X-ray diffraction curves of organoclay and 1 phr organoclay/epoxy nanocomposites at different mixing speeds: hand mixing and 24,000 rpm high mixing for 60 minutes are showed in Fig. 2.22. The d-spacing or interlayer distance corresponding to the gap between clay layers is calculated according to Bragg's law: $n\lambda = 2d\sin\theta$. The pristine organoclay has a single sharp peal at $2\theta = 3.9°$, which corresponds to d-spacing of 22.6 Å. Clear peaks are not detected in the case of the nanocomposites.

Comparison of viscosity of neat resin and 1 phr organoclay/epoxy suspensions at different mixing speeds for 60 minutes is shown in Fig. 2.23. With the presence of the clay, the viscosities of the organoclay/epoxy suspensions are higher than that of neat epoxy. Increasing mixing speed obviously affect the viscosity. The observed increase in the viscosities of suspensions after mixing at high shear rate may imply to improve clay dispersion compared to hand mixing.

Figs. 2.24 and 2.25 show flexural strength and modulus of neat resin and 1 phr

organoclay/epoxy mixtures at different mixing speeds for 60 minutes. Both flexural strength and modulus of nanocomposites are higher than those of the neat resin. Also, flexural strength and modulus of the nanocomposites are improved with increased mixing speed. As discussed above, more homogenous clay dispersion in nanocomposites results to the improvement of mechanical properties due to dispersion of fixing point of organoclay with the matrix.

Figs. 2.26 and 2.27 show TEM micrographs of 1 phr organoclay/epoxy nanocomposite under 60 minute hand mixing and 24,000rpm high speed mixing preparation for 60 minutes at different magnifications. The results show that the d-spacing of clay in the epoxy matrix via the high speed mixing is larger than that of hand mixing. It obviously confirms that mixing speed has an effect on the clay interlayer distance.

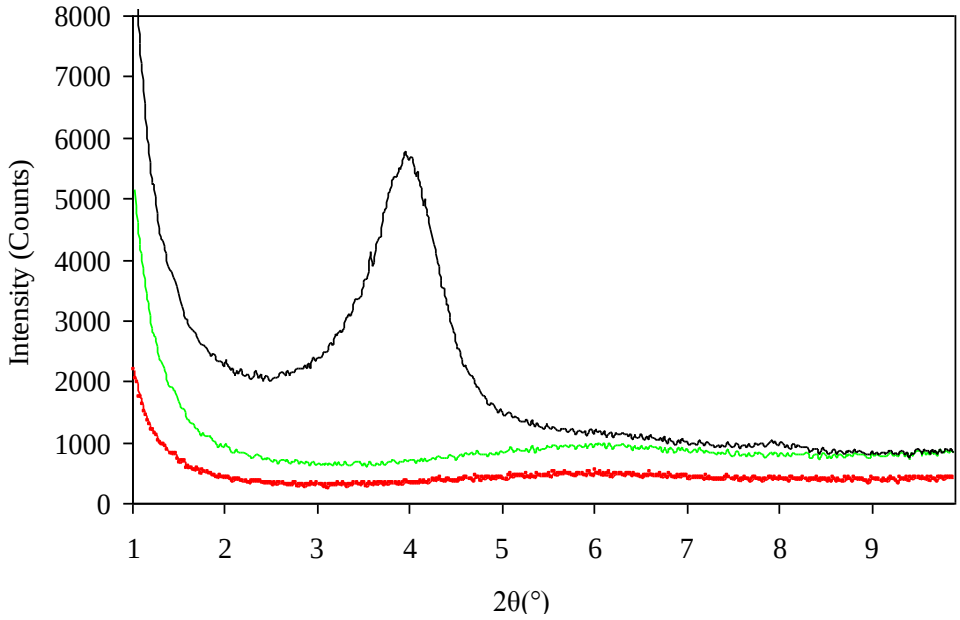

Fig. 2.22 X-ray diffraction curves of organoclay - I.30E (–) and 1 phr organoclay/epoxy nanocomposites at different mixing speeds for 60 minutes: hand mixing (–) and 24,000 rpm high mixing speed (–)

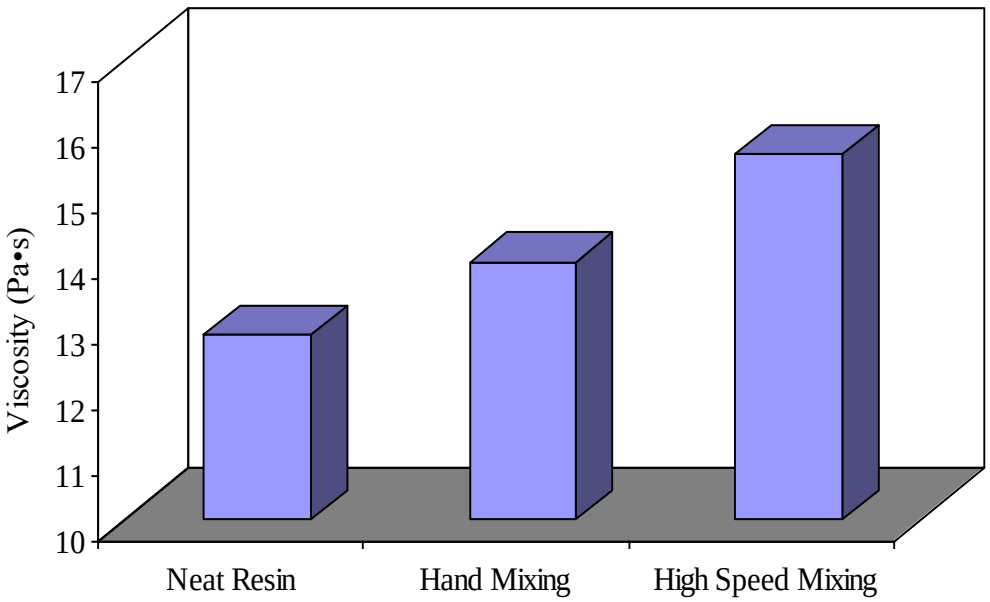

Fig. 2.23 Comparison of viscosity of neat resin and 1 phr organoclay/epoxy suspensions at different mixing speeds for 60 minutes

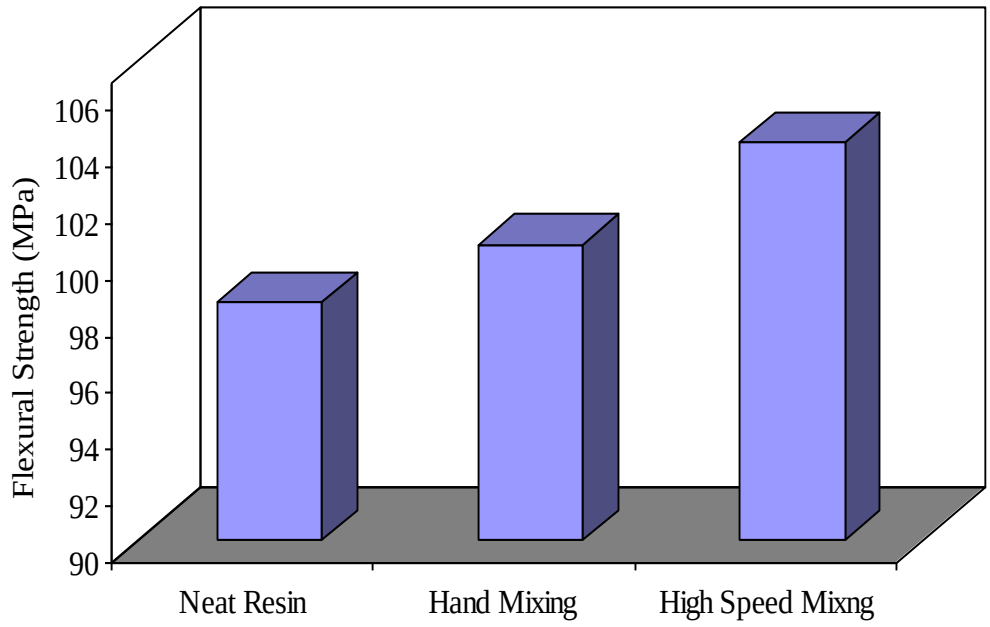

Fig. 2.24 Flexural strength of neat resin and 1 phr organoclay/epoxy mixtures at different mixing speeds for 60 minutes

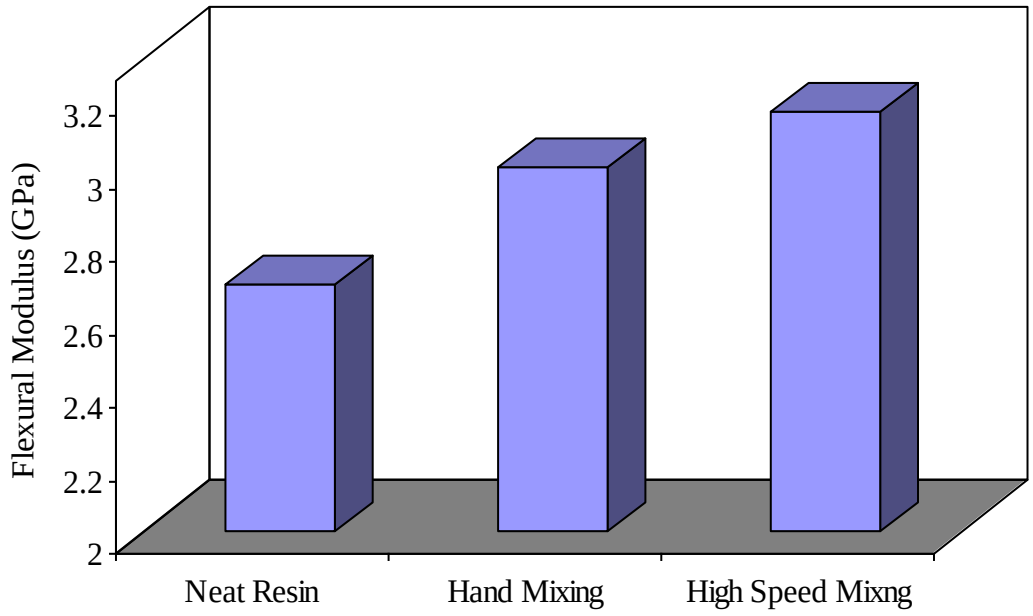

Fig. 2.25 Flexural modulus of neat resin and 1 phr organoclay/epoxy mixtures at different mixing speeds for 60 minutes

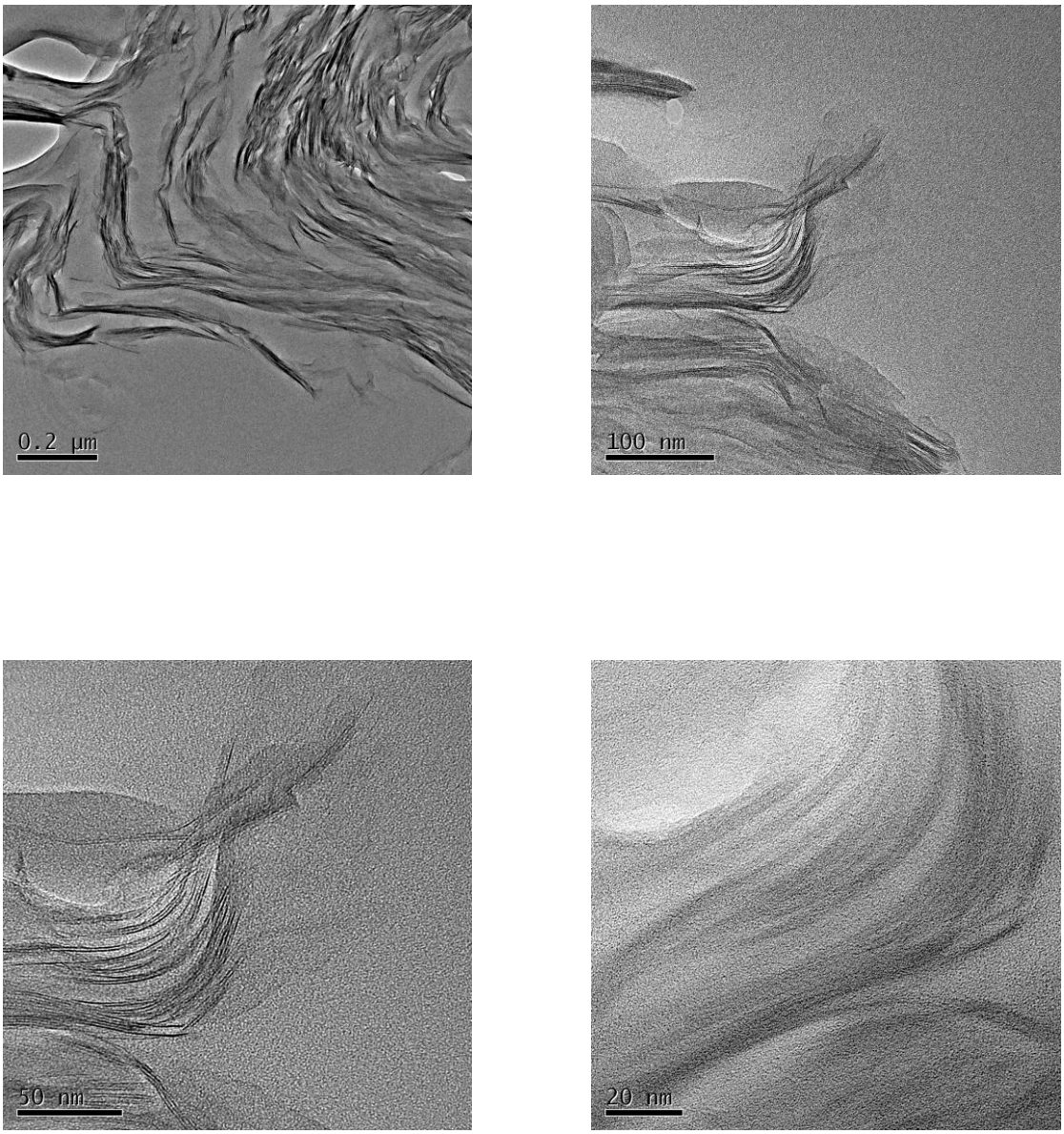

Fig. 2.26 TEM micrographs of 1 phr organoclay/epoxy nanocomposite under 60 minute hand mixing preparation at different magnifications

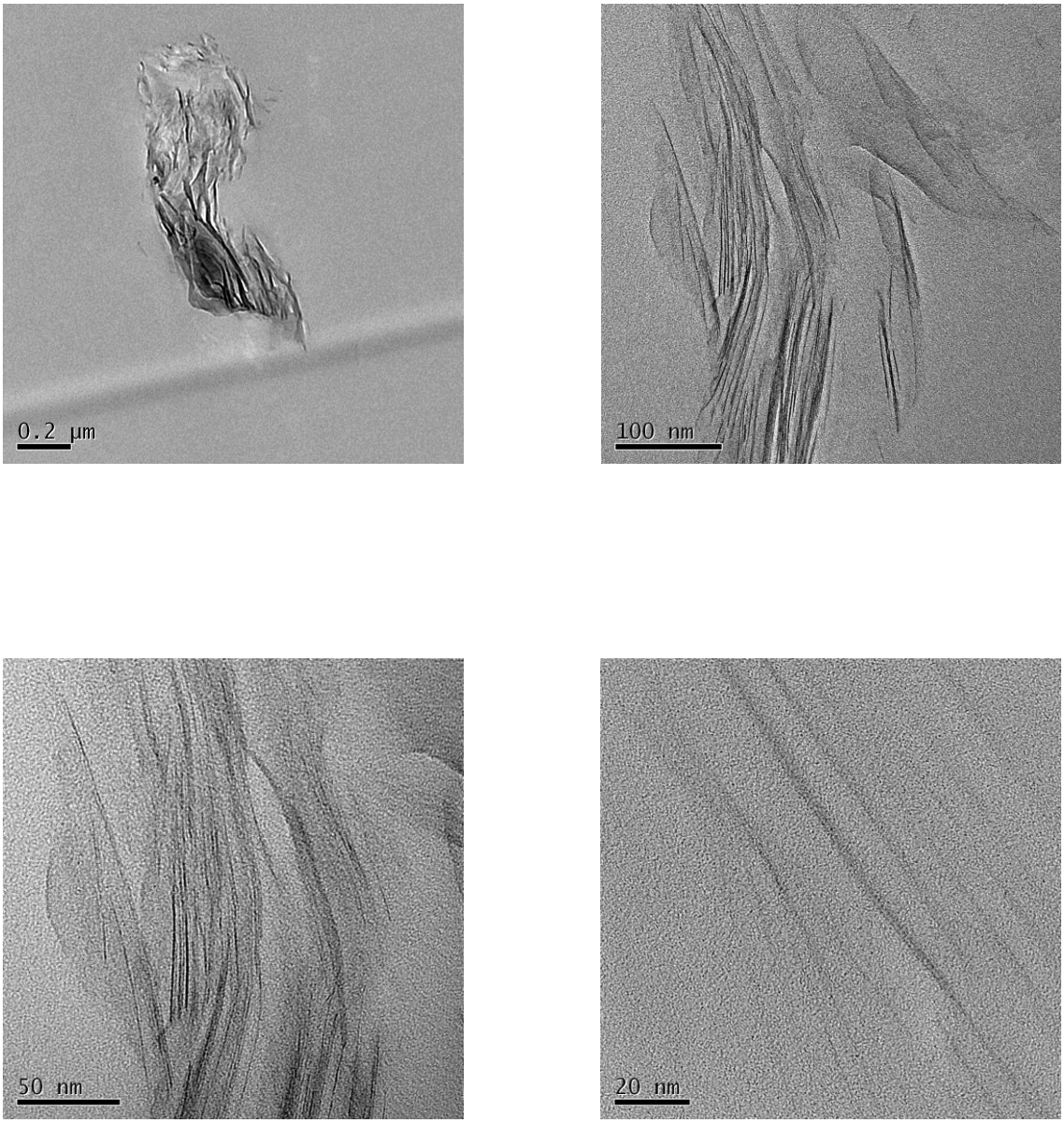

Fig. 2.27 TEM micrographs of 1 phr organoclay/epoxy nanocomposite under 24,000rpm high speed mixing preparation for 60 minutes at different magnifications

2.4.2 Mixing Duration

From 2.4.1, there is an effect of mixing speed, but the organoclay is still not fully exfoliated dispersion in the epoxy matrix. Then, mixing duration was examined. The samples were prepared at 1 phr organoclay filler loading under only 24,000 rpm for different mixing durations.

X-ray diffraction curves of organoclay and 1 phr organoclay/epoxy nanocomposites at 24,000 rpm mixing speeds for different mixing durations are shown in Fig. 2.28. The results show no peak of the nanocomposites under the 24,000 rpm high speed mixing at any mixing duration. It could be implied the structure of clay intercalation/exfoliation is able to achieve even at the short mixing duration – 30 minutes.

The viscosities of the 1phr organoclay/epoxy suspensions after being mixed at 24,000 rpm for different durations are shown in Fig. 2.29. The results indicate that the viscosity of the suspension increases with increasing mixing duration. The increase in viscosity of the suspension may be related to two possible reasons: first, the microscopic transformation of clay structure from the clay galleries to intercalated/exfoliated structure, and second, the finer macroscopic dispersion of the clay galleries in epoxy matrix.

Fig. 2.30 shows the effect of mixing duration on flexural strength of 1 phr organoclay/epoxy nanocomposites under 24,000 rpm mixing speeds. Flexural strength is recommeded at 60 minutes due to the expansion of clay interlayer distance with the appropriate mixing duration.

Effect of mixing duration on flexural modulus of 1 phr organoclay/epoxy nanocomposites at 24,000 rpm mixing speeds is shown in Fig. 2.31. Flexural modulus is unexpectedly decreased with increasing mixing duration. It implies that long-term mixing duration is not good in the enhancement of stiffness due to a lower aspect ratio of organoclay which will be discussed below with the TEM micrographs in details in Chapter 5.

Fig. 2.32 and 2.33 show TEM micrographs of 1 phr organoclay/epoxy nanocomposite under 24,000 rpm high speed mixing for 60 and 240 minutes mixing duration. The results obviously show that the organoclay length of the 60 minutes mixing duration is much longer than the 240 minute mixing duration or on the other words, the aspect ratio (plate width/plate thickness) of organoclay under mixing for 60 minutes is greater than 240 minutes for the reason that the aspect ratio of clay is decreased due to long application of shear force which results to accidental plate breakage. As the results, the high aspect ratio is achieved the increase of the properties i.e. strength and stiffness.

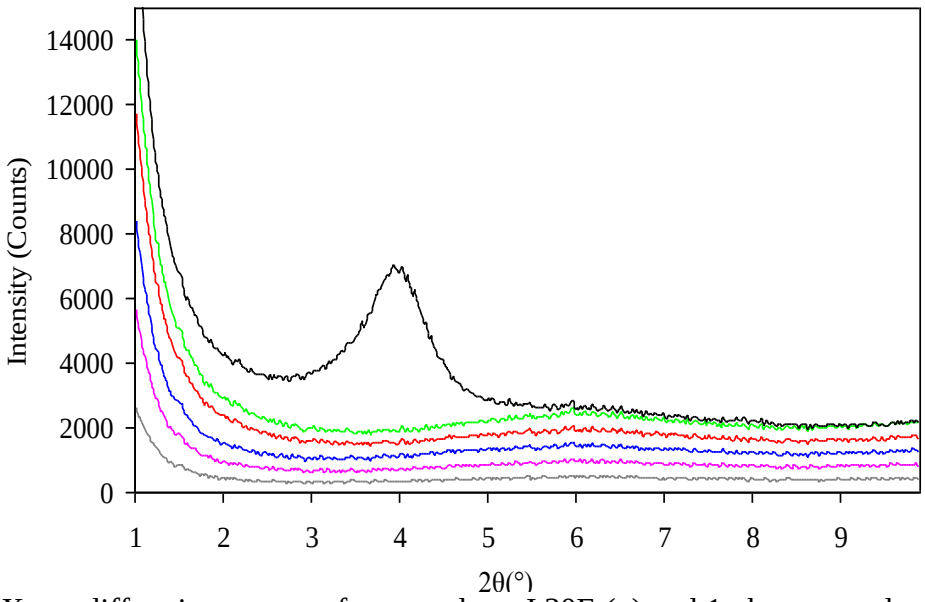

Fig. 2.28 X-ray diffraction curves of organoclay - I.30E (–) and 1 phr organoclay/epoxy nanocomposites under 24,000 rpm mixing speeds at different mixing durations: 30 min (–), 60 min (–), 120 min (–), 180 min (–), and 240 min (–)

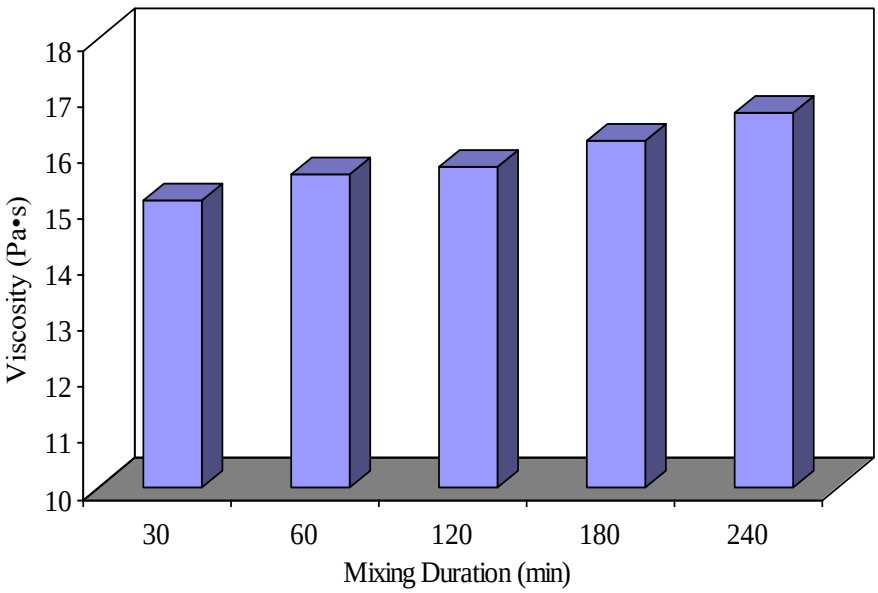

Fig. 2.29 Effect of mixing duration on viscosity of 1 phr organoclay/epoxy suspensions under 24,000 rpm mixing speeds

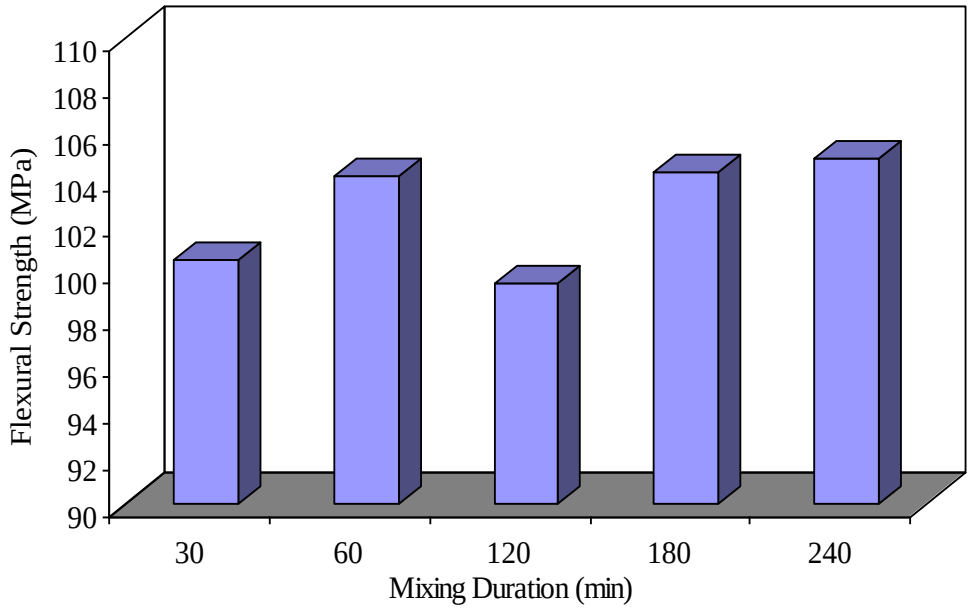

Fig. 2.30 Effect of mixing duration on flexural strength of 1 phr organoclay/epoxy nanocomposites under 24,000 rpm mixing speeds

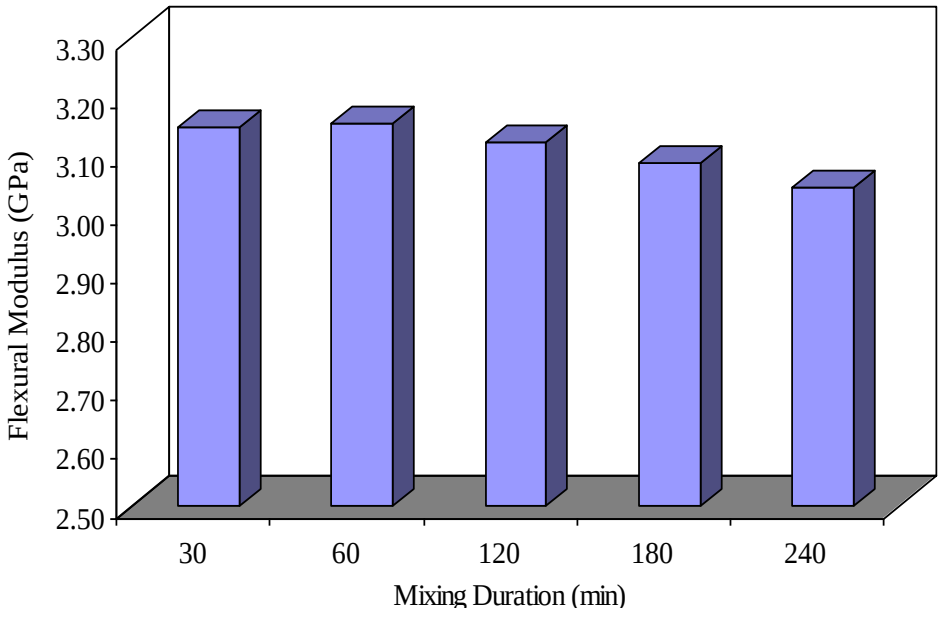

Fig. 2.31 Effect of mixing duration on flexural strength of 1 phr organoclay/epoxy nanocomposites under 24,000 rpm mixing speeds

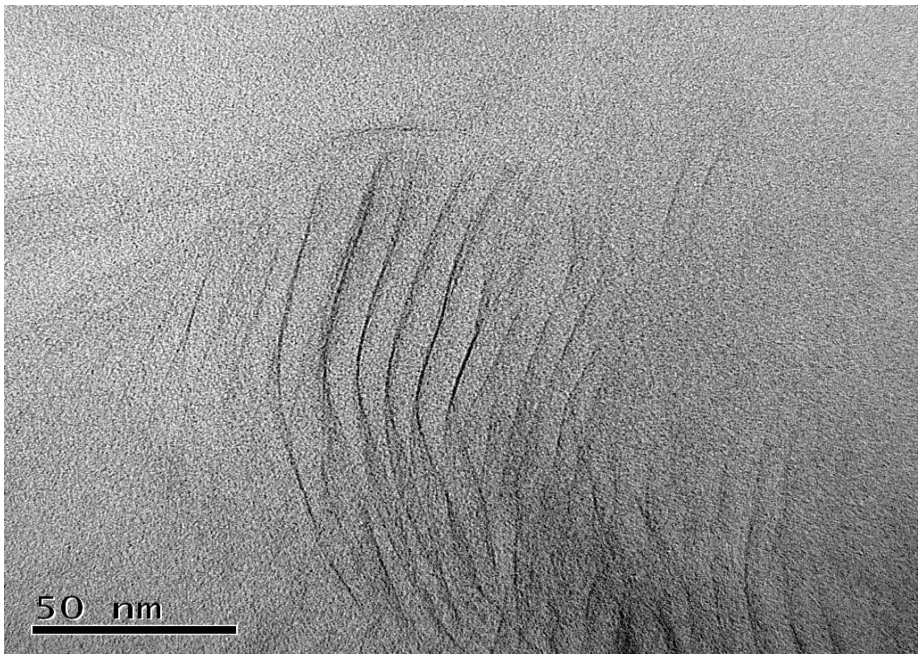

Fig. 2.32 TEM micrographs of 1 phr organoclay/epoxy nanocomposite under 24,000rpm high speed mixing preparation for 60 minutes mixing duration

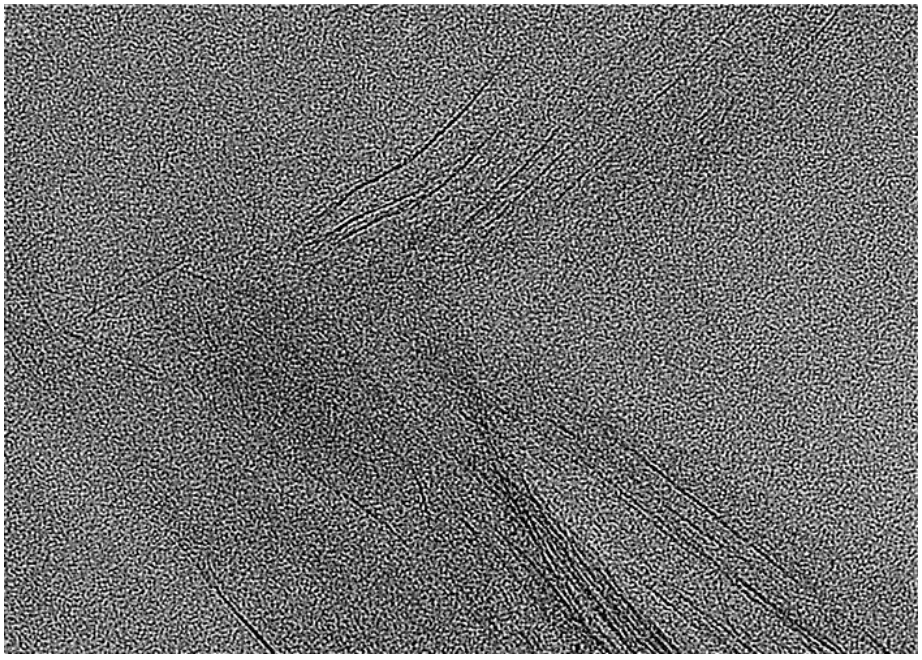

Fig. 2.33 TEM micrographs of 1 phr organoclay/epoxy nanocomposite under 24,000rpm high speed mixing preparation for 240 minutes mixing duration

2.5 Effect of Ultrasonic Application

From to previous results, the organoclay dispersion showed intercalated/exfoliated structure, but not fully exfoliation. Ultrasonic appication is commonly used to disperse particles into liquid substances. In this study, ultrasonic application was selected to apply during mixing process to enhance the clay dispersion. The samples were prepared at 1 phr organoclay/epoxy nanocomposites under 24,000 rpm mixing speeds for 60 minute mixing durations at different conditions: with and without ultrasonic application

X-ray diffraction curves of organoclay and 1 phr organoclay/epoxy nanocomposites under 24,000 rpm mixing speeds for 60 minute mixing duration at different conditions: without ultrasonic application and with ultrasonic application are shown in Fig. 2.34 Again, the results show no peak of the nanocomposites under 24,000 rpm mixing speeds for 60 minute mixing durations either with or without ultrasonic application.

Effect of ultrasonic application on viscosity of 1 phr organoclay/epoxy suspensions under 24,000 rpm mixing speeds for 60 minute mixing duration at different mixing conditions - with and without ultrasonic application are shown in Fig. 2.35. The results show the effect of ultrasonic application is slightly increased the viscosity. It implies that ultrasonic application is assisted the finer dispersion of the clay and enhanced to obtain the intercalated/exfoliated clay structure in the epoxy matrix.

Figs 2.36 and 2.37 show the effect of ultrasonic application on flexural strength, flexural modulus of 1 phr organoclay/epoxy nanocomposites under 24,000 rpm mixing speeds

for 60 minute mixing duration. There results show that the flexural strength of the nanocomposits with ultrasonic application increase about 3 MPa and the flexural modulus increase 80 MPa compared to nanocomposits without ultrasonic application. They confirm that enhancement of properties corresponded well with clay dispersion and the exfoliated clay structure due to added ultrasonic application.

TEM micrographs of 1 phr organoclay/epoxy nanocomposite under 24,000rpm high speed mixing preparation for 60 minute mixing duration without, and with 60 minute ultrasonic application at different magnifications are shown in Fig. 2.38 and Fig. 2.39, respectively. The results noticeably show that the clay galleries of the nanocomposites without the ultrasonic treatment is more tighten compared to with the ultrasonic treatment. The clay dispersion and d-spacing after ultrasonic treatment are higher that before the treatment.

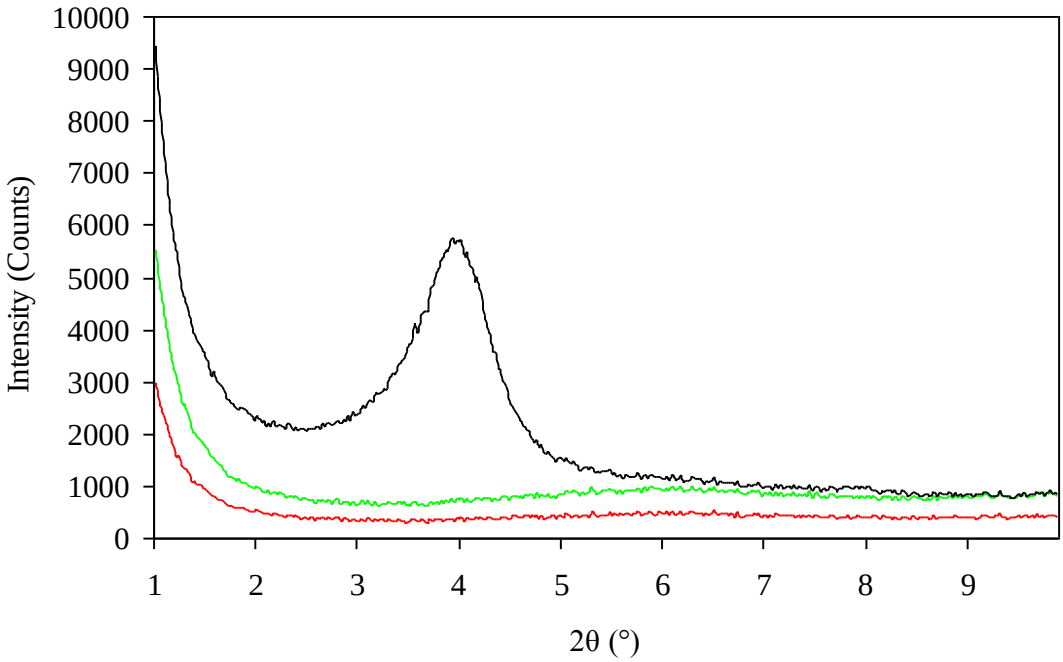

Fig. 2.34 X-ray diffraction curves of organoclay - I.30E (–) and 1 phr organoclay/epoxy nanocomposites under 24,000 rpm mixing speeds for 60 minute at different conditions - without ultrasonic application (–) and with ultrasonic application (–) for 60 minutes

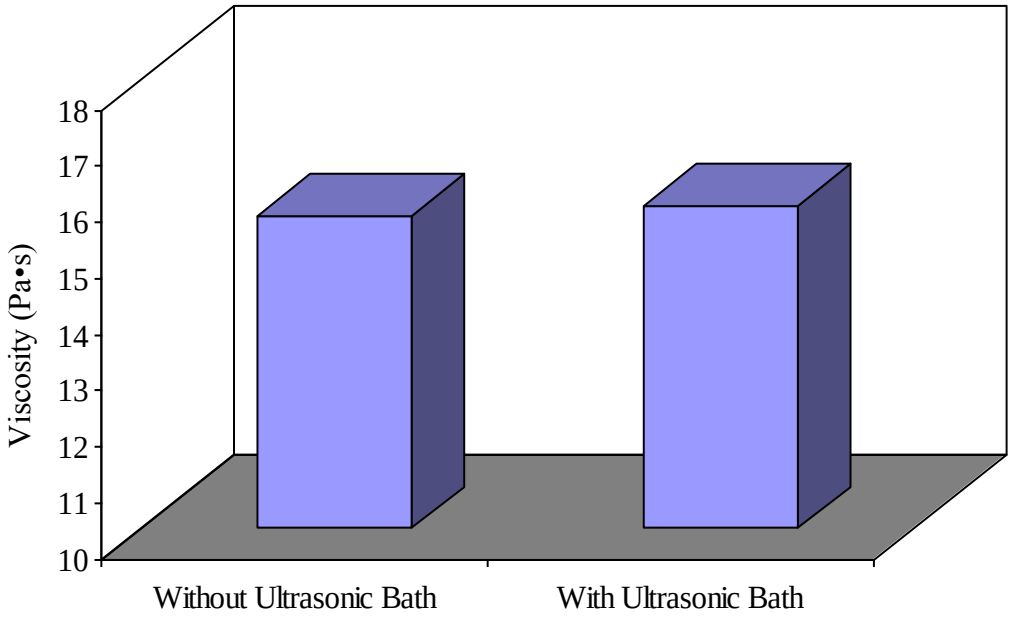

Fig. 2.35 Effect of ultrasonic application on viscosity of 1 phr organoclay/epoxy suspensions under 24,000 rpm mixing speeds for 60 minute at different conditions- without ultrasonic application and with ultrasonic application for 60 minutes

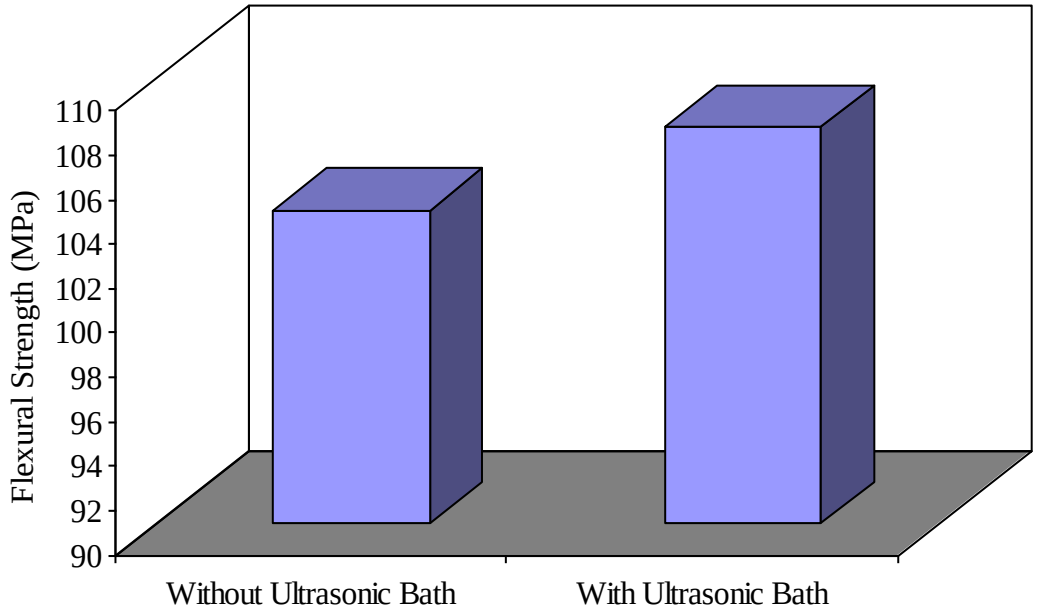

Fig. 2.36 Effect of ultrasonic application on flexural strength of 1 phr organoclay/epoxy nanocomposites under 24,000 rpm mixing speeds for 60 minutes (treatment with ultrasonic application is 60 minutes)

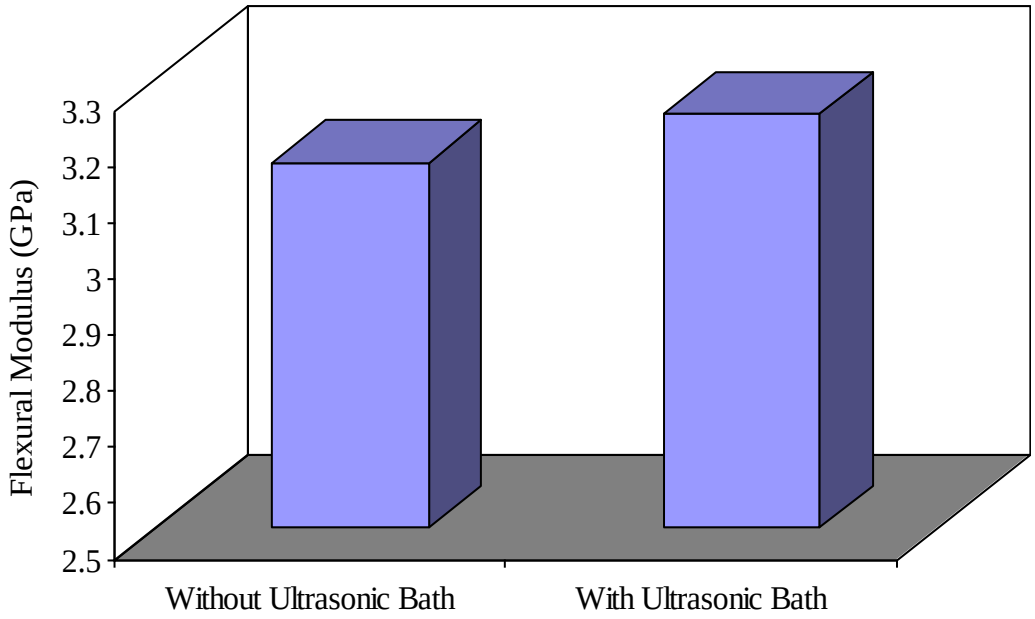

Fig. 2.37 Effect of ultrasonic application on flexural modulus of 1 phr organoclay/epoxy nanocomposites under 24,000 rpm mixing speeds for 60 minutes (treatment with ultrasonic application is 60 minutes)

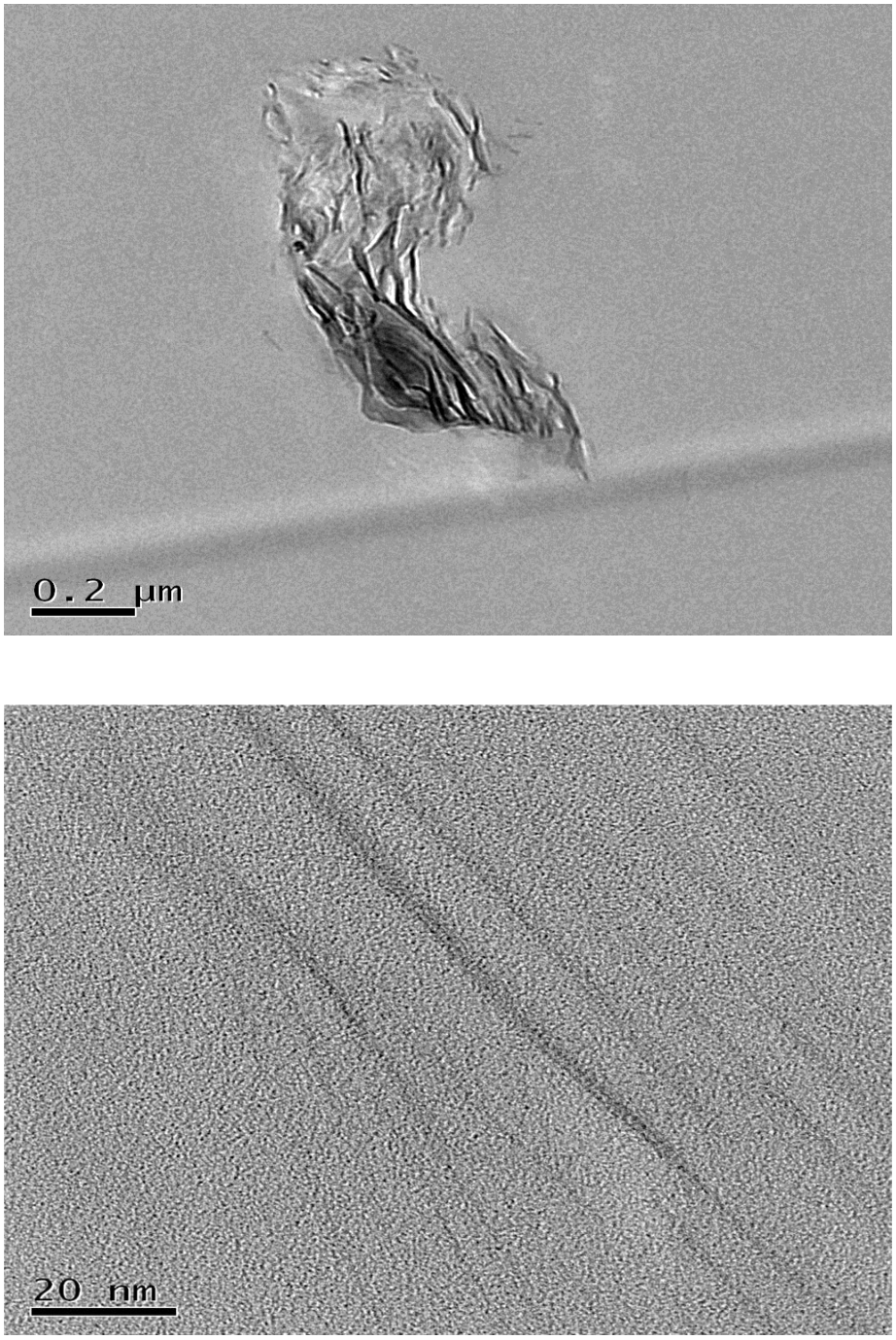

Fig. 2.38 TEM micrographs of 1 phr organoclay/epoxy nanocomposite under 24,000rpm high speed mixing preparation for 60 minute mixing duration without ultrasonic application at different magnifications

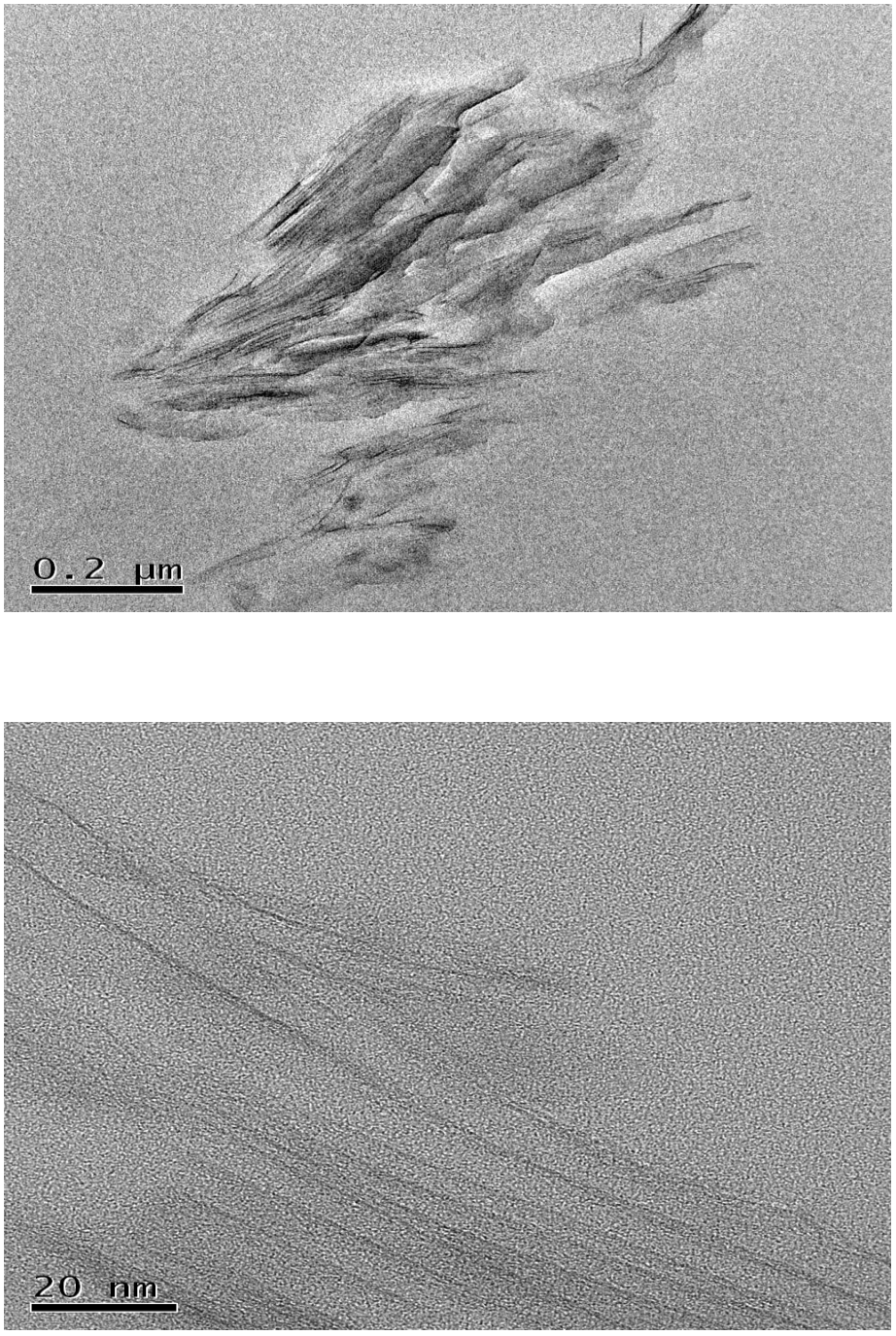

Fig. 2.39 TEM micrographs of 1 phr organoclay/epoxy nanocomposite under 24,000rpm high speed mixing preparation for 60 minute mixing duration with 60 minute ultrasonic application at different magnifications

2.6 Effect of clay loading in epoxy nanocomposites

The samples were prepared via 24,000 rpm mixing speeds for 60 minute mixing durations at different clay loadings from 0.5 phr to 5 phr.

X-ray diffraction curves of organoclay - I.30E and organoclay/epoxy suspensions under 24,000 rpm mixing speeds for 60 minute mixing duration at different clay loadings: 0.5-5 phr are shown in Fig. 2.40. The results show no peak of the nanocomposites under 24,000 rpm mixing speeds for 60 minute mixing durations at all clay loadings from 0.5 phr to 3 phr. As mentioned before, it implies that at any clay loadings, liquid epoxy resin is able to diffuse into the clay galleries, and supplementary to obtain the high degree of clay intercalation/ exfoliation in the epoxy matrix.

Effect of clay loading on viscosity of organoclay/epoxy suspensions under 24,000 rpm mixing speeds for 60 minute mixing duration at different clay loadings are shown in Fig. 2.41. The results show the increasing of clay loading is increased viscosity. The higher the clay loading (higher surface area), the higher shear force requires to apply (the higher viscosity is obtained).

Fig. 2.42 and Fig. 2.43 show effect of clay loading on flexural strength and flexural modulus of organoclay/epoxy nanocomposites under 24,000 rpm mixing speeds for 60 minute mixing duration at different clay loadings. There results show that flexural strength and flexural modulus are increased with increasing clay loading up to 3phr, and than, significantly declined after there. The increase in flexural properties follows the basic rule of mixing; the higher the concentration of filler in the composites, the higher

load the material can support since the applied stress is transferred form the matrix to the more rigid particulates. Also, the increased number of organoclay provides additional reinforcement and restriction to the mobility of polymer chain. On the other hand, the decrease is because of clay agglomeration which is created the initial crack on the materials.

TEM micrographs of 3 phr organoclay/epoxy nanocomposite under 24,000 rpm high speed mixing preparation for 60 minute mixing duration are shown in Fig. 2.44. The results considerably show that there are larger agglomerations on the 3 phr compared to the 1 phr organoclay/epoxy nanocomposite as shown before (Fig. 2.38).

Briefly, the appropriate clay loadings for the organoclay/epoxy nanocpmposites are 3 phr in the case of the flexural property.

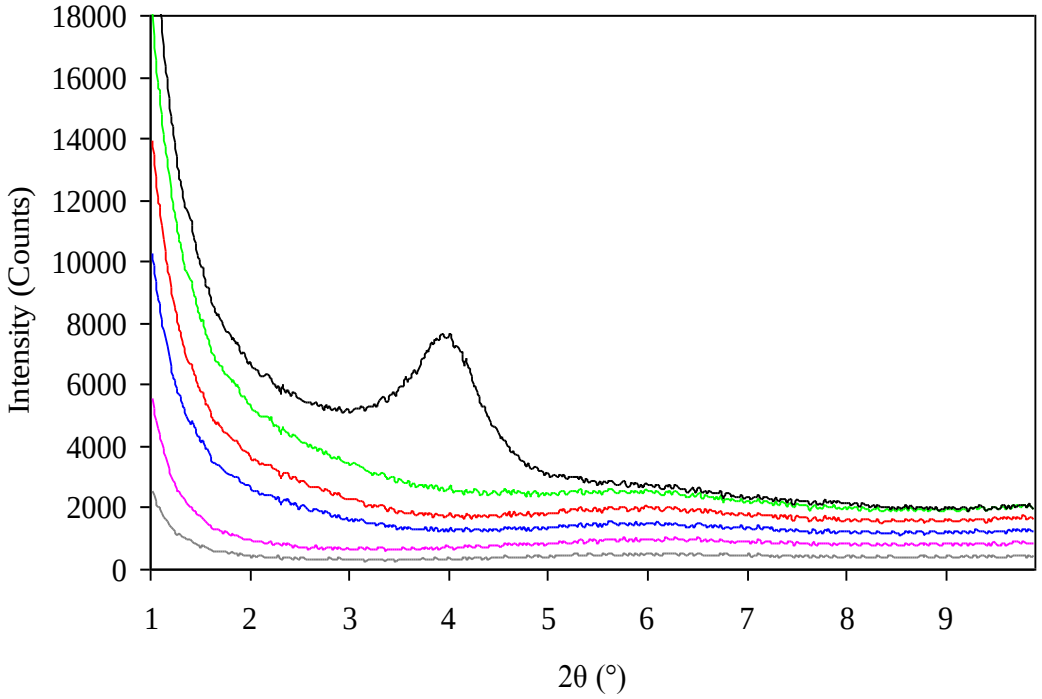

Fig. 2.40 X-ray diffraction curves of organoclay - I.30E (–) and organoclay/epoxy nanocomposites under 24,000 rpm mixing speeds for 60 minutes at different clay loadings: 0.5 phr (–), 1 phr (–), 2 phr (–), 3 phr (–), and 5 phr (–)

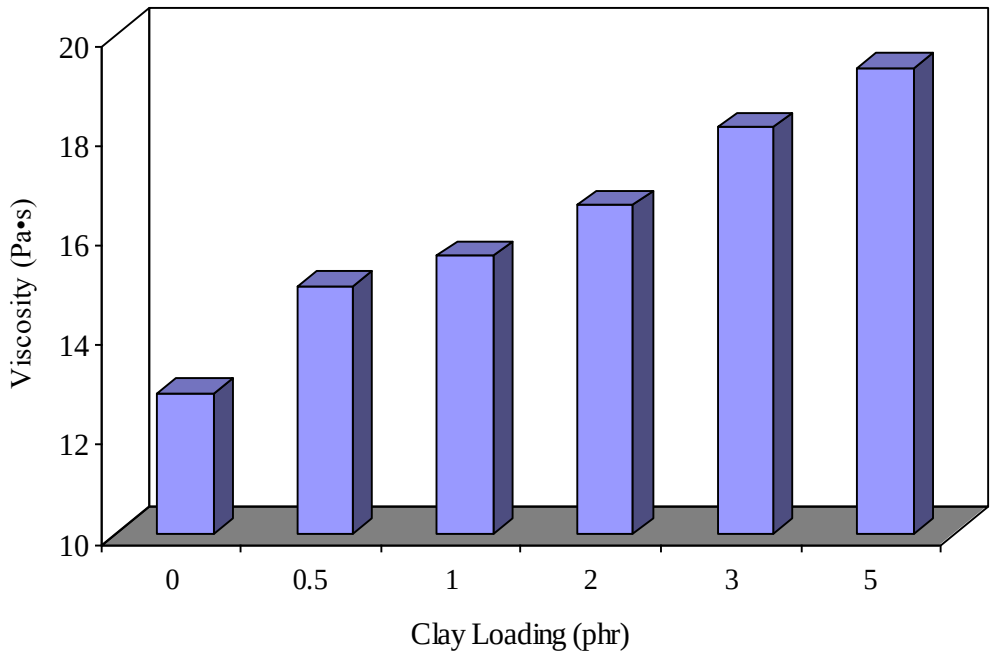

Fig. 2.41 Effect of clay loading on viscosity of organoclay/epoxy suspensions under 24,000 rpm mixing speeds for 60 minutes at different clay loadings

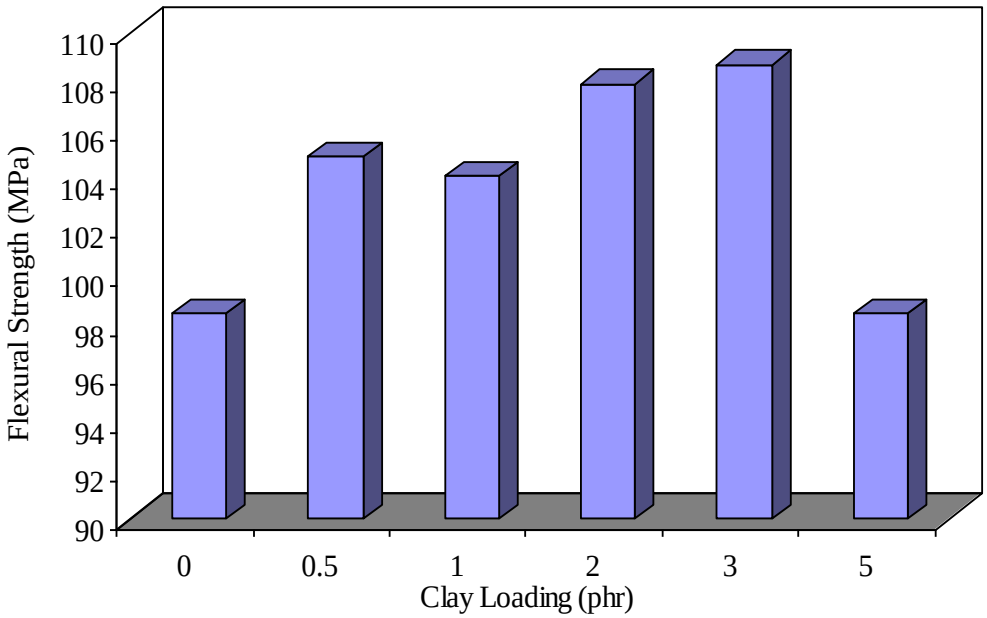

Fig. 2.42 Effect of clay loading on flexural strength of organoclay/epoxy nanocomposites under 24,000 rpm mixing speeds for 60 minutes at different clay loadings

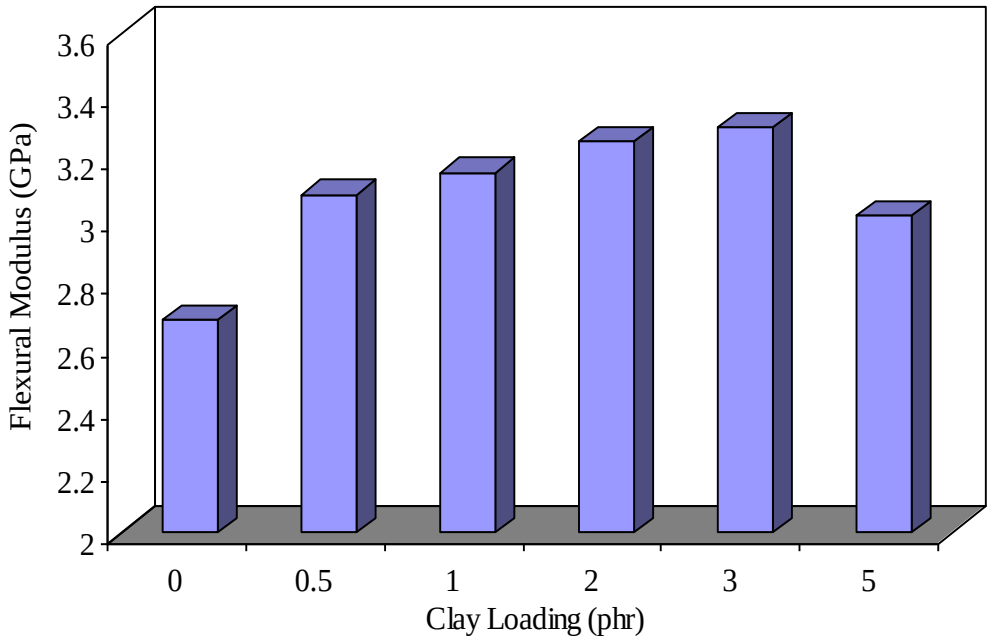

Fig. 2.43 Effect of clay loading on flexural modulus of organoclay/epoxy nanocomposites under 24,000 rpm mixing speeds for 60 minutes at different clay loadings

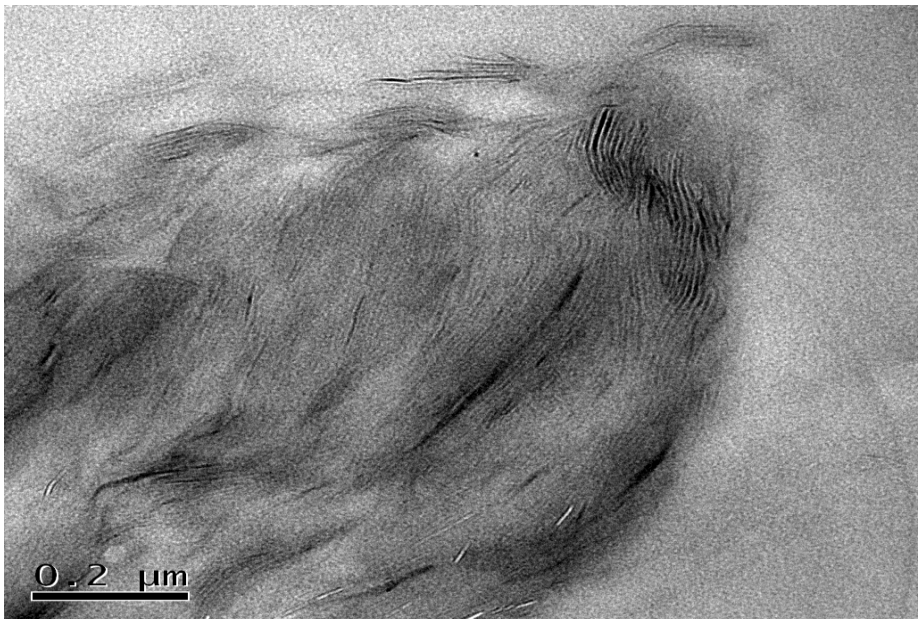

Fig. 2.44 TEM micrographs of 3 phr organoclay/epoxy nanocomposite under 24,000rpm high speed mixing preparation for 60 minutes

2.4 Conclusion

Mixing method of epoxy nanocomposites plays an important role in clay dispersion in epoxy resin and is a main key parameter of epoxy/organoclay nanocomposites on improvement of properties. In order to obtain knowledge of anti-corrosion performance of epoxy nanocomposites, three sample composites were prepared by different three mixing method. Corrosion behavior was investigated under immersion test, and evaluated by penetration depth and penetration profile. All samples have almost similar penetration rate. On the other hand, high speed mixing sample and neat epoxy resin reached equilibrium at similar time and earlier compared to normal mixing and shear mixing samples. Epoxy/organoclay nanocomposite preparation under high speed mixing method which creates exfoliated clay dispersion in the epoxy matrix performs better

corrosion resistant compared to normal and shear mixing methods regarding to weight gain and penetration depth.

The effects of mixing parameters, ultrasonic application and clay loading on the dispersion, intercalation/exfoliation of clay and mechanical properties of nanocomposites have been studied. Mixing speed is one of the key factors in order to achieve exfoliated epoxy/organoclay nanoncomposites due to high shear force. The optimum mixing duration is about 60 minutes. The increase in properties from mixing duration is attributed to good clay dispersion and large clay interlayer distance. Ultrasonic treatment is applied to induce well dispersion of clay, slightly large interlayer distance. The optimum clay loadings for epoxy/organoclay nanocomposites are at 3 phr for flexural strength and stiffness.

Chapter 3

Chemical nanoclay dispersion using chemical exfoliators

3.1 Introduction

The improvement of various properties has been reported about the epoxy/clay nanocomposites by ammonium modified clay in many reports [56-59]. Kornmann, *et al*.[60-61] prepared the epoxy resins filled with various amine modifiers and showed the morphologies and thermal, mechanical properties influenced with the addition of amine modifiers on the organoclays. They reported the enhancements of flexural modulus and fracture properties on nanocomposites

In the case of MMT, this is commonly achieved by treating it with large organic surfactants, usually ammonium ions. In their natural state, the MMT layers have a net negative charge and are held together by electrostatic forces between the sheets and interlaying inorganic cations. These ions are effectively exchanged with the ammonium ions which penetrate the clay gallery and increase the distance between the sheets. The clay gets more or less hydrophobic depending on the exact structure of the ammonium ion tails.

To a great extent the outcome relies on the processing technique used. PLSNs can be made either by adding the filler in the polymerization step, in a solution or straight into a polymer melt. The latter is very attractive due to its simplicity; existing machinery and procedures can be used. The result is, however, strongly affected by parameters such as

shear forces, processing time, temperature, etc. as shown in several studies [62-63]. The impact of these parameters also depends on the polymer matrix used.

Many attempts have been made so far to use epoxy as the matrix, however, only few have fully successed. Clay dispersion methods and corrosion behavior of epoxy/organoclay nanocomposites in our previous study in Chapter 2 showed that high speed mixing plays an important role on clay dispersion. Epoxy/organoclay nanocomposite via high speed mixing method performed better corrosion resistant compared to propeller and three-roll calendar mixing method, however, still have a challenge on homogeneous clay dispersion in the epoxy matrix.

The pre-mixing substances are designed to various functional groups (epoxy and amine functional groups which are compatibility with epoxy resins and ability for the curing accelerator) and different size of molecular chain, which could be adaptable to interlayer spaces, and to investigate mechanical property and diffusion behavior of epoxy/organoclay nanocomposites. The aim of this study is to acquire fully exfoliated organoclay into epoxy matrix using pre-mixing substances as well as to investigate mechanical property and diffusion behavior of epoxy/organoclay nanocomposites.

3.2 Experimental Method

3.2.1 Materials

Commercially available diglycidyl ether of bisphenol A type epoxy (DGEBA), Epomik R140 was purchased from Mitsui Chemical Co., Ltd. used as matrix, which had an epoxide equivalent weight of 188 g/equiv. Diamine curing agent, Jeffamine D230 produced from Huntsman Corporation was used as curing agent. Figure 3.1 shows the structures of the materials used in this study. Montmorillonite-based organoclay (Nanomer I.30E) from Nanocor Inc., was used in this study to produce the nanocomposites. Nanomer I.30E nanoclays are surface compatabilized montmorillonites. In addition to traditional inner gallery cation exchange modification, Nanomer I.30E uses n-octadecyl ammonium as treatment agent as shown in Fig. 3.2 and surface modifier concentration is 28-32 mass%.

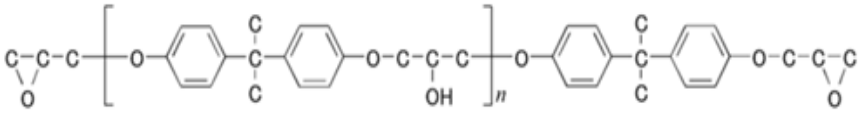

n = 0.15

DGEBA

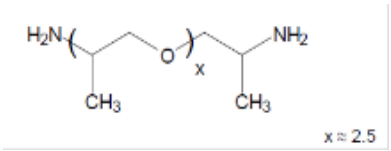

D230

Fig. 3.1 Chemical structures of materials used in this study.

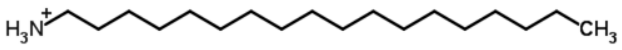

Fig. 3.2 Chemical structures of n-octadecyl ammonium

Pre-mixing substances employed in this study were selected two functional groups with two variants. First pre-mixing substance is epoxy reactive diluents (EPICLON 703, EPICLON 720 and EPICLON 705 produced from Huntsman Corporation) which are different sizes of molecular structures, and the other pre- mixing substance is diamine curing agents (D400 and D2000 produced from Huntsman Corporation, short and long molecular structure, respectively). The structures and properties of the pre-mixing substances used in this study are shown in Table 3.1.

Table 3.1 Structures of pre-mixing substances.

Pre-mixing substance	Commercial name	Epoxide or Amine hydrogen equivalent weight (g/eq.)	Chemical structure
E1	EPICLON 703	284	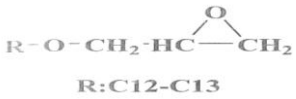
E2	EPICLON 720	154	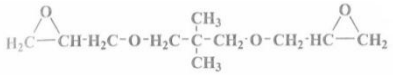
E3	EPICLON 705	203	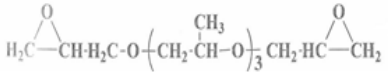
D1	D400	100	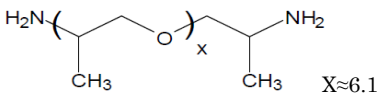
D2	D2000	520	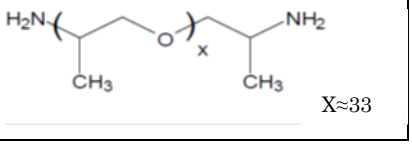

3.2.2 Method

Initially, to prepare organoclay/pre-mixing substance, pre-mixing substances were mixed with 10 mass% organoclay via high speed homogenizer (Ultra-TURRAX T18, IKA.) for 15 minutes, following by 15 minutes ultrasonic bath, and repeating both processes for 4 times. After that, the 10 mass% mixtures were mixed with epoxy via high speed mixing homogenizer at 24,000 rpm for 10 minutes. After mixing according to the above conditions, the mixtures were degassed under vacuum for 10minutes. Thereafter, cooling down to room temperature, and then, epoxy resin and curing agent were added according to stoichiometric ratio to the mixtures stirred with degassing again for 10 minutes before casting. Finally, the pre-mixed organoclay and epoxy with diamine curing agent was cured at 80°C in oven for six hours and followed by post curing at 120°C in the oven for 12 hours.

3.2.3 Characterization

3.2.3.1 Clay Dispersion

3.2.3.1.1 Viscosity

To evaluate clay dispersion, viscosities of organoclay/pre-mixing substance suspensions after mixing process were measured at 25°C on Anton Paar – Physica MCR 100 viscometer using cone and plate geometry.

3. 2.3.1.2 D – spacing

D-spacing of organoclay was measured using a Philips MRD X'Pert with a rotation anode and CuKα radiation (Å). The scanning range was from 1.05° to 9.95°. The step size was 0.02° and the step time was 3 sec for the measurement of the d-spacing. The d-spacing of different mixing conditions were investigated. For the analysis of the clay

powder, particles were mounted on a sample holder with a large cavity and a smooth surface was obtained by passing the particles with a glass plate. Analysis of organoclay swollen in the epoxy resin with the curing agent was performed by placing the sample composites on the sample holder. The nanocomposite plates produced during the molding process had a fairly smooth surface which has been directly analyzed. The d-spacing was calculated according to Bragg's equation regarding to Chapter 2.

3.2.3.2 Mechanical property

Flexural property was evaluated by three-point bending test using a bending machine according to ASTM D790. To study corrosion behavior of the nanocomposites, immersion test at 60°C under 10 mass% of sulfuric acid was selected to determine diffusivity and equilibrium mass change.

3.2.3.3 Immersion test

The immersion test specimens of 60×25×2 mm^3 for measurement of initial mass were dried at 50°C in oven for more than 75 hours. All specimens holding with a Teflon tube, in order to avoid sample overlapping, were tested in beaker containing 10% of sulfuric acid solution separately. The beakers were sealed with plastic film to avoid evaporation of the solution. The samples were performed in water bath controlled at 60°C according to the previous study [18]. Specimens were removed at regular time, washed by water and then carefully wiped to remove excess of acid on the specimens. The mass change was determined by obtaining the change in mass of specimen, relative to the initial mass and is calculated according to Eq. 2.1.

3.2.3.4 Morphology

The nanoclay composite structure and clay distribution were examined using Transmission Electron Microscopy (TEM). TEM images were obtained by a JEOL 2010F equipped with a field-emission gun operating at 200kV. TEM samples were prepared by ultramicrotome to be thin sections of the polymer nanocomposite with a diamond knife. These thin sections were then captured on coated Cu grids. The samples were tested at different magnifications from 2 μm to 200 nm scale bar.

3.3 Clay Dispersion

To evaluated clay dispersion in the substances, viscosity and XRD were selected to exam.

3.3.1 Viscosity

Viscosity was selected as one parameter in this study to detect degree of clay exfoliation in clay/pre-mixing substance suspension. Table 3.2 and Fig. 3.3 show viscosity and % change of neat pre-mixing substance and pre-mixing substance with 10 mass% organoclay after mixing with high speed homogenizer base on neat pre-mixing substances. As shown in Fig.6, pre-mixing substances significantly affected to increase viscosity. For epoxy functional group, small epoxy reactive diluent (E1) remarkably increase viscosity more than 7,400% after pre-mixing compared to neat E1 pre-mixing substances. For amine functional group, on the other hand, long molecular chain of diamine curing agents (D2) markedly increases viscosity after pre-mixing process. The

result of viscosity can imply that pre-mixing substance is necessary in mixing process to obtain fully exfoliation PLSNs.

Table 3.2 Viscosities of samples

Sample	**Viscosity [Pa・s]**	**% Change of viscosity base on neat sample**	**% Change of viscosity base on sample before mixing**
Neat resin	12.82		
resin+clay (before mixing)	19.93	55.41	
resin+clay (after mixing)	22.36	74.40	12.22
E1	0.01		
E1+clay (before mixing)	0.03	222.02	
E1+clay (after mixing)	0.61	7305.32	2199.61
E2	0.03		
E2+clay (before mixing)	0.07	106.07	
E2+clay (after mixing)	0.24	590.75	235.20
E3	0.02		
E3+clay (before mixing)	0.05	116.42	
E3+clay (after mixing)	0.20	748.99	292.28
D1	0.05		
D1+clay (before mixing)	0.11	135.33	
D1+clay (after mixing)	0.07	47.90	-37.16
D2	0.39		
D2+clay (before mixing)	0.80	103.78	
D2+clay (after mixing)	4.38	1010.69	445.04

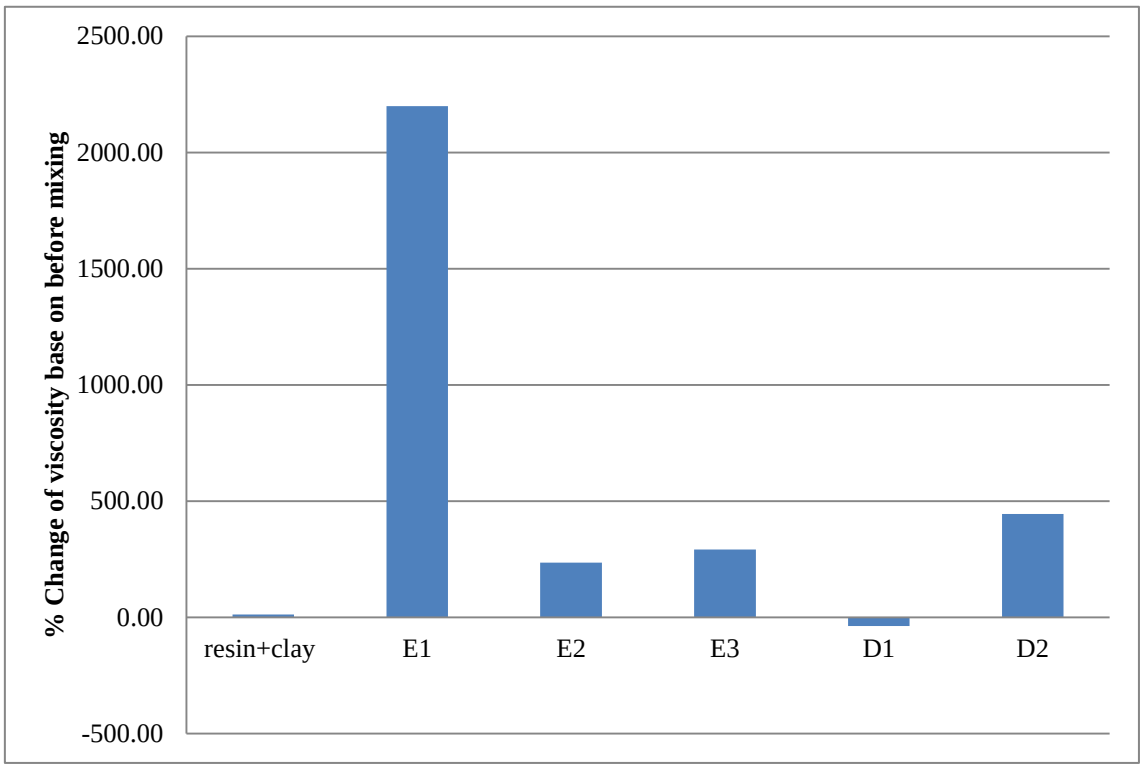

Fig. 3.3 % of change of viscosity of different pre-mixing substances with 10 mass% organoclay after mixing

3.3.2 D – spacing

Fig. 3.4 shows XRD patterns of organoclay and epoxy/organoclay nanocomposites with various pre-mixing substances. The d-spacing or interlayer distance corresponding to the gap between clay layers is calculated according to Bragg's law. The pristine organoclay has a single sharp peak at $2\theta = 3.9°$, which corresponds to d-spacing of 22.6 Å. For epoxy/organoclay nanocomposites with pre-mixing substances, clear peaks are not detected. It implies that organoclay mixing appropriate pre-mixing substances archive fully exfoliated clay structure in epoxy/clay nanocomposites.

More details on XRD result of epoxy/organoclay nanocomposites with different pre-mixing substances, XRD patterns of E1 and D2 pre-mixing substances observed shifts of diffraction peaks to not only smaller angles (It means stretches of distances between the silicate layers of the organoclays), but also flatter in comparison with E2 and D1 pre-mixing substances, respectively. The XRD result was confirmed that firstly pre-mixing substances help to obtain high degree of clay exfoliation in epoxy matrix, and secondly both XRD and viscosity proved that small molecular structure of epoxy reactive diluent and long molecular structure of diamine curing agent would obtain higher clay exfoliation on epoxy matrix compared to long molecular structure of epoxy reactive diluent and short molecular structure of diamine curing agent, respectively (These “long” and “short” are under comparison of compounds selected in this study).

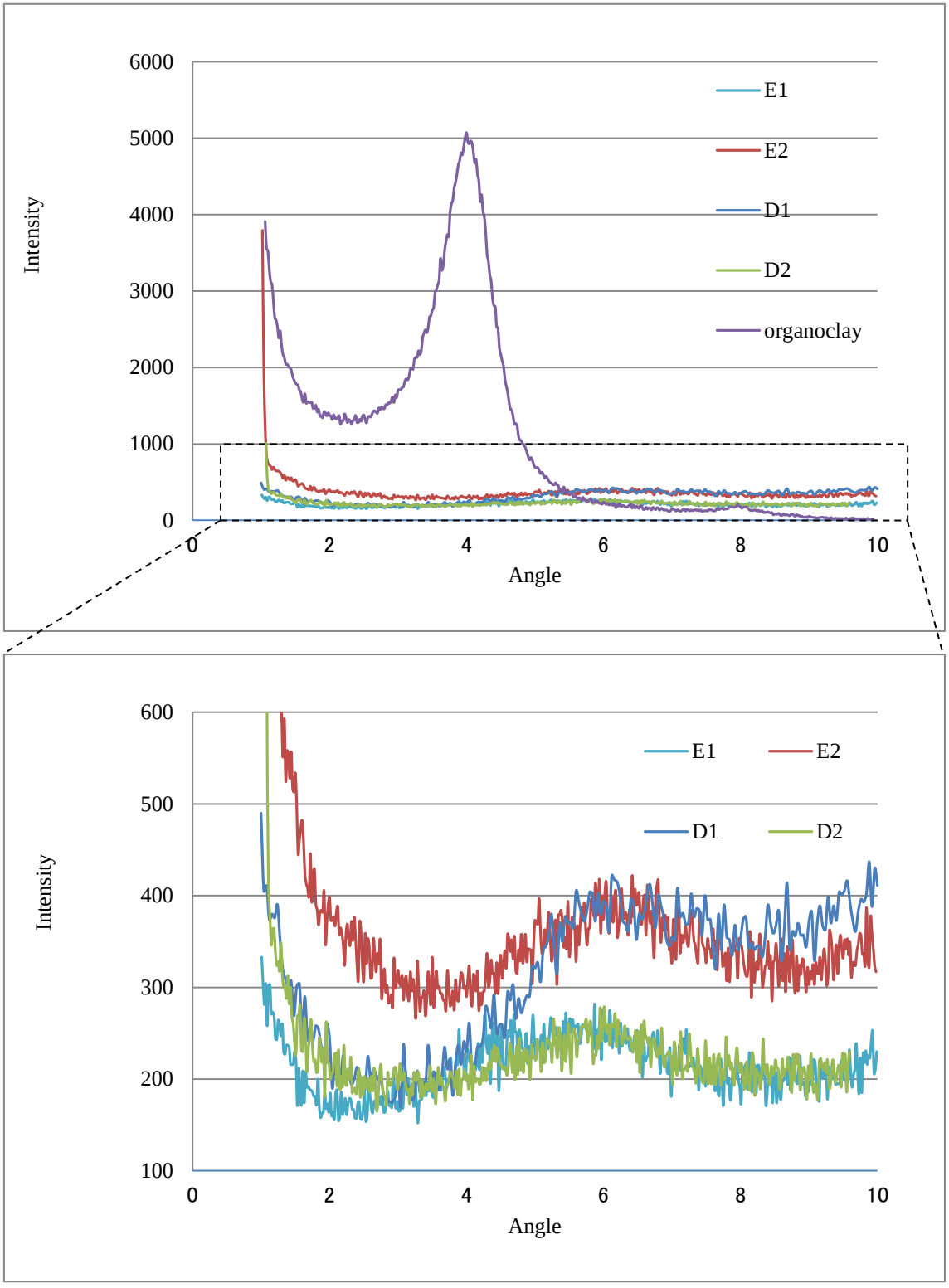

Fig. 3.4 XRD patterns of organocaly and epoxy/organoclay nanocomposites with various pre-mixing substances

3.4 Mechanical property

Fig. 3.5 shows effect of pre-mixing substances on flexural strength of epoxy/organoclay nanocomposites. Flexural strength of epoxy/organoclay nanocomposites with epoxy pre-mixing substances was slightly increased. It implies a possibility of which clay exfoliated structure in epoxy matrix would enhance to increase flexural strength. However, flexural strength of epoxy/ organoclay nanocomposites with diamine pre-mixing substances was decreased.

Fig. 3.6 shows effect of pre-mixing substances on flexural modulus of epoxy/organoclay nanocomposites. Flexural modulus of epoxy/organoclay nanocomposites with diamine pre-mixing substances was obviously increased. Flexural modulus of nanocoposites with E1, D1, D2 increases 13%, 88%, 67% compared to neat resin, respectively. It would be due to additional pre-mixing process which obtained exfoliated clay structure in the epoxy matrix. It implies that clay exfoliated structure would increase flexural modulus.

Especially, flexural diamine pre-mixing substance significantly increases in comparison with epoxy pre-mixing substance. It would be because of not only improvement in clay exfoliation effect, but also long alkyl group exchange effect which stiffs molecular chain mobility compared to short alkyl group of modified. As a result, the improvement of flexural modulus of epoxy/organoclay nanocomposites is recommended to have organoclay pre-mixing process with diamine pre-mixing substance before mixng with epoxy resin and curing agent.

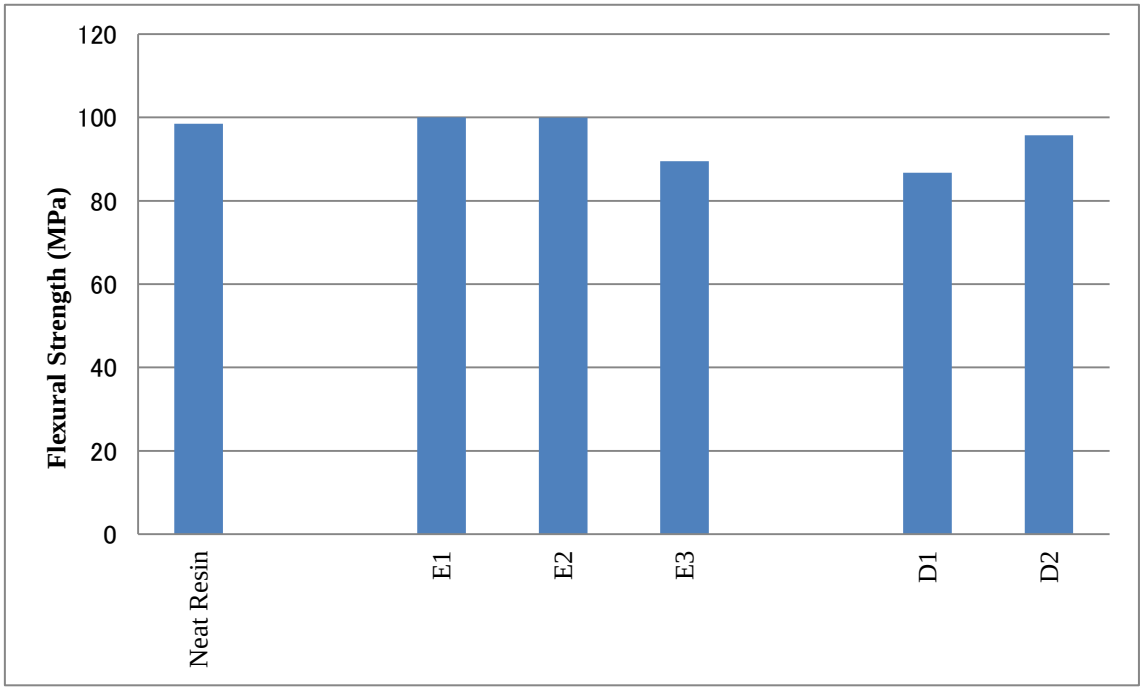

Fig. 3.5 Effect of pre-mixing substances on flexural strength of epoxy/organoclay nanocomposites.

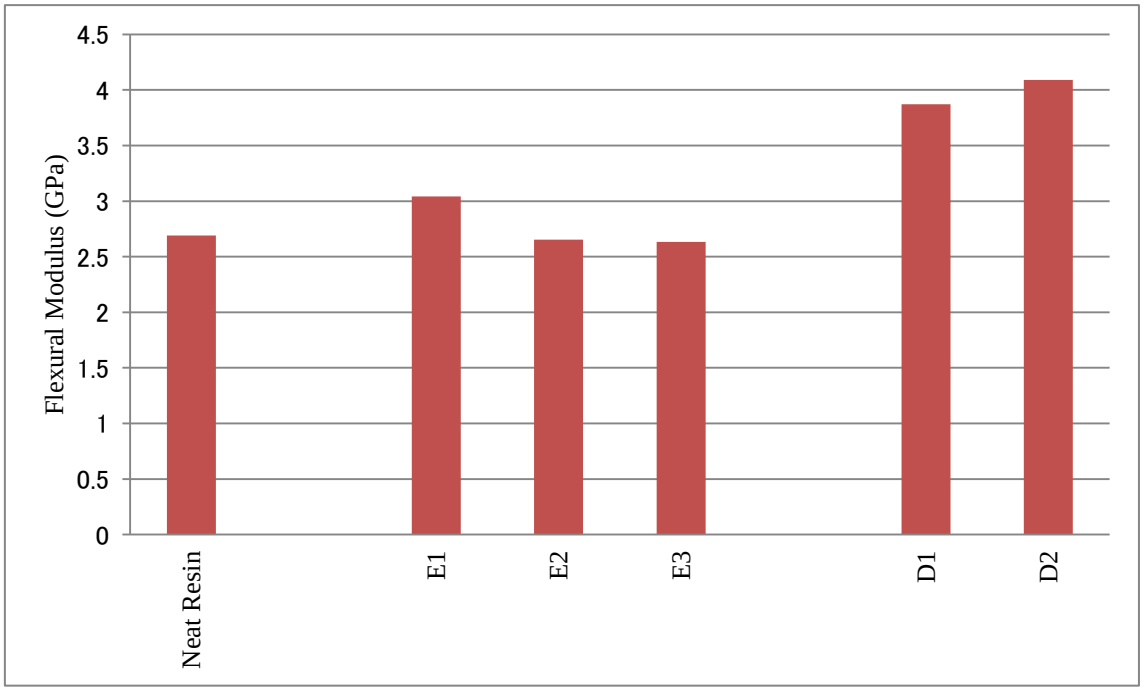

Fig. 3.6 Effect of pre-mixing substances on flexural modulus of epoxy/organoclay nanocomposites.

3.5 Corrosion Behavior

For the polymeric materials, one of the most common parameters in Chemical engineering fields and factories is corrosion performance of materials. Immersion test was employed to investigate anti-corrosion performance of the nanocomposites. Fig. 3.7 shows % weight change of neat epoxy and epoxy/organoclay nanocomposite with different pre-mixing substances in term of square root of time. In this study, corrosion in the composite is described by its percentage of weight change in immersed corrosive environment. Percentage of weight saturation of all nanocomposite with pre-mixing substances improvingly decrease compared to neat resin. Typically, percentage of weight saturation of nanocomposite with D2 pre-mixing substance significantly decreases compared to neat resin and nanocomposite with the other pre-mixing substances. It is due to high degree of clay exfoliation in epoxy matrix.

One curious discussion is that epoxy/organoclay nanocomposite with epoxy different pre-mixing substance do not show much improvement on decreasing percentage of weight change as expected. The reason would be that there are two effects on the nanocomposites. Firstly, effect from clay exfoliation which decreases percentage of weight saturation. Secondly, effect from free volume which increases percentage of weight saturation because epoxy functional group of pre-mixing substance reacts with modified surface amine. It will be discuss more in Chapter 5.

However, in case of diamine pre-mixing substance, short alkyl group of modified amine of organoclay would exchange with long molecular chain of diamine pre-mixing

substance which make longer structure and stronger epoxy matrix. As a result, corrosion behavior could be improved by adding appropriated pre-mixing substance which is recommended to use long molecular chain of diamine pre-mixing substance.

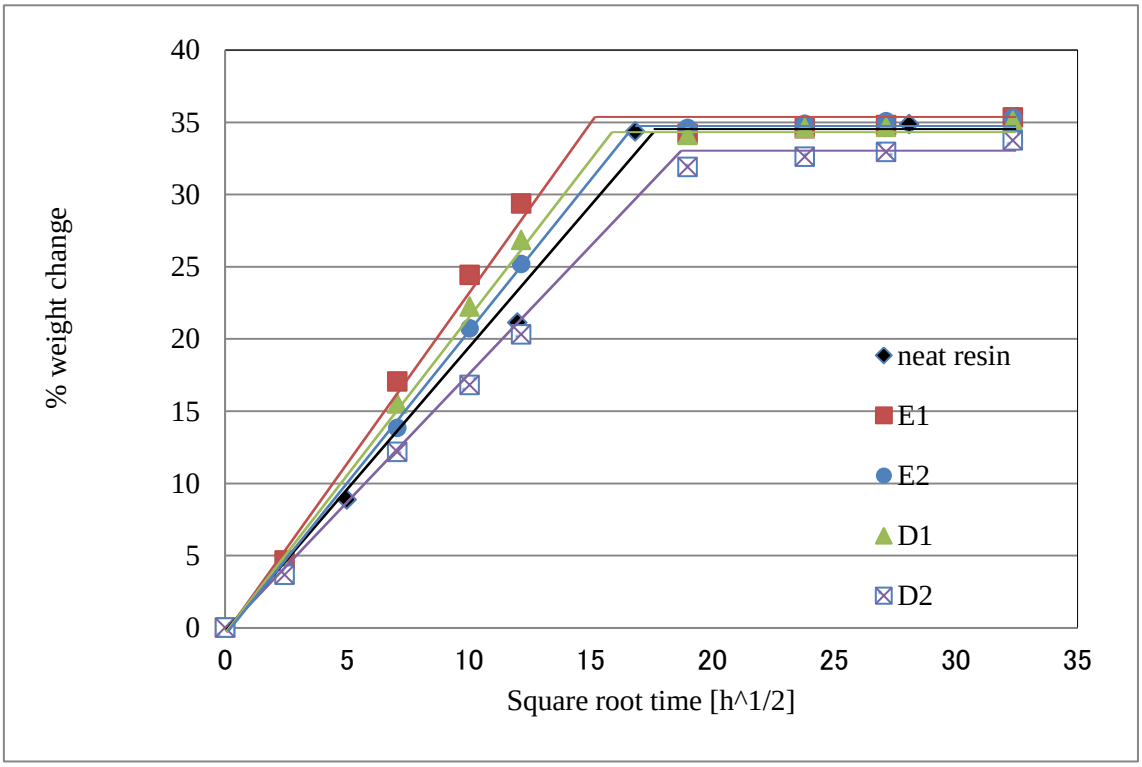

Fig. 3.7 % weight change of neat epoxy and epoxy/organoclay nanocomposite with different pre-mixing substances in term of square root of time.

3.6 Morphology

The structure and morphology of clay dispersion in nanocomposites were determined by TEM as shown in Fig. 3.8. TEM micrographs of epoxy/clay nanocomposites containing E1 and D2 pre-mixing substances are shown in Fig. 3.8(a,b) and Fig. 3.8(c,d), respectively. The dark lines on the bright-scattered images correspond to organoclay.

The exfoliated and homogeneously dispersed silicate layers in both epoxy and diamine pre-mixing substances were obviously observed. The clay layers are more uniformly and exfoliately dispersed in the epoxy that was prepared with E1 compared to D2 compounds.

The increase in the exfoliation of the layered clay as shown in Fig. 3.8a and 3.8b has a positive effect on the exfoliated dispersion of the clay in the materials, demonstrating that the pre-mixing substances of the system plays an important role in the clay dispersion.

Again, the TEM micrographs were corresponding to viscosity and XRD results higher degree of clay exfoliation in epoxy pre-mixing substances (Fig. 3.8a and 3.8b) was observed in compared to diamine pre-mixing substances (Fig. 3.8c and 3.8d). This confirms that pre-mixing substances have an effect on the degree of clay exfoliation and the improvement of dispersion of silicate layers in epoxy nanocomposite requires pre-mixing substance in the production process.

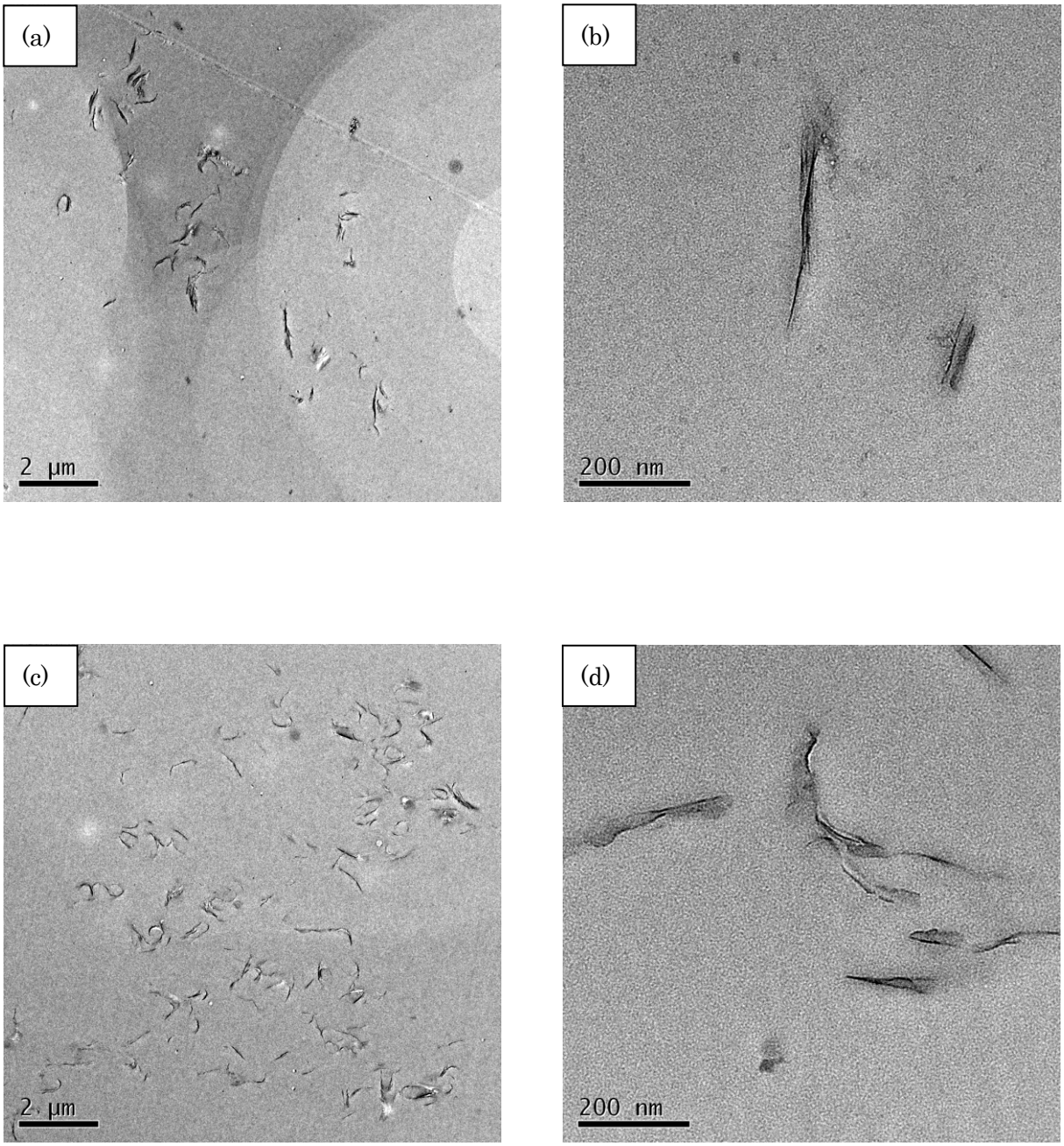

Fig. 3.8 TEM images of epoxy/clay/pre-mixing substance nanocomposites containing: epoxy/organoclay/E1 nanocompostie with (a) low and (b) high magnification; epoxy/organoclay/D2 nanocompostie with (c) low and (d) high magnification

3.7 Conclusions

Fully epoxy/organoclay nanocomposites have been successfully obtained with epoxy reactive diluents and diamine curing agents pre-mixing as clay exfoliators. Epoxy reactive diluents and diamine curing agents pre-mixing substances play an important role on clay exfoliation into epoxy matrix. Pre-mixing process with epoxy and diamine exfoliators assists to obtain fully exfoliated epoxy/clay nanocomposites confirming from all viscosity, XRD and TEM micrographs. Epoxy exfoliator has more affected on increasing degree of clay exfoliation compared to diamine exfoliator. Flexural modulus and diffusivity of epoxy/organoclay nanocomposites with diamine exfoliator obtains significantly improving, however, with epoxy exfoliator is not much improving. On these results, the developments of properties for the epoxy/organoclay nanocomposites are now planning.

Chapter 4

Effect of amine exfoliators on organoclay dispersion

4.1 Introduction

Due to complex parameters involved the fully exfoliation behaviour of the clay in the epoxy thermosetting matrix, work in this area must be deeply studied, especially the question of at which stage a complete clay exfoliation will be taken place must be clearly understood. Previous study on Chapter 3, pre-mixing process with chemical exfoliators plays an important role on the clay dispersion.

Amine exfoliators have more potential on increasing both clay exfoliation and nanocomposite properties. Focusing on corrosion property, nanocomposites with amine exfoliators showed better anti-corrosion property compared to epoxy exfoliators.

In this chapter, amine exfoliators are paid much attention to study on organoclay dispersion for fully epoxy/organoclay nanocomposites and their properties. Amine compounds are selected to be various amine functional groups which are compatible with epoxy resins and able to act as curing accelerators. Regarding to the knowledge from Chapter 3, the amine clay exfoliators were varied sizes of molecular chains of the compounds. Viscosity, clay interlayer distance using XRD and morphology of the nanocomposites using TEM are investigated. Flexural property and corrosion behaviour of nanocomposites with different amine compounds were examined.

4.2 Experiments

4.2.1 Materials

The epoxy resin used was a liquid diglycidyl ether of bisphenol A (DGEBA) (Epomik R140 form Mitsui Chemical Co., Ltd.) used as matrix, which has an epoxide equivalent weight of 188 g/equiv. Diamine curing agent (Jeffamine D230 from Huntsman Corporation) was used as curing agent which has an amine hydrogen equivalent weight of 60 g/equiv. Fig. 4.1 shows chemical structures of the materials used in this study. The clay used for synthesis of the nanocomposites was a commercial treated organoclay (Nanomer I.30E from Nanocor Inc.). It is basically n-octadecyl ammonium salt of mor

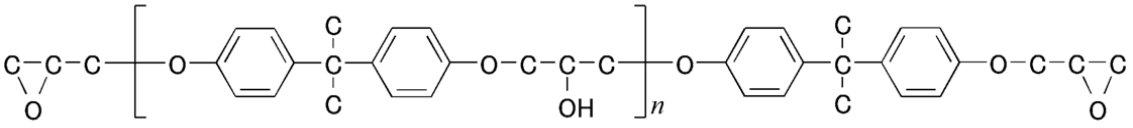

DGEBA

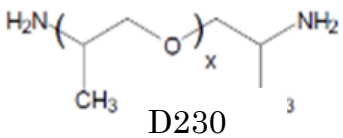

D230

Fig. 4.1 Chemical structures [illegible] used in this study.

Pre-mixing substances were selected two amine functional groups with two variants of molecular chain. Monoamine pre-mixing substances (Jeffamine M600 and M2070) are monofunctional primary amine. Diamine pre-mixing substances (Jeffamine D400 and D2000) are diffusional primary amine. All pre-mixing substances are supplied by Huntsman Corporation. The structures and properties of the pre-mixing substances are shown in Table 4.1.

Table 4.1 Structures and properties of pre-mixing substances

Pre-mixing substance	Commercial name	Number average molecular weight	Amine hydrogen equivalent weight *(g/eq)*	Chemical structure
M1	M600	600	291	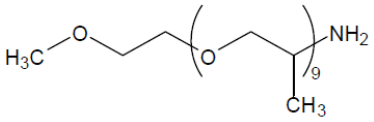
M2	M2070	2070	1040	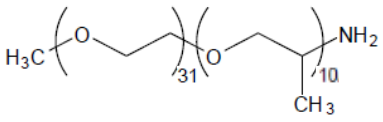
D1	D230	230	60	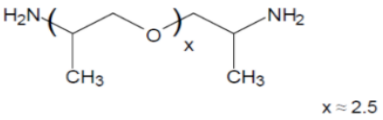
D2	D400	400	100	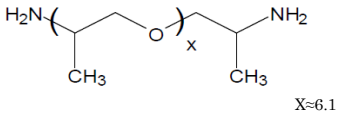
D3	D2000	2000	520	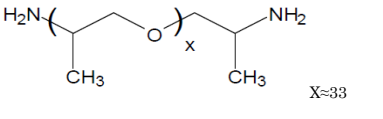
T1	T403	440	81	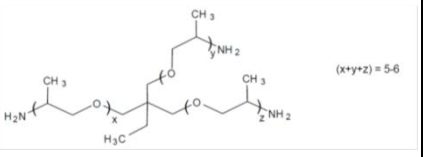
T2	T3000	3000	530	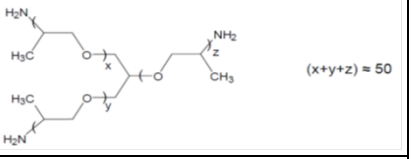
T3	T5000	5000	952	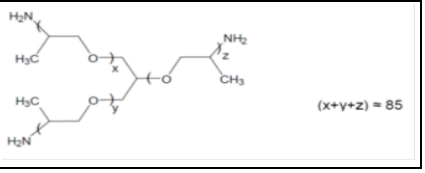

4.2.2 Method

Initially, to prepare suspensions of organoclay/pre-mixing substance, pre-mixing substances were mixed with 10 mass% organoclay via high speed homogenizer (Ultra-TURRAX T18, IKA.) at 24,000 rpm for 15 minutes, following by 15 minutes ultrasonic bath, and repeating both processes for 4 times. After that, the 10 mass% suspensions were mixed with epoxy via the homogenizer for 10 minutes. After mixing according to the above conditions, the mixtures were degassed under vacuum for 10minutes. Thereafter, cooling down to room temperature, and then, epoxy resin and curing agent were added to the mixtures stirred with degassing again for 10 minutes before casting. Finally, the organoclay/pre-mixing substance mixture of epoxy with diamine curing agent was cured at 80 °C in oven for six hours and followed by post curing at 120 °C in the oven for 12 hours.

4.2.3 Characterization

4.2.3.1 Viscosity

Viscosities of suspensions of organoclay/pre-mixing substance after pre-mixing process were measured at 25°C on Anton Paar – Physica MCR 100 viscometer using cone and plate geometry to evaluate clay dispersion in pre-mixing substance.

4.2.3.2 D-spacing

The clay dispersion was examined using Transmission Electron Microscopy (TEM). D-spacing of the organoclay and the nanocomposites were measured using a Philips MRD X'Pert with a rotation anode and CuKα radiation (Å). The scanning range was

from 1.05° to 9.95°. The step size was 0.02° and the step time was 3 sec for the measurement of the d-spacing. The d-spacing of different mixing conditions were investigated. For the analysis of the clay powder, particles were mounted on a sample holder with a large cavity and a smooth surface was obtained by passing the particles with a glass plate. Analysis of organoclay in the epoxy resin with the curing agent was performed by placing the sample composites on the sample holder. The nanocomposite plates produced during the molding process had a fairly smooth surface which has been directly analyzed. TEM samples were prepared by ultra-microtome to be thin sections of the nanocomposite with a diamond knife. These thin sections were then captured on coated Cu grids. The interlayer distance was calculated according to Bragg's equation. The samples were tested at different magnifications from 200 to 500 nm scale bar.

4.2.3.3 Flexural Property

Three-point bending is a convenient way to determine flexural property. Flexural strength and modulus were evaluated by three-point bending test using a bending machine, Shimazu Autograph AGS-1KNJ. The bending test specimens of 60×25×2 mm^3 for flexural property according to ASTM D790 were tested at room temperature as shown in Chapter 2. Operating condition of the bending test was 40 mm span distance and 2 mm/min cross head speed.

4.2.3.4 Immersion test

The immersion test specimens of 60×25×2 mm^3 for measurement of initial weight were dried at 50°C in oven for more than 75 hours according to Chapter 2. All specimens holding with a Teflon tube, in order to avoid sample overlapping, were tested in beaker

containing 10% of sulfuric acid solution separately. The beakers were sealed with plastic film to avoid evaporation of the solution. The samples were performed in water bath controlled at 60°C.

4.2.3.5 Morphology

Transmission Electron Microscopy (TEM) images in this study were obtained using a JEOL 2010F equipped with a field-emission gun operating at 200kV. TEM specimens need to be sufficiently thin to allow the transmission of electrons. TEM samples were prepared by ultramicrotoming thin sections of the polymer nanocomposite with a diamond knife. These thin sections were then captured on coated Cu grids. The samples were tested at different magnifications from 0.2 µm to 50 nm.

4.3 Clay dispersion

4.3.1 Viscosity

One parameter to detect clay dispersion in pre-mixing substance in this study was viscosity. Table 4.2 showed viscosity of neat sample and samples with clay 10 mass% before and after mixing using high speed homogenizer and % change of viscosity based on neat samples and samples before mixing. Pre-mixing substances had an important effect on viscosity of samples. Viscosity of almost samples significantly increased when adding pre-mixing substance during pre-mixing process, except some of small molecular chain of diamine compounds (D1 and D2).

In case of monoamine compounds, both M1 and M2 showed positive values of % change of viscosity base on sample before mixing. Longer molecular structure of monoamine (M2, 1315%) showed higher percentage change of viscosity compare to smaller molecular structure of monoamine compound (M1, 582%). It implied that the longer molecular structure of monoamine (M2) would assist to obtain better exfoliation of organoclay in the epoxy matrix compared to short molecular chain of monoamine compound (M1). These phenomena would be discussed in details next chapter.

In case of diamine compounds, D1 and D2 showed negative values of % change of viscosity base on sample before mixing, -10% and -37%, respectively. Only D3 showed positive value, 445%, of % change of viscosity base on sample before mixing. Again, long molecular structure of dioamine showed higher percentage change of viscosity compare to smaller molecular structure of monoamine compound (D1 and D2). It confirmed that long molecular structure of monoamine (D3) would assist to achieve

better exfoliation of organoclay in the epoxy matrix compared to short molecular chain of monoamine compound (D1 and D2).

In order to discuss the reasons for the negative values of % change of viscosity base on sample before mixing of diamine compounds, molecular chains of D1 and D2 amine compounds are shorter than the clay modifier (n-octadecyl ammonium salt). During pre-mixing stage, the amine compounds would be exchanged their short alkyl group with alkyl group of the clay modifier. As these phenomena, it would cause organoclay to be shrunken as shown negative value of the viscosity. These phenomena will be discussed in details next chapter.

In case of triamine compounds, all T1, T2 and T3 showed positive values of % change of viscosity base on sample before mixing, 43%, 471% and 504%, respectively. Conformingly, long molecular structure of triamine showed higher percentage change of viscosity compared to smaller molecular structure of monoamine compound. As the other amine compounds, it confirmed that long molecular structure of triamine compound would assist to achieve better exfoliation of organoclay in the epoxy matrix compared to short molecular chain of triamine compound.

Appropriate amine compound was necessary in pre-mixing process. Monoamine compound shows higher % change of viscosity of viscosity base on sample before mixing compared to diamine and triamine compounds. Amine compounds with long molecular chain are recommended for synthesis fully exfoliated epoxy/organoclay nanocomposites.

Table 4.2 Viscosity and % change of viscosity of samples

Sample	Viscosity [Pa・s]	% Change of viscosity base on neat sample	% Change of viscosity base on sample before mixing
M1	0.0248		
M1+organoclay (before mixing)	0.0542	118	
M1+organoclay (after mixing)	0.3700	1389	582
M2	0.343		
M2+organoclay (before mixing)	0.667	94.	
M2+organoclay (after mixing)	9.440	2652	1315
D1	0.013		
D1+organoclay (before mixing)	0.023	76	
D1+organoclay (after mixing)	0.021	57	-10
D2	0.048		
D2+organoclay (before mixing)	0.114	135.33	
D2+organoclay (after mixing)	0.071	47.90	-37
D3	0.394		
D3+organoclay (before mixing)	0.803	103.78	

Table 4.2 Viscosity and % change of viscosity of samples (cont.)

Sample	Viscosity [Pa・s]	% Change of viscosity base on neat sample	% Change of viscosity base on sample before mixing
D3+organoclay (after mixing)	4.377	1010	445
T1	0.087		
T1+organoclay (before mixing)	0.131	50	
T1+organoclay (after mixing)	0.188	115	43
T2	0.450		
T2+organoclay (before mixing)	0.718	59	
T2+organoclay (after mixing)	4.100	811	471
T3	0.850		
T3+organoclay (before mixing)	1.420	67	
T3+organoclay (after mixing)	8.580	909	504

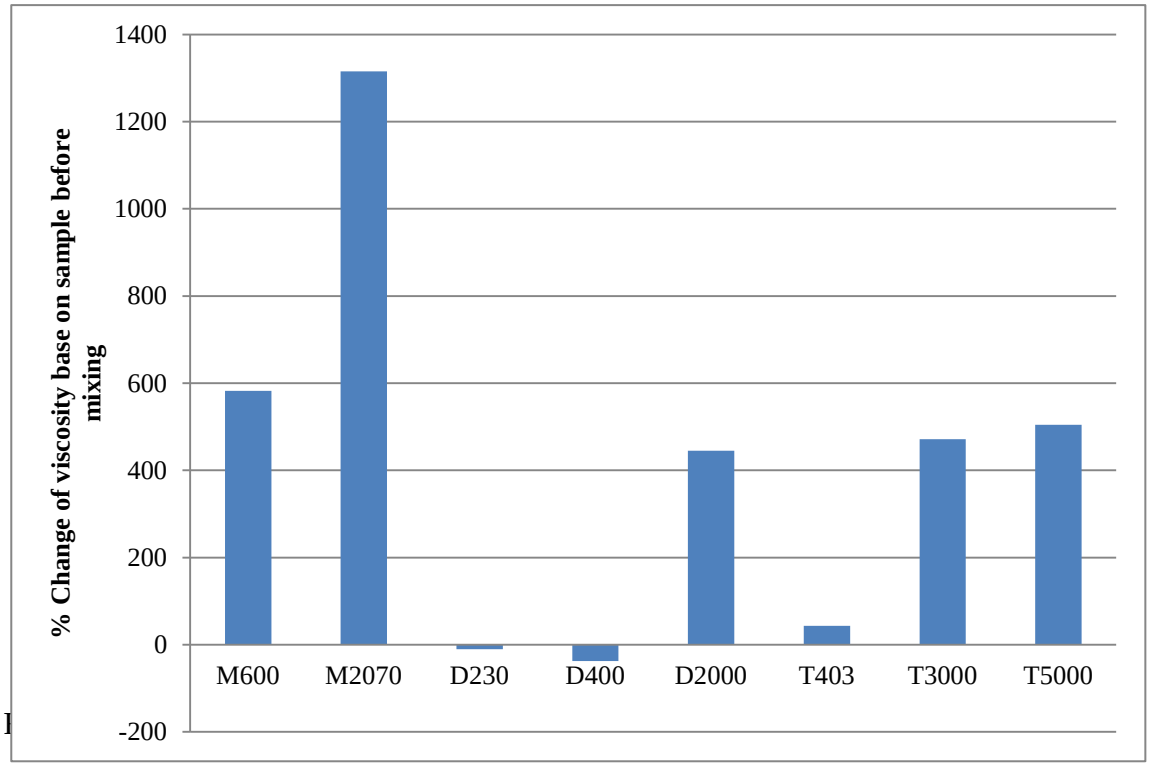

pre-mixing base on sample before mixing

4.3.2 D-spacing

The d-spacings of the organoclay and the nanocomposites were examined by X-ray diffraction. Fig. 4.3 shows XRD spectra for organoclay and epoxy/organoclay nanocomposites with different pre-mixing substances. The pristine organoclay has one single sharp peak at 3.9° and this is related to the d-spacing of 22.6 Å according to Bragg's equation.

In the case of the nanocomposites with amine compounds, the XRD curves of nanocomposites with M1, M2, D3, T1 and T3 pre-mixing substances appear similar pattern shifting of diffraction peaks to lower angles and flatter compared to organoclay and nanocomposite without pre-mixing substance except nanocomposites with D1

which shows peak at similar angle to the nanocomposite without pre-mixing substance. A shift of the peak to lower angle proves that clay exfoliation in epoxy matrix had taken place from amine compounds. The clay layer separation of nanocomposites with amine compounds was considerably higher than without amine compounds.

XRD results showed that monoamine compound had lower angle and flatter compared diamine and triamine compounds. Moreover, long molecular structure of amine compounds would obtain higher clay exfoliation in the epoxy matrix compared to short molecular structure.

Again, XRD results were corresponding to the viscosity. They also confirmed that clays exfoliation by the amine compounds at the pre-mixing step. Amine compounds as clay exfoliators were able to obtain high degree of clay exfoliation in the epoxy matrix.

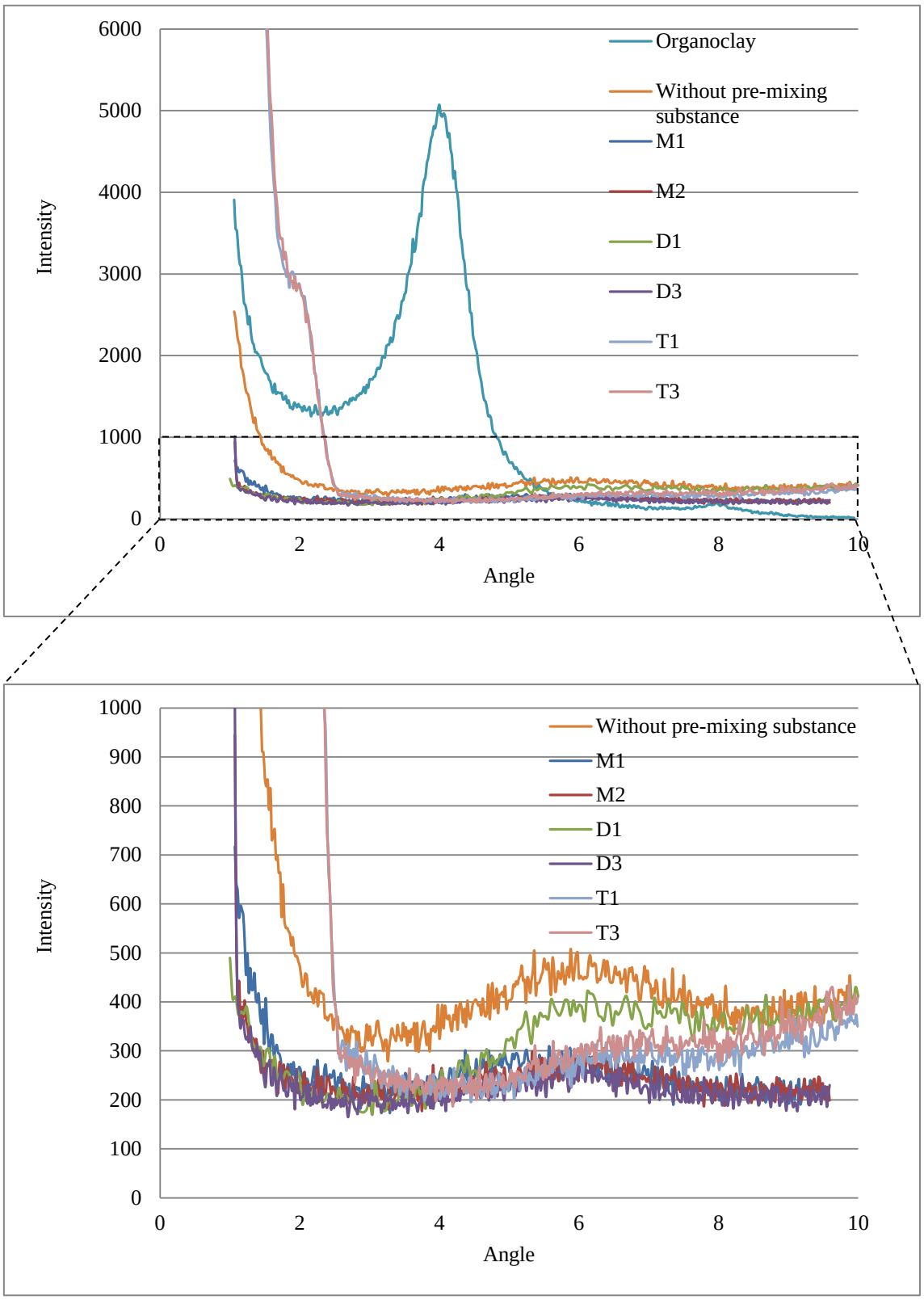

Fig. 4.3 XRD spectra for organoclay and epoxy/organoclay nanocomposites with different amine compounds

4.4 Flexural property

Fig. 4.4 shows effect of amine compounds on flexural strength of epoxy/organoclay nanocomposites. Flexural strength of epoxy/organoclay nanocomposites with monoamine and diamine compounds increase with increasing molecular size of the compounds. Flexural strength of epoxy/ organoclay nanocomposites with only monoamine compound was higher than nanocomposite without any amine compounds. Unexpectedly, flexural strengths of epoxy/ organoclay nanocomposites with diamine and triamine compounds were lower than neat resin and nanocomposites without any amine compounds. It implies that clay exfoliated structure in epoxy matrix would be just a small factor to increase flexural strength.

Fig. 4.5 shows effect of amine compounds on flexural modulus of epoxy/organoclay nanocomposites. Flexural modulus of epoxy/organoclay nanocomposites with monoamine and diamine compounds increase with increasing molecular size of the compounds. Flexural modulus of epoxy/organoclay nanocomposites with both monoamine and diamine compounds was obviously increased compared to except D1, and all triamine compounds. Flexural modulus of nanocomposites with M1, D1 and D2 increases 22%, 28%, 33% compared to nanocomposites without any amine compounds, respectively. It suggested that flexural modulus would be increased with clay exfoliated structure in the epoxy matrix except triamine compounds. Epoxy/organoclay nanocomposites with triamine compounds will be separately discussed below from the others. In comparison between monoamine and diamine compounds, flexural modulus of exfoliated nanocomposite with D3 diamine compound increases more compared to monoamine compounds, however, viscosity of monoamine compound was higher than

diamine compound. It noticeably implied that not only factor of exfoliated clay structure plays an important rule on increasing flexural modulus, but there is something else.

As discussed before, during pre-mixing process, diamine compounds would be exchanged with alkyl group of the clay modifier (monoamine functional group). As these phenomena, surface of modified organoclay after pre-mixing process would change from monoamine functional group to diamine functional group. In the curing process, organoclay containing modified diamine functional group on the surface would be able to fix better with the main matrix compared to modified monoamine organoclay. As these results, flexural modulus of nanocomposite with modified diamine organoclay would be better performance than nanocomposite with modified monoamine organoclay.

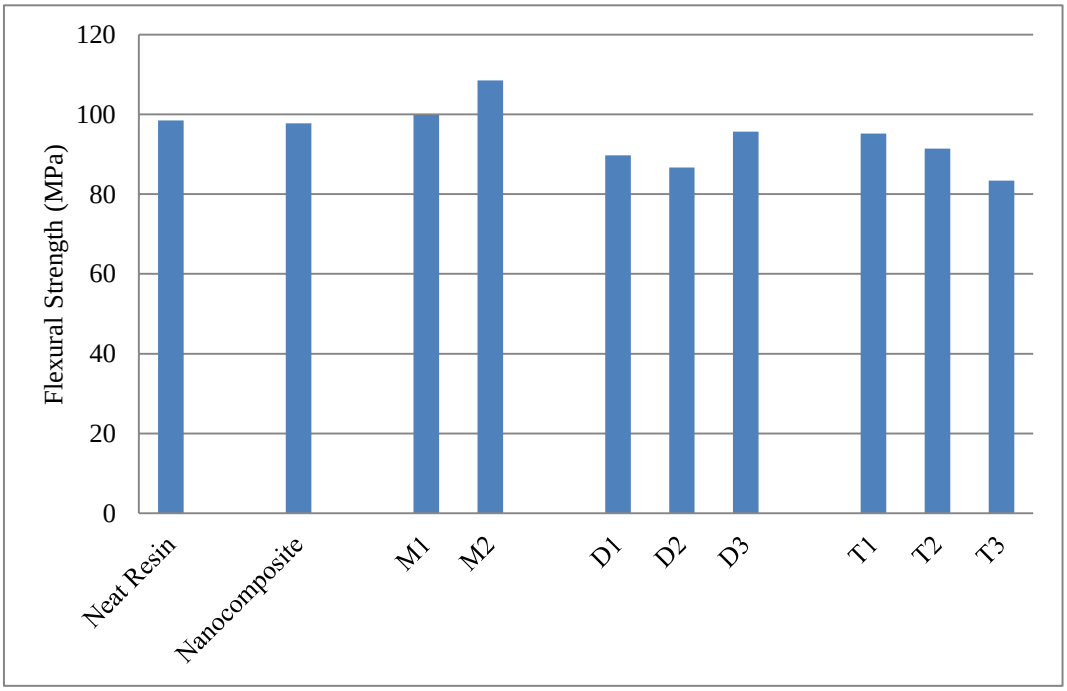

Fig. 4.4 Effect of amine compounds on flexural strength of epoxy/organoclay nanocomposites.

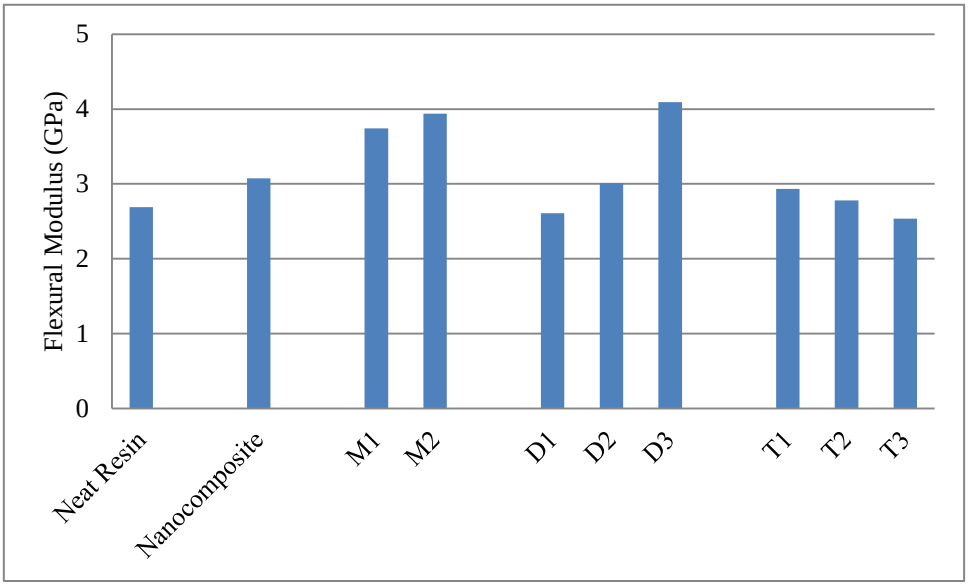

Fig. 4.5 Effect of amine compounds on flexural modulus of epoxy/organoclay nanocomposites.

In case of triamine compounds, flexural strength and modulus of epoxy/organoclay nanocomposites with f triamine compounds decrease with increasing molecular size of triamine compounds which was opposite tendency rom monoamine and diamine compounds. There would be some different behaviour from triamine compounds. Checking in details from stress-strain curves of neat resin and epoxy/organoclay nanocomposites with different triamine compounds as shown on Fig. 4.6, nanocomposites with T1 triamine compound showed brittle behavior nanocomposites. However, epoxy/organoclay nanocomposites with T2 and T3 triamine compounds showed ductile behavior which is unusual characterization of epoxy nanocomposites. Toughness (area below stress-strain curves) of nanocomposites with T2 and T3 triamine compounds remarkably increase compared to nanocomposites with T1 triamine compounds. It implied that triamine compounds with organoclay after pre-mixing

process would be mainly affect to change the characterization of the materials. More details, it will be discussed with TEM images.

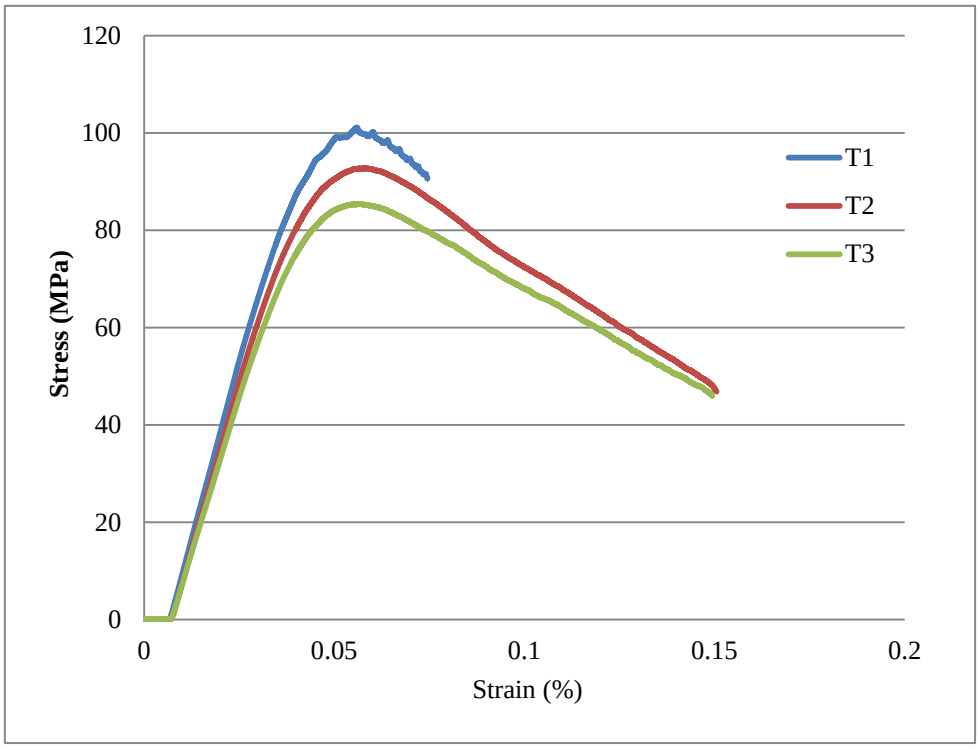

Fig. 4.6 stress-strain curves of epoxy/organoclay nanocomposites with different triamine compounds

After checking on stress-strain curve of nanocomposites with different triamine compounds, one more parameter was checked about curing process. It might be from incompletely curing epoxy and/or triamine compounds in the samples. Additional 130 °C for 4 hours curing process for neat resin and nanocomposites with different triamine compounds was set to confirm that the materials would be surely completely cured. Fig. 4.7 and 4.8 show flexural strength and modulus of neat resin and different epoxy/organoclay nanocomposites with additional 130 °C for 4 hours. Flexural strength and modulus of nanocomposites with triamine compounds decreased after additional

curing process. It might be from thermal degradation from too high temperature from the additional curing process. However, it was confirmed that the materials that prepared from the experimental procedure are completely cured.

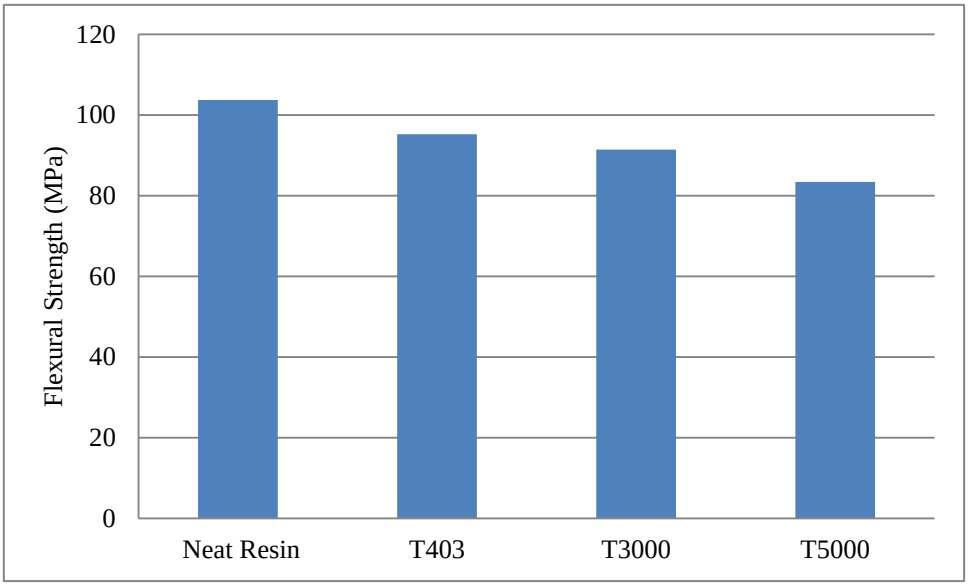

Fig. 4.7 Flexural strength of neat resin and epoxy/organoclay nanocomposites with different triamine compounds additional 130 °C for 4 hours on curing process

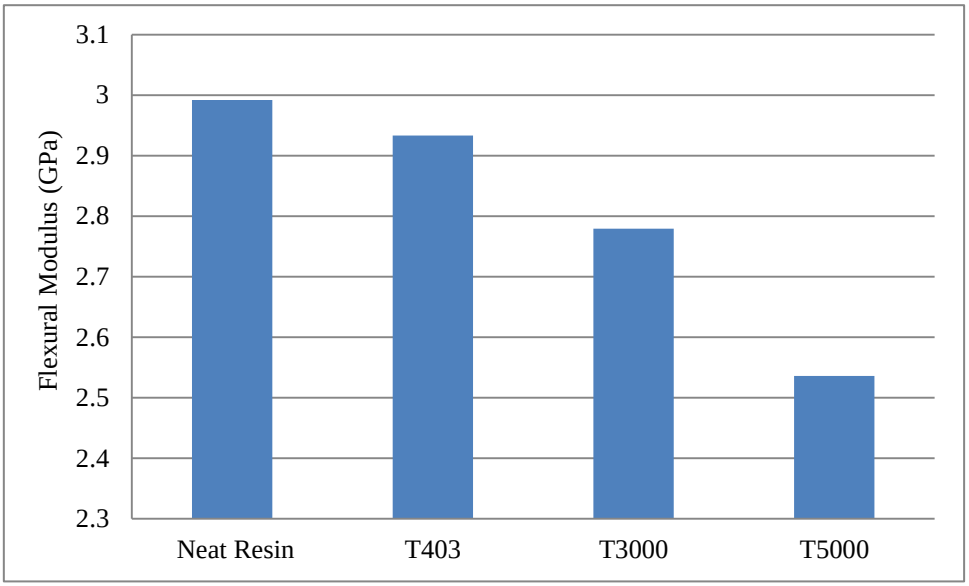

Fig. 4.8 Flexural modulus of neat resin and epoxy/organoclay nanocomposites with

different triamine compounds additional 130 °C for 4 hours on curing process

4.5 Corrosion behaviour

Percentage of weight change of neat epoxy and epoxy/organoclay nanocomposite with different amine compounds in term of square root of time under 10 mass % sulfuric acid solution with fix temperature at 60 °C was shown on Fig. 4.9. To identify a term of "corrosion" in this study, corrosion in the composite is described by its percentage of weight change in immersed corrosive environment. Generally, for an amine cured epoxy, sulfuric acid permeates into the resin easily. In here, high weight gain is recognized. Compared with neat epoxy, only nanocomposite with D3 diamine compound shows a slower penetration and lower percentage of weight saturation. This difference is quite large, more than 2.5 mass % of initial weight of specimen which corresponds to the same value of pure water uptake [64]. It is due to high degree of clay exfoliation in epoxy matrix and higher amount of amine functional group on surface of orgonoclay after pre-mixing which are able to bond and fix with main epoxy matrix.

More discussion on nanocomposite with diamine compound, during pre-mixing process, short monoamine alkyl group of pristine modified amine of organoclay would exchange with long molecular chain of diamine compound (D3) which make exfoliated clay structure and stronger to fix clay with the epoxy matrix. As a result, corrosion behavior could be improved by pre-mixing organoclay with long molecular chain of diamine pre-mixing substance.

Expectedly, nanocomposites with triamine compound would obtain the best corrosion performances because of high amount of amine functional group compared to nanocomposites with monoamine and diamine compounds. However, nanocomposites with triamine compound showed the worst corrosion performances compared to the others. As discussed before, triamine compounds with organoclay after pre-mixing process would change behaviors of the materials. In details, it will be discussed with TEM images.

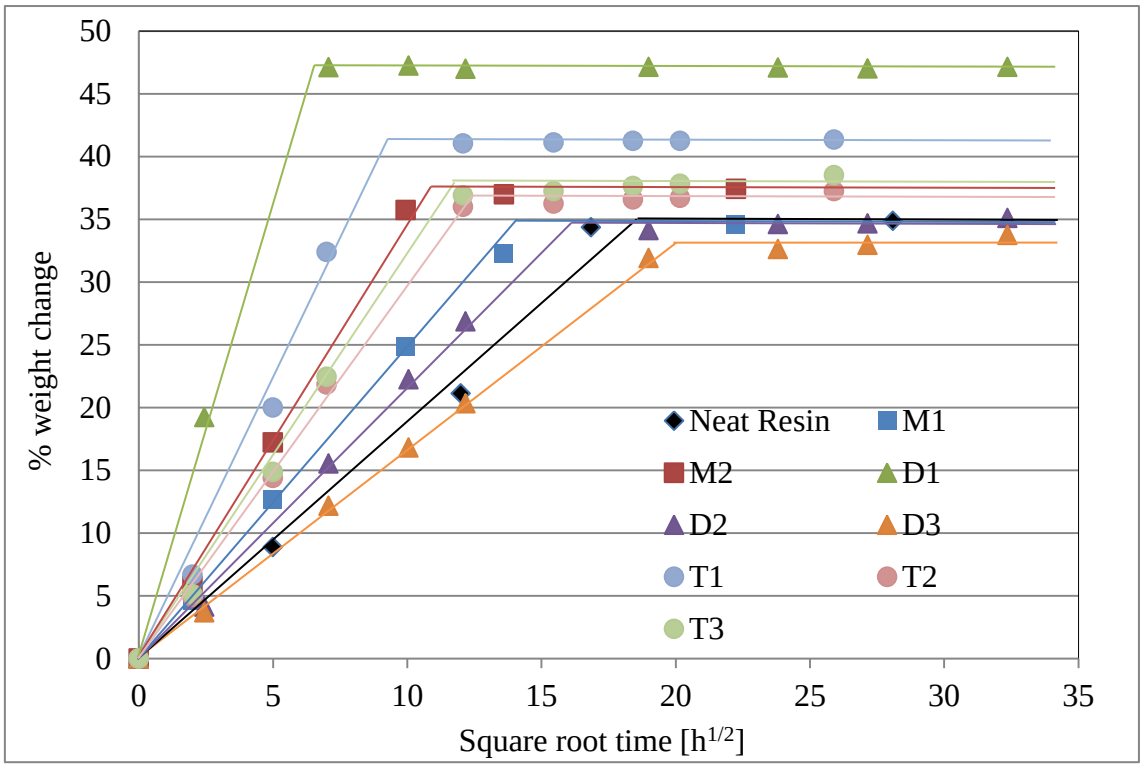

Fig. 4.9 % weight change of neat epoxy and epoxy/organoclay nanocomposite with different amine compounds in term of square root of time under 10 mass % sulfuric acid solution at 60 °C.

4.6 Morphology

Morphology and dispersion of organoclay in the epoxy matrix was observed in micro- and nano-scales by TEM. Figs. 4.10 to 4.13 show TEM images of epoxy/organoclay nanocomposites with M2 monoamine, D2 diamine, T1 triamine and T3 triamine compounds at different magnifications. The dark lines on bright-scattered images correspond to organoclay. Figs. 4.10, 4.11 and 4.12 shows exfoliated and uniform dispersion of the organoclays in the epoxy matrix under micro scale bar, and single layered clay to prove the fully exfoliated clay structure in the nanocomposites in nano scale bar. In comparison of nanocomposites with monoamine, diamine and triamine compounds, monoamine compound shows the highest clay exfoliation and the most uniform dispersion in the nanocomposites, on the other hands, triamine compound shows the lowest clay exfoliation and the worst dispersion in the nanocomposites. Conformingly, TEM micrographs were corresponding to viscosity and XRD results.

In order to discuss on matrix of the materials, nanocomposites with monoamine and diamine compounds obtained single phase of the matrix, however, nanocomposites with triamine compound showed phase separation of the matrix. Generally, triamine compound does not easily mix and blend with epoxy and/or the other amine compounds. To mix triamine compounf with the others, the ratio of triamine to the others has to be quite low. However, in this study, the ratio has to fix as a standard in order to surely recognize only effect of amino compound on clay exfoliation.

Considering on nanocomposites with short molecular chain (T1, Fig. 4.12) and long molecular chain (T3, Fig. 4.13) of triamine compounds, both nanocomposites with T1

and T3 triamine compounds show phase separation of the matrix. Organoclay in nanocomposites with T3 long molecular triamine compounds obtains more exfoliated and more homogenous compared to T1 short molecular triamine compounds. Nanocomposites with T3 triamine compounds obtain bubble in the material which is the main reason on decreasing flexural property and corrosion behaviour.

In order to discuss flexural property and corrosion behaviour with TEM images of nanocomposites with triamine compounds, the longer triamine compounds the more bubbles contain in the material which is cause on decreasing flexural property and also, corrosion behaviour.

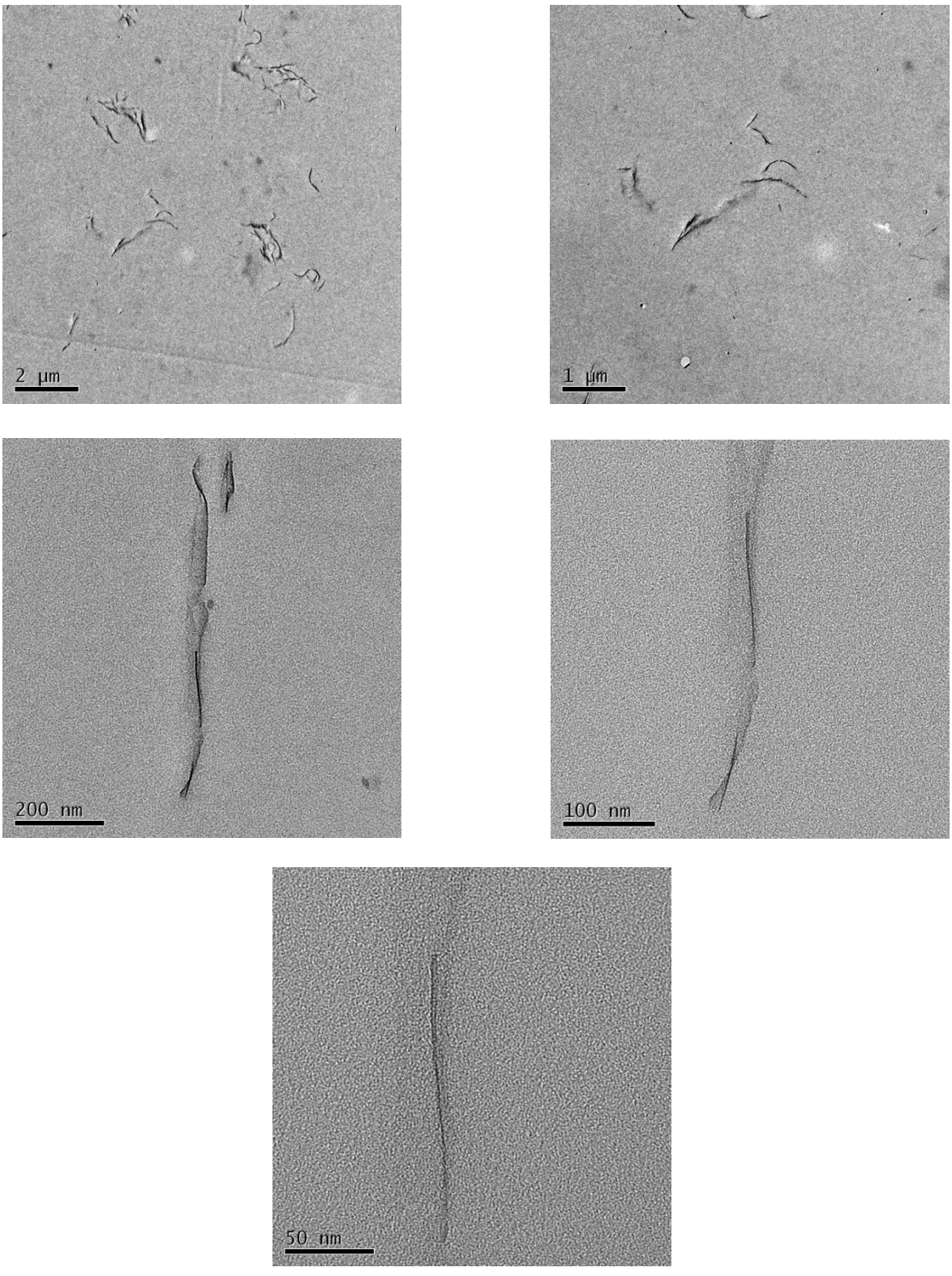

Fig. 4.10 TEM images of epoxy/organoclay nanocomposites with M2 monoamine compound at different magnifications

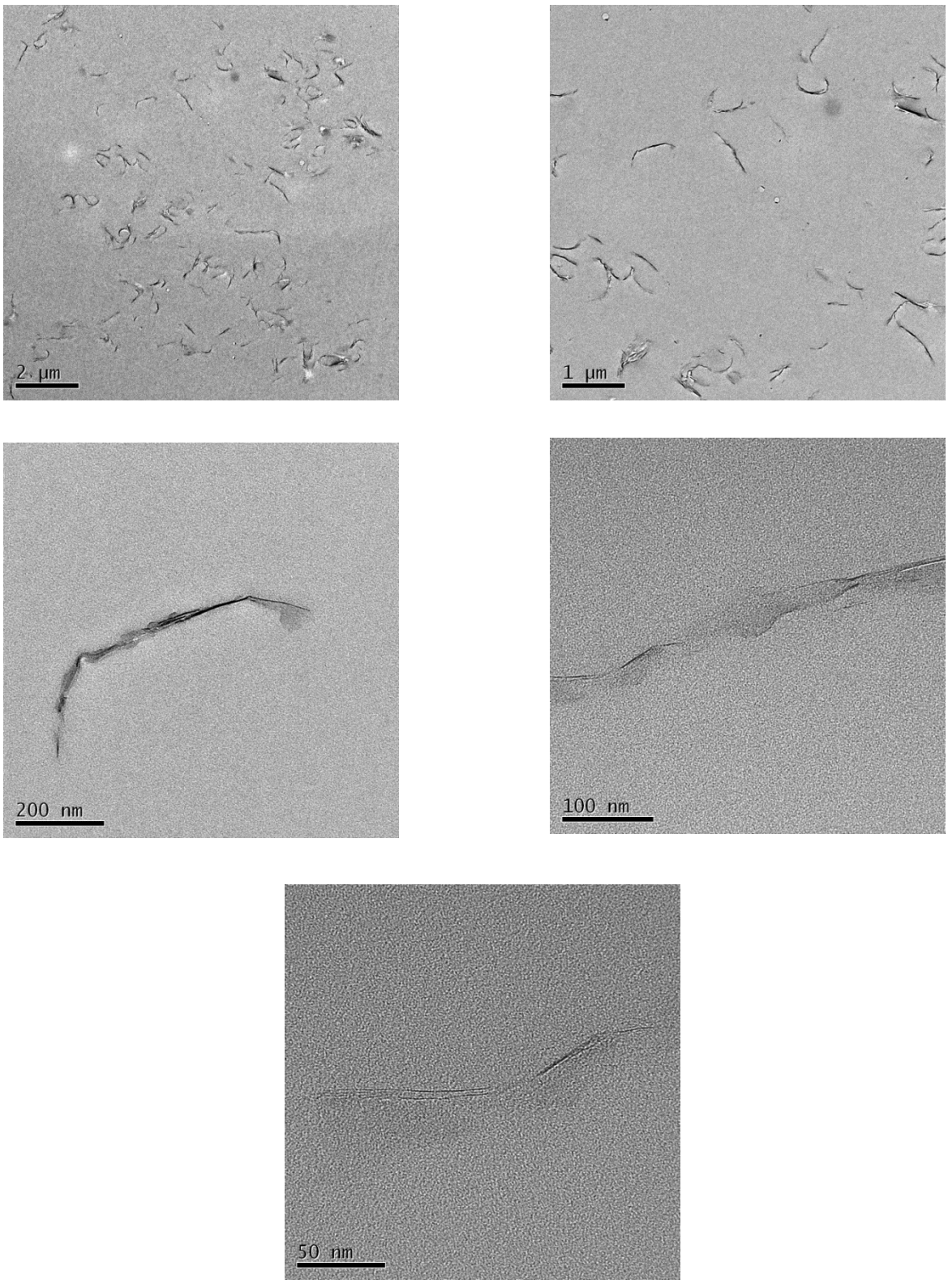

Fig. 4.11 TEM images of epoxy/organoclay nanocomposites with D3 diamine compound at different magnifications

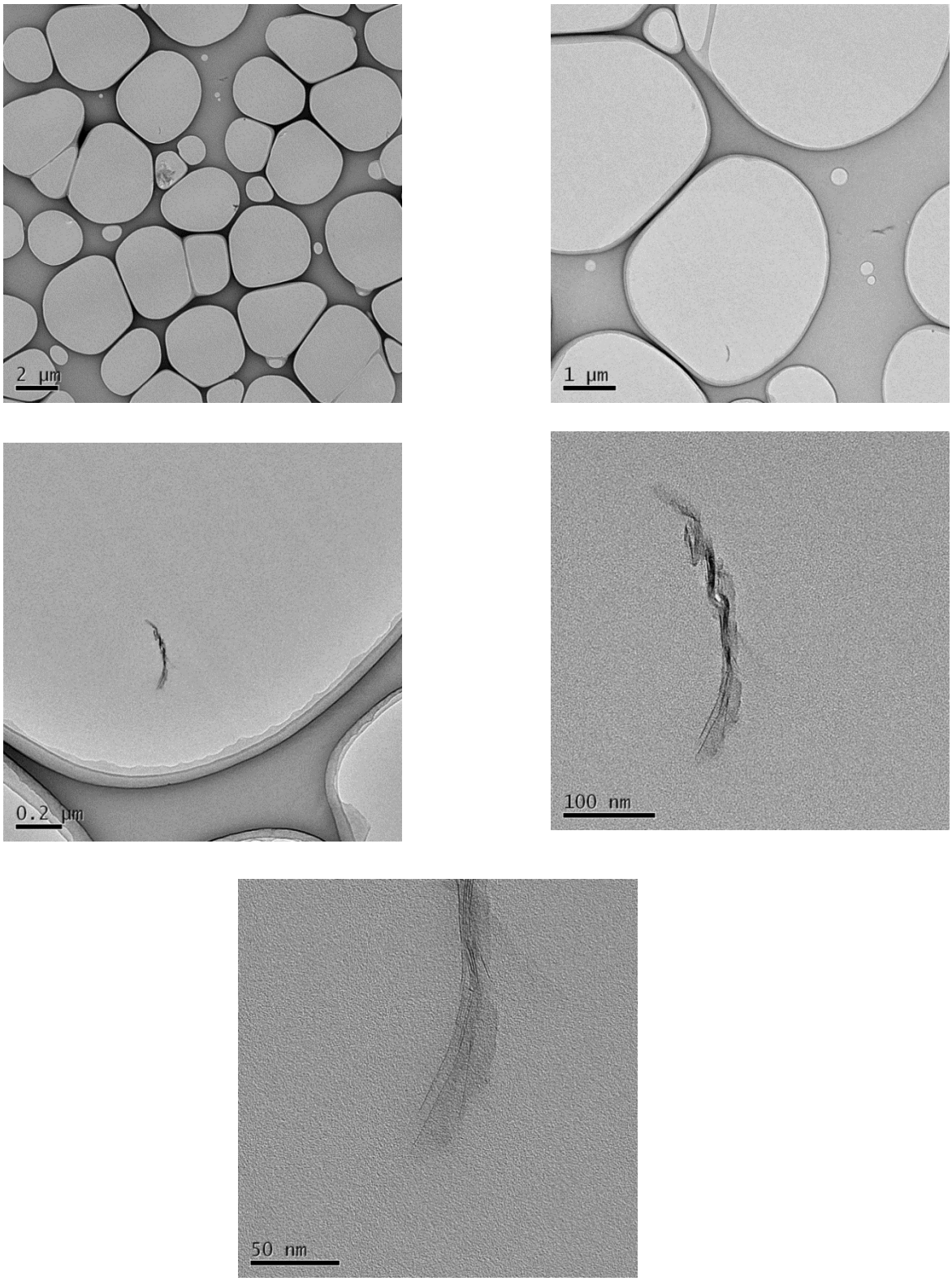

Fig. 4.12 TEM images of epoxy/organoclay nanocomposites with T1 triamine compound at different magnifications

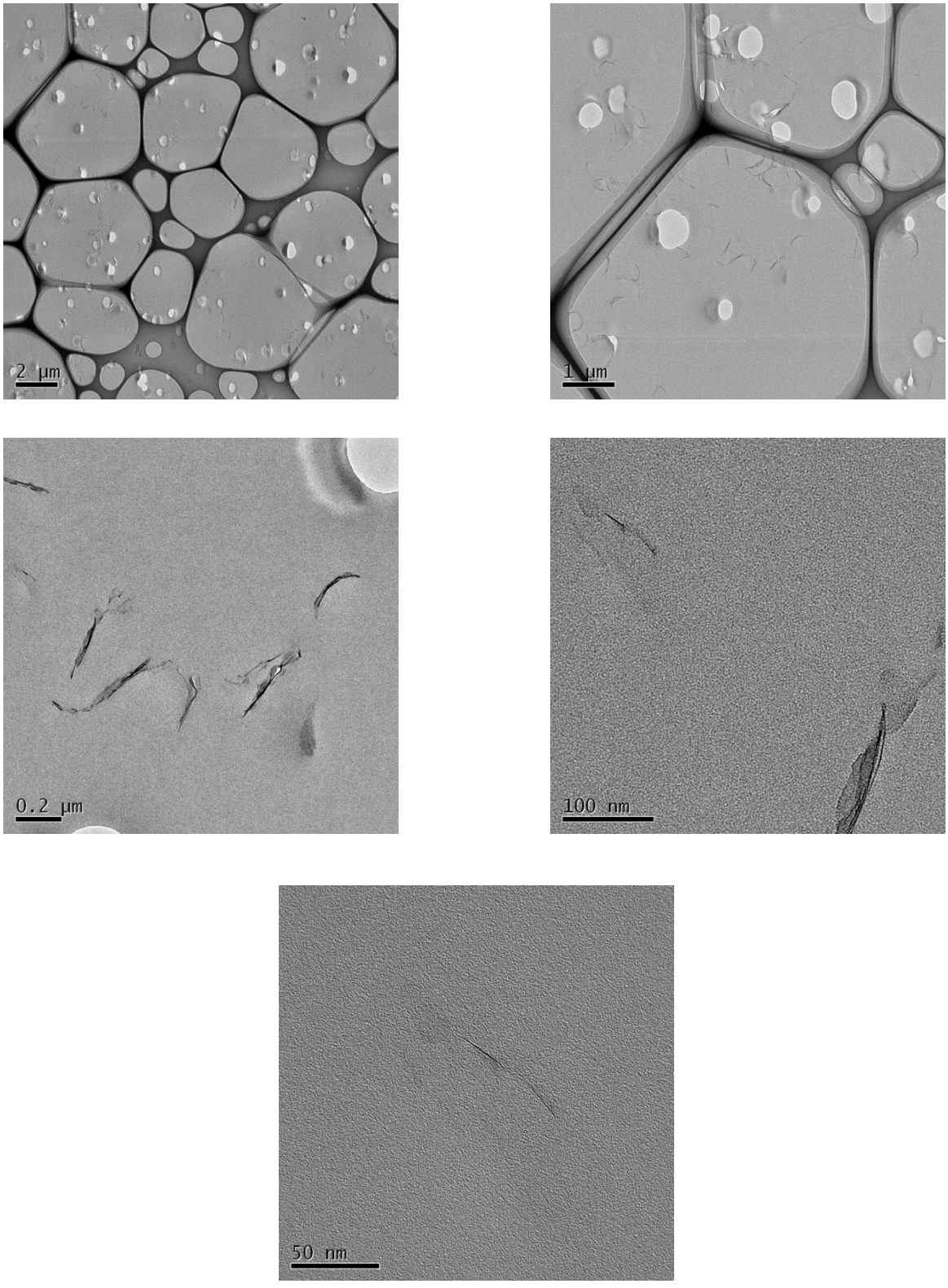

Fig. 4.13 TEM images of epoxy/organoclay nanocomposites with T3 triamine compound at different magnifications

4.7 Conclusions

Amine compounds play an important role on the clay dispersion and exfoliation in epoxy matrix and act as clay exfoliators during pre-mixing process. Epoxy/organoclay nanocomposites with monoamine clay exfoliator show the highest clay exfoliation and the most uniform dispersion regarding to viscosity, XRD and TEM results. Long molecular structure of clay exfoliators are recommend for synthesis fully epoxy/organoclay nanocomposites. Flexural property of epoxy/organoclay nanocomposites with only monoamine clay exfoliator increase compared to neat resin and nanocomposites without clay exfoliators. Corrosion of epoxy/organoclay nanocomposites with only long molecular chain diamine clay exfoliator shows better performance compared to neat resin. Epoxy/organoclay nanocomposites with triamine clay exfoliator were not able to homogeneously mix and shows phase separation which is cause to decrease flexural property and corrosion behaviour of the nanocompoistes.

Chapter 5

Mechanisms of clay exfoliation and nanocomposite properties development

This chapter is described mechanisms of epoxy/organoclay nanocomposites with different methods base on the results from previous chapters.

5.1 Effect of physical dispersion methods

From the TEM observation in Chapter 2, Figure 5.1 illustrates the assumed distribution of clay platelets at different mixing methods. Model of three kinds of nanocomposites made by normal mixing, shear mixing and high speed mixing is shown in Fig. 5.1. Black dot represents crosslink between epoxy resin and curing agent, and gray dot represents onium ion.

Normal mixing includes random dispersed stacked fillers with small gaps as shown in Fig. 5.1 (a). Shear mixing dispersed clay stacks into smaller stacks of clay platelets as intercalation with larger interlayer distance compared to normal mixing as shown in Fig.5.1 (b). High speed mixing results to intercalated/exfoliated layered fillers as shown in Fig. 5.1 (c). Due to the low degree of shear via normal and shear mixing involves, the energy is not enough to break clay stacks and hence do not enhance degree of intercalation/exfoliation. On the other hand, due to the higher degree of shear via high speed mixing involves the dispersion of large stacks into smaller ones took place and hence increases degree of intercalation/exfoliation.

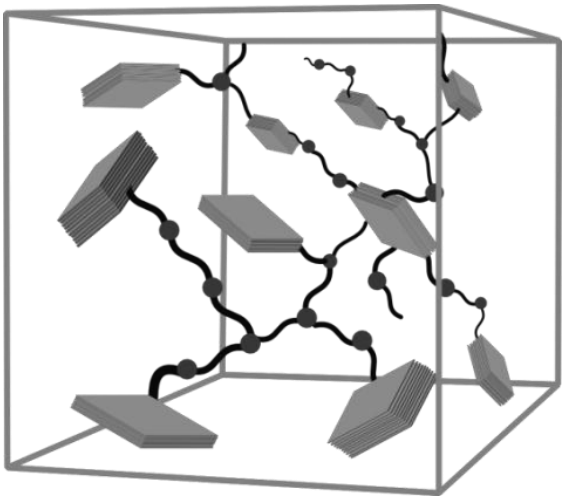

(a) normal mixing

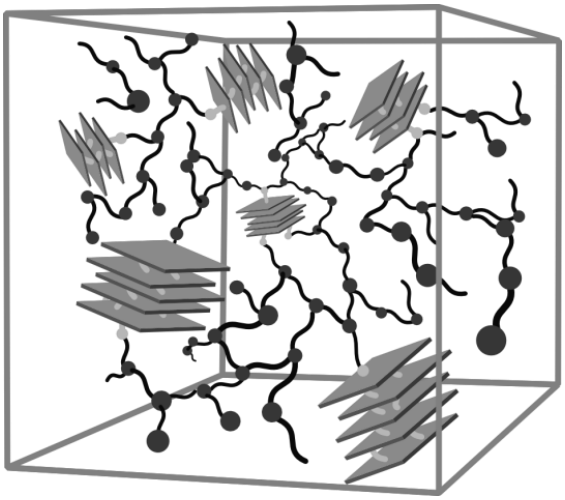

(b) shear mixing

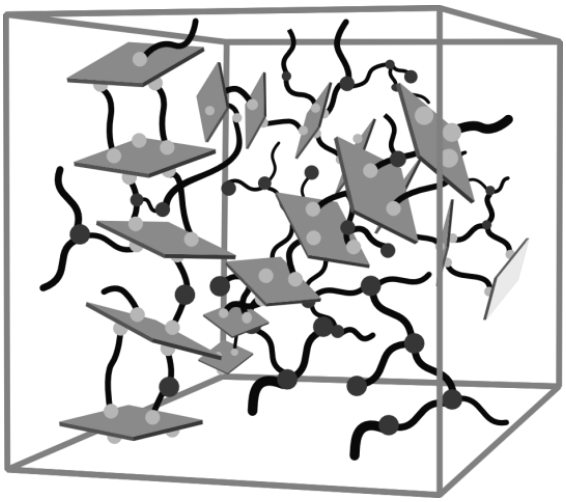

(c) high speed mixing

Fig. 5.1 Model of three kinds of nanocomposites made by normal mixing, shear mixing and high speed mixing (black dot represents crosslink between epoxy resin and curing agent, and gray dot represents onium ion).

5.2 Effect of mixing parameter

From above model, high speed mixing shows good clay intercalation/exfoliation in the matrix. In this sub-chapter, it illustrates the phenomena for clay dispersion in the epoxy matrix with different high shear mixing parameters and ultrasonic application base on TEM images in Chapter 2. Model of clay dispersion under several mixing parameters is shown on Fig. 5.2.

Fig. 5.2A shows a typical clay gallery. There are 2 to 10 sheets in each gallery. The d-spacing or interlayer distance is corresponding to the gap between clay layers. Fig. 5.2B shows the clay gallery is subjected and dispersed by shear force by share force. The individual layered- clay is started to peel apart due to high share force. The d-spacing of clay is enlarged to future forming up the intercalated/exfoliated clay structure as shown on Fig. 5.2C. Regarding to the results from Chapter 2, it obviously confirms that mixing speed has an effect on clay interlayer distance.

However, if the clay gallery is operated under overloaded-shear rate, layered-clays are damaged as shown in Fig. 5.2D base on TEM image (Fig. 2.33). As the results, properties of the nanocomposites would be decreased. Fig. 5.2F shows assisted clay dispersion by ultrasonic energy base on TEM image (Fig. 2.39). After the ultrasonic application, clay galleries would be less tighten and slightly more open at the end of the galleries.

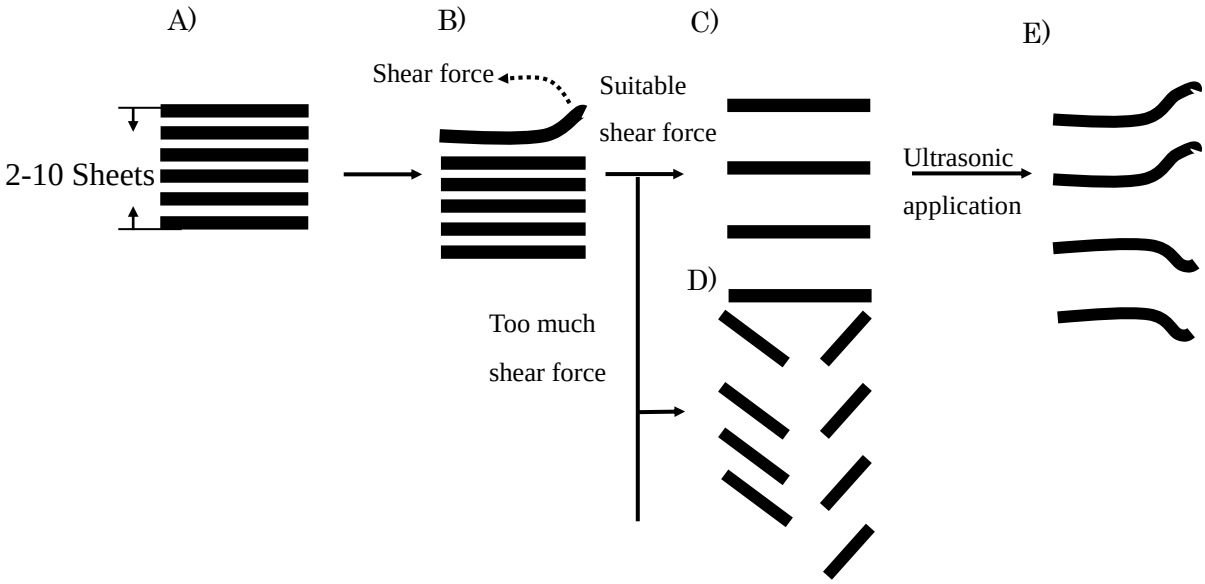

Fig. 5.2 Model of clay dispersion under several mixing parameters (black thick line represents nanoclay).

5.3 Effect of clay exfoliators

From 5.2, physical method using high speed mixing with suitable mixing parameters shows good clay dispersion, but still not fully exfoliated clay structure in the epoxy matrix. Combine physical and chemical clay dispersion method is applied. Chemical compounds are designed to various functional groups (epoxy and amine functional groups which are compatibility with epoxy resins and ability for the curing accelerator).The clay exfoliation mechanisms are proposed base on TEM observation. The mechanism for breaking down initial organoclay galleries to become exfoliated clay structure in epoxy matrix is discussed. Initially, the penetration of adoptable

pre-mixing substances between clay layers has taken place. The adoptable pre-mixing substances tend to diffuse into the space between the clay galleries. Adoptable pre-mixing substances are called “Exfoliators”, which assist to achieve clay exfoliation structure.

5.3.1 Epoxy exfoliator

Fig. 5.3 shows mechanism of clay exfoliation with epoxy exfoliator in epoxy matrix. In case of “epoxy exfoliators”, it requires smaller molecular size than clay interlayer spacing which allows penetrating into clay spacing. Epoxy exfoliator/ modified interlayer amine modifier reaction starts from clay interlayer and/or the neighborhood. After the reaction, clay interfacial energy would be reduced much lower than non-exfoliator. As these phenomena, clay layers could be much easier to separate from clay gallery to exfoliated layered clay compared to pristine and commercial modified clay. As these phenomena, individual silicate nanolayers were homogeneously and randomly dispersed throughout epoxy matrix. Therefore, small molecular structure of epoxy exfoliator would be one of the key parameters to achieve clay exfoliation.

Unfortunately, during epoxy curing to form the matrix, the clays after pre-mixing process with epoxy exfoliator were not able to bond with main epoxy matrix because epoxy functional group of exfoliator reacts with amine functional group of modified surface clay which occur free volume surrounding layered clays themselves. There phenomena could affect to reduce performance of the nanocomposites.

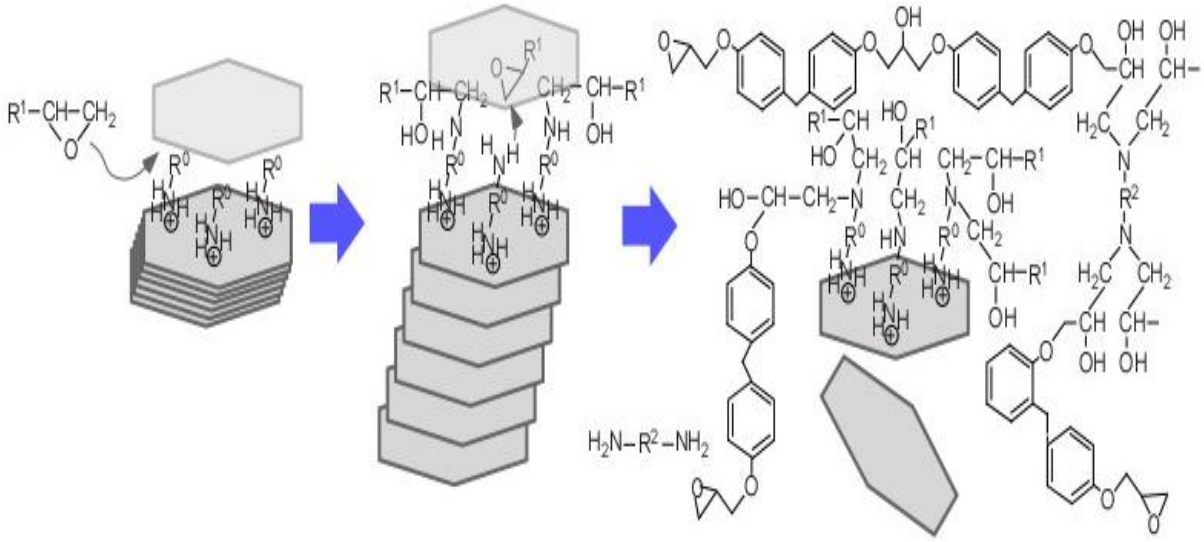

Fig. 5.3 Mechanism of clay exfoliation with epoxy exfoliator in epoxy matrix

5.3.2 Monoamine exfoliator

Mechanism of clay exfoliation with monoamine exfoliator in epoxy matrix is illustrated in Fig. 5.4. In case of "amine exfoliators", the first step of clay dispersion would be required how easy exfoliators penetrate into the clay gallery which required the same functional group of ammonium salt of organoclay. The left side of Fig. 5.4 shows a typical clay gallery immersing in amine compounds which were required longer molecular chain than clay surface modifier, *n*-octadecyl ammonium in this study. If molecular chains of amine compounds were shorter than the clay modifier, organoclay was shrunken after pre-mixing process which obtained lower viscosity after pre-mixing compared to resin/organoclay suspension without any amine compounds regarding to viscosity of D1 and D2 diamine exfoliators as shown in Chapter 4. After that, the suspension of organoclay/amine compounds would exchange their long alkyl group with the alkyl group of the clay modifier during pre-mixing process. While these phenomena occurred, interlayer distance of the clays would be enlarged regarding to the

molecular chain of the amine clay exfoliators. Therefore, the exfoliated clay dispersion in the epoxy matrix was synthesized during pre-mixing process.

Monoamine exfoliator obtained high degree of clay distribution. It would be because monoamine exfoliator is the same functional group to primary organoclay modifier compared to the other exfoliators. In general, if functional group of substances is the same, it would be easier to penetrate into each other. In the same reason, monoamine exfoliator which is the same functional group as ammonium salt of organoclay would be easier to penetrate into the clay. While continues mixing with appropriate condition, clay galleries would be separated down to exfoliated clay.

Compared to epoxy exfoliator, properties such as mechanical and barrier properties of nanocomposites with monoamine exfoliator would be performed much better. As these phenomena, amine exfoliator has a significant positive effect on clay exfoliated synthesis in the epoxy matrix and long molecular chain of monamine exfoliator is recommended.

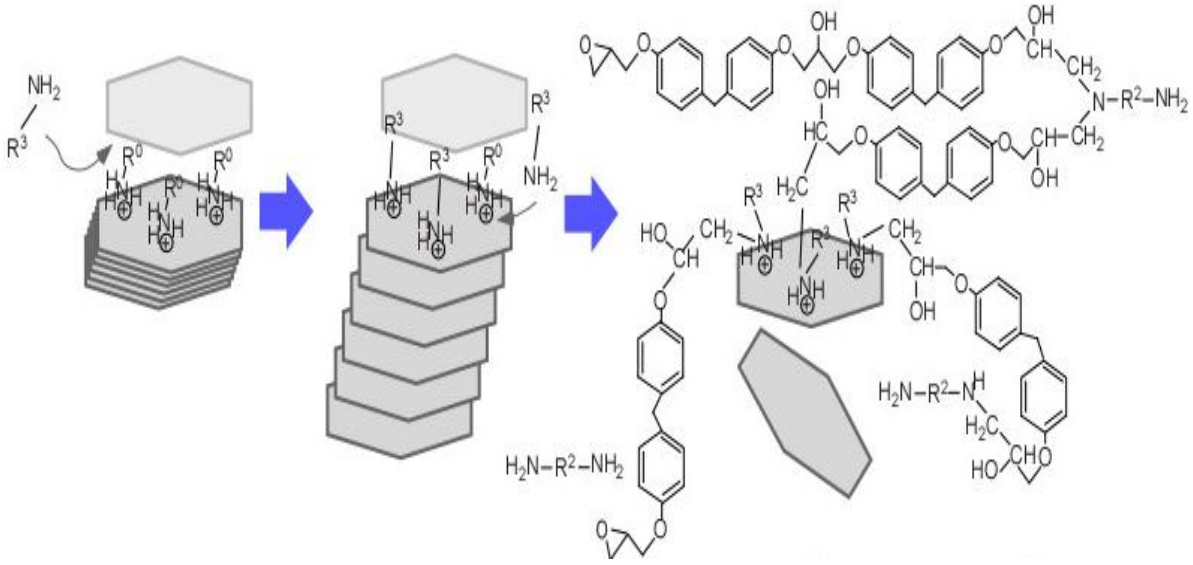

Fig. 5.4 Mechanism of clay exfoliation with monoamine exfoliator in epoxy matrix

5.3.3 Diamine exfoliator

Mechanism of clay exfoliation with diamine exfoliator in epoxy matrix is illustrated in Fig. 5.5. As discuss before, the first step of clay dispersion with “amine exfoliators” would be required required the same functional group of ammonium salt of organoclay. In case of diamine functional group of exfoliator requires long molecular which would exchange its long alkyl group of the exfoliator with short alkyl group of amine interlayer modifier during pre-mixing process. These phenomena would enhance to enlarge interfacial clay spacing, and hence, exfoliated clay structure in epoxy matrix was produced. Moreover, exchanged long amine alkyl group from diamine exfoliator on layered clays are able to bond with main epoxy matrix which is one of the key factors to improve higher properties of nanocomposites compared to monoamine exfoliator. Similar to monoamine exfoliator, long molecular chain of diamine exfoliator is recommended.

In comparison between monoamine and diamine exfoliators, mechanical and barrier properties of nanocomposites with diamine exfoliator obtains better performances. Noticeably, improving effects of the nanocomposites with diamine exfoliator is not only exfoliated clay structure, but also stiffer materials because nanoclay after treating with diamine exfoliators would has two bonding reaction and fix stronger with the epoxy matrix compared to monoamine exfoliator which has only one bonding reaction.

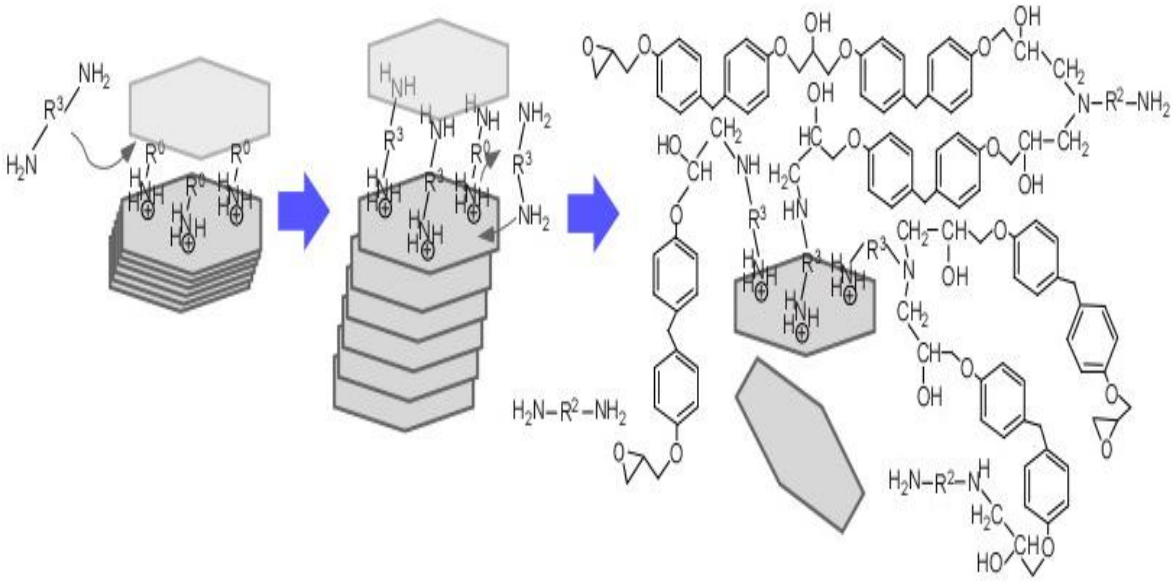

Fig. 5.5 Mechanism of clay exfoliation with diamine exfoliator in epoxy matrix

5.3.4 Triamine exfoliator

From TEM observation, illustration of morphology of epoxy/organoclay nanocomposites with triamine is shown in Fig. 5.6. Gray circle represents amine pahse. Black line represents organoclay. As discuss before, triamine exfoliator does not easily mix with epoxy and/or the other amine compounds. Considering on morphology of nanocomposties with triamine exfoliator, they obviously show phase separation. Organoclay in nanocomposites with triamine compounds would be able to obtain exfoliated structure. However, nanocomposites with long molecular triamine exfoliator would obtain with bubbles in the material. The longer triamine compounds the more bubbles contain in the material which is cause on decreasing flexural property and also, corrosion behaviour.

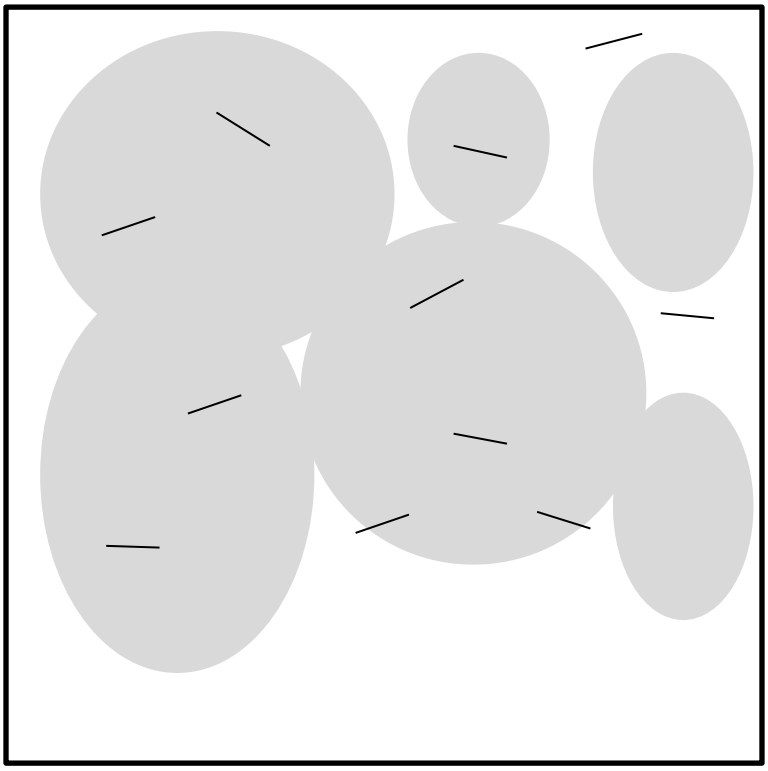

Fig. 5.6 Illustration of morphology of epoxy/organoclay nanocomposites with triamine exfoliator (Gray circle represents amine pahse and black line represents organoclay).

5.4 Flexural property

5.4.1 Effect of types of clay exfoliator

Figure 5.7 illustrates the assumed unbounded and bonded organoclay in the epoxy matrix. There are two main types of clay exfoliators in this study: first type is epoxy exfoliator which obtains unboned organoclay, and second is amine exfoliator which obtains boned organoclay in the nanocomposites clay. Black line represents c epoxy network, and hexagonal plat represents layered clay.

Fig. 5.7 (above) shows unbonded organoclays which are not fixed with the main matrix. Flexural modulus of the nanocomposites with unbonded organoclays would not increase.

To increase the stiffness of the materials, it needs to fix the mobility of the molecular chains of the polymer. Noticeably, improving stiffness of the nanocomposites with unbonded organoclays would be not expected.

Fig. 5.7 (below) shows bonded organoclays which are fixed with the main matrix. Flexural modulus of the nanocomposites with bonded organoclays would increase. Bonded organoclays are fixed with the matrix and decrese the mobility of the molecular chains of the polymer. As these phenomena, stiffness of the nanocomposites with bonded organoclays would be increased.

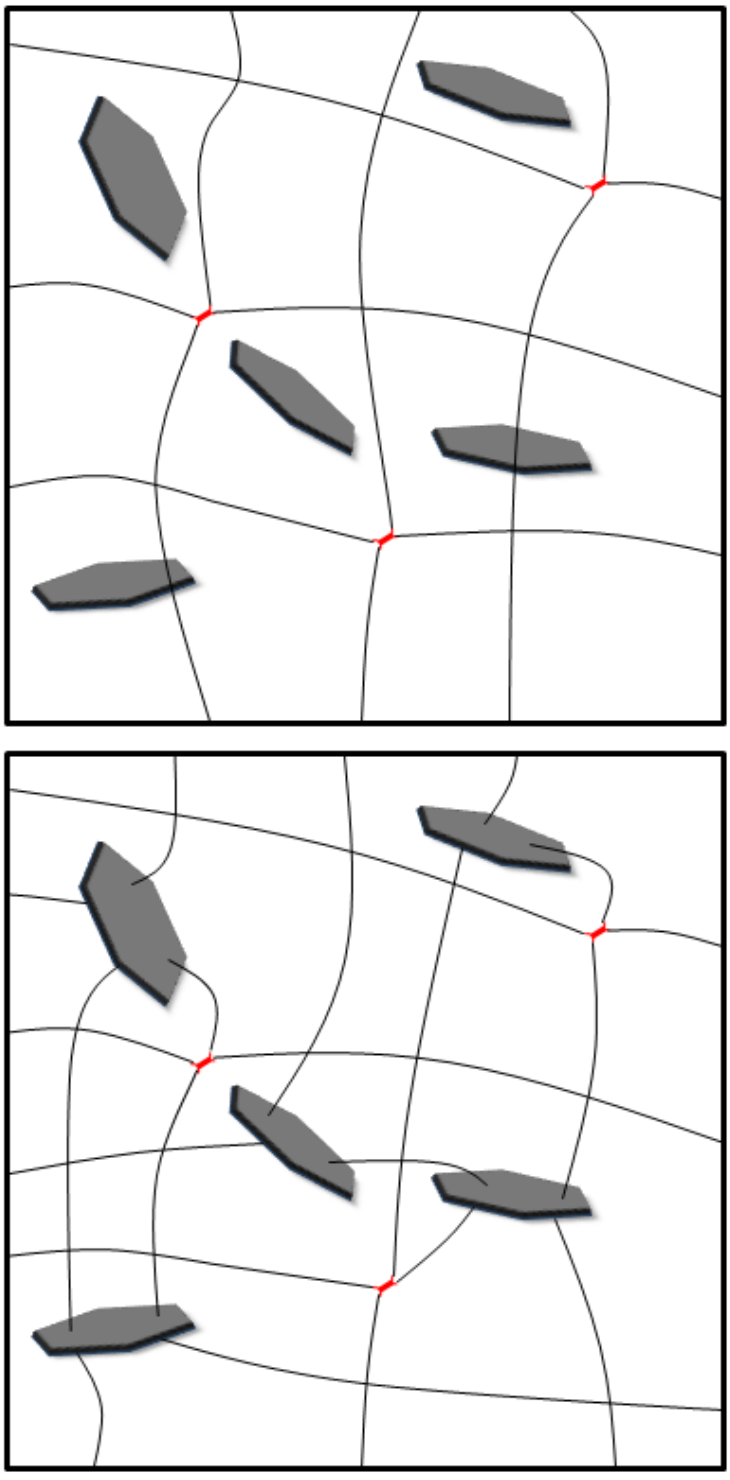

Fig. 5.7 Illustration of unbonded (above) and bonded (below) organoclays in epoxy matrix (red object represents crosslink between epoxy resin and curing agent, hexagonal shape represents clay, and black line represents epoxy matrix)

5.4.2 Effect of clay loading

Figure 5.8 illustrates model of high clay loading of epoxy/organoclay nanocomposites. Red object represents crosslink between epoxy resin and curing agent. Hexagonal shape represents clay. Black line represents epoxy matrix.

Increasing clay loading increase flexural modulus of the nanocomposites because bonded organoclays increase and fixed stronger with the matrix. As there phenomena, it would be decrease the mobility of the molecular chains of the polymer. Stiffness of the nanocomposites with bonded organoclays would be increased.

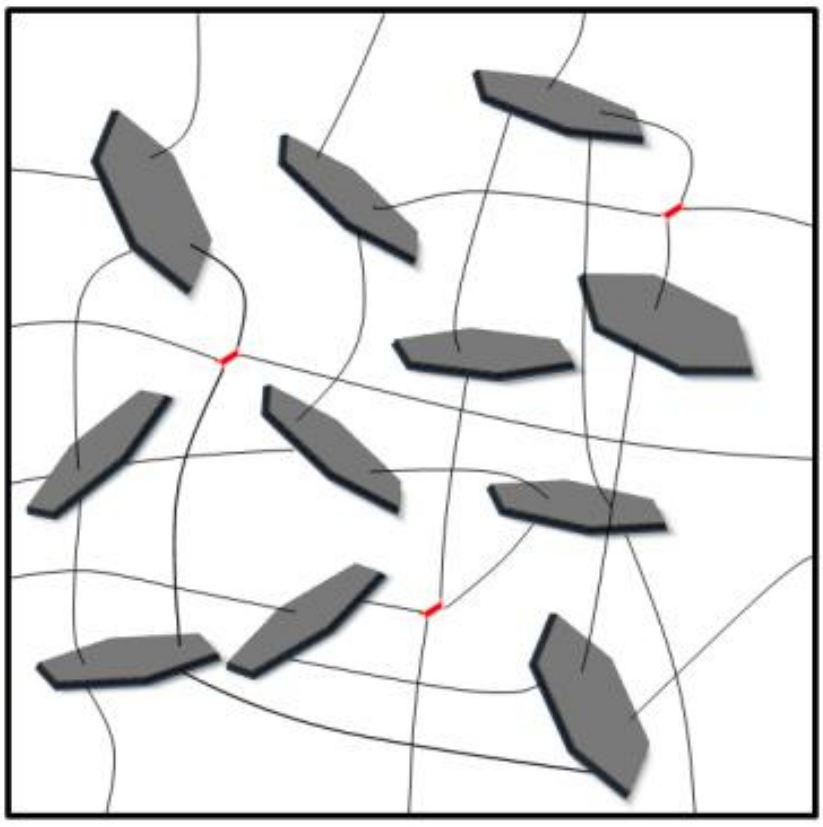

Fig. 5.8 Model of high clay loading of epoxy/organoclay nanocomposites (red object represents crosslink between epoxy resin and curing agent, hexagonal shape represents clay, and black line represents epoxy matrix).

5.5 Corrosion behaviour

Figure 5.9 shows mechanism of sulfuric acid diffusion in organoclay and epoxy network. Black dot represents crosslink between epoxy resin and curing agent, and gray dot represents onium ion. Solution equilibrium of epoxy/organoclay nanocomposite with several exfoliators shows noticeable different tendency. Epoxy/organoclay nanocomposite with long molecular diamine exfoliators (D3) has low weight uptake than other samples. However, epoxy/organoclay nanocomposite with epoxy and triamine exfoliators has high weight uptake than other samples. It would be divided in three structures: 1) bonded organoclay/epoxy nanocomposite, 2) unboned organoclay/epoxy nanocomposite and 3) nanocomposite with phase separation. They may be explained by following mechanism.

Firstly, bonded organoclay/epoxy nanocomposite, epoxy polymerization may occur with onium ions on clay layers (at the gray dots in illustration), after that, reacts with initially amine organic agent and makes epoxy-network. They would obtain not only exfoliated clay structure in epoxy matrix but also, strong bonding between organoclay and epoxy network. Especially exfoliated clay structure could be fixed more into polymeric matrix and hindrance to the transport of fluid by clay surface area and occupied volume pre platelet compared to the other structures. These phenomena could affect to decrease polymer mobility and lead to lower weight uptake of sulfuric acid.

Sexcondly, unbonded organoclay/epoxy nanocomposite, epoxy polymerization may occur with only amine curing agent without clay layer boding because onium ions on clay layers have reacted with epoxy exfoliator during pre-mixing process. Even though

the nanocomposites obtain extremely high degree of clay exfoliation, they could not achieve high corrosion performance It would not be able to decrease polymer mobility and also, occur the free volume.. These phenomena would not be able to obtain lower weight uptake of sulfuric acid. Therefore, corrosion performance would be low.

Finally, nanocomposites with phase separation, they would obtain with bubbles in the materials. The bubbles are mainly cause on decreasing corrosion behaviour. So, this material structure would obtain the worst performance compare to the others

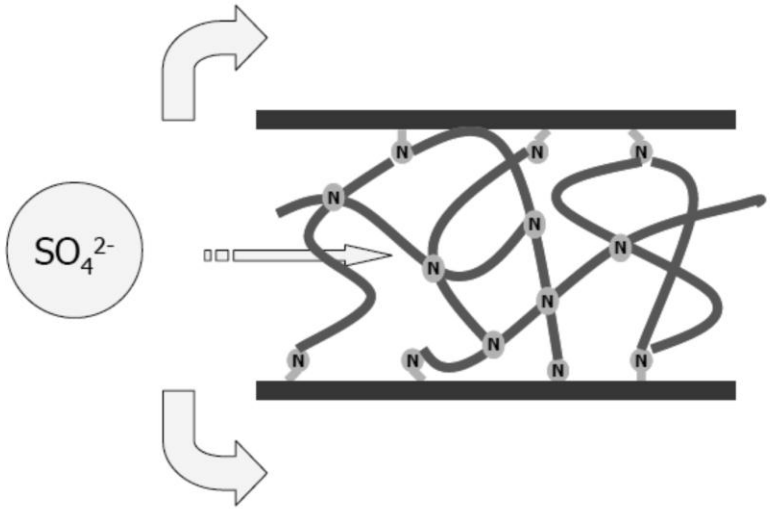

Fig. 5.9 Mechanism of sulfuric acid diffusion in organoclay and epoxy network.

Chapter 6

General conclusion

6.1 Physical clay dispersion

6.1.1 Effect of physical clay dispersion methods

Mixing method of epoxy nanocomposites plays an important role in clay dispersion in epoxy resin and is one of the main key parameters of epoxy/organoclay nanocomposites on improvement of properties. In order to obtain knowledge of mechanical clay dispersion in the epoxy matrix, epoxy/organoclay nanocomposites were prepared by different three mixing method. Viscosity, d-spacing weight gain results and mechanism of protection against liquid penetration and nanocomposites morphology were discussed.

Corrosion behaviour was investigated under immersion test, and evaluated by penetration depth and penetration profile. All samples have almost similar penetration rate. On the other hand, high speed mixing sample and neat epoxy resin reached equilibrium at similar time and earlier compared to normal mixing and shear mixing samples. Epoxy/organoclay nanocomposite preparation under high speed mixing method which creates exfoliated clay dispersion in the epoxy matrix performs better corrosion resistant compared to normal and shear mixing methods regarding to weight gain and penetration depth.

6.1.2 Effect of mixing parameters and ultrasonic application

The effects of mixing parameters and ultrasonic application on clay dispersion in the epoxy matrix and their properties have been studied. Mixing speed which is at 24,000 rpm is one of the factors to achieve fully exfoliated organoclay structure in the epoxy nanoncomposites. The recommended mixing duration was about 60 minutes. The increase in properties from mixing duration is due to fine clay dispersion and enlargement of clay interlayer distance. Ultrasonic application is applied to induce better clay dispersion and slightly enlarge interlayer clay distance.

6.1.2 Effect of clay loading

The appropriate clay loadings for epoxy/organoclay nanocomposites was at 3 phr for flexural strength and stiffness. The improvement in properties was due to fixation of organoclay in the epoxy matrix.

6.2 Effect of chemical nanoclay dispersion using chemical exfoliators

Fully epoxy/organoclay nanocomposites have been successfully obtained with epoxy reactive diluents and diamine curing agents pre-mixing as clay exfoliators. Epoxy reactive diluents and diamine curing agents pre-mixing substances play an important role on clay exfoliation into the epoxy matrix. Pre-mixing process with epoxy and diamine exfoliators assists to obtain fully exfoliated epoxy/clay nanocomposites confirming from all viscosity, XRD and TEM micrographs. Epoxy exfoliator has more effect on increasing degree of clay exfoliation compared to diamine exfoliaotor.

Flexural modulus and diffusivity of epoxy/ organoclay nanocomposites with diamine exfoliator obtains significantly improving, however, with epoxy exfoliator is not much improving due to unboned organoclay with the epoxy matrix.

6.3 Effect of amine exfoliators on organoclay dispersion

Amine compounds which act as clay exfoliators during pre-mixing process were one of the key successes factors to achieve fully exfoliated organoclay dispersion in epoxy matrix. Epoxy/organoclay nanocomposites with monoamine clay exfoliator show the highest clay exfoliation and the most uniform dispersion regarding to viscosity, XRD and TEM results. Long molecular structure of clay exfoliators are recommend for synthesis fully epoxy/organoclay nanocomposites. Flexural property of epoxy/organoclay nanocomposites with only monoamine clay exfoliator increase compared to neat resin and nanocomposites without clay exfoliators. Corrosion of epoxy/organoclay nanocomposites with only long molecular chain diamine clay exfoliator shows better performance compared to neat resin. Epoxy/organoclay nanocomposites with triamine clay exfoliator shows phase separation because it was not able to homogeneously mix and cause to decrease flexural property and corrosion behaviour of the nanocompoistes.

6.4 Mechanisms of clay exfoliation and nanocomposites properties development

Regarding experimental results and TEM observation, they were illustrated to describe mechanisms of epoxy/organoclay nanocomposites with different methods as well as

their flexural property and corrosion behaviour. The higher degree of shear via high speed mixing involves the dispersion of large stacks into smaller ones took place and hence increases degree of intercalation/exfoliation. As the results, exfoliated clay dispersion in the epoxy matrix performs better corrosion resistant compared to normal and shear mixing methods.

Mixing speed has an effect on clay interlayer distance because suitable shear force would enhance d-spacing of layered clay. Assisting clay dispersion with ultrasonic application, clay galleries would be less tighten and slightly more open at the end of the galleries.

Epoxy exfoliator would reduce clay interfacial energy which makes fully exfoliated clay structure. However, the organoclays after pre-mixing process with epoxy exfoliator were not able to bond with main epoxy matrix because epoxy functional group of exfoliator reacts with amine functional group of modified surface clay instance. There phenomena would affect to reduce performance of the nanocomposites with epoxy exfoliator.

In comparison between monoamine and diamine exfoliators, mechanical and barrier properties of nanocomposites with diamine exfoliator obtains better performances because diamine exfoliators would has two bonding reaction and fix stronger with the matrix compared to monoamine exfoliator which has only one bonding reaction.

Triamine exfoliator does not easily mix with epoxy and/or the other amine compounds. As these phenomena, phase separation and bubbles were obtained in the nanocomposites with triamine exfoliator which is cause on decreasing flexural property and corrosion behaviour.

References

1. The American Heritage Dictionary of the English Language, Fourth Edition, Copyright © 2000 by Houghton Mifflin Company.

2. P. M. Ajayan, L. S. Schadler, and P. V. Braun. Nano Comp. Sci. Tech. Wiley, 2003.

3. Pinnavia T. J., Sci., 365, 1983.

4. MSDA and product data of montmorillonite-based organoclay I.30E from Nanocor Inc. , USA.

5. A. Usuki, M. Kawasumi, Y. Kojima, A. Okada, T. Kurauchi, and O. Kamigaito, J. Material. Res., 1174, 1993.

6. A. Okada, and A. Usuki, Mat. Sci. Eng. C, 3109, 1995.

7. P. C. LeBaron, Z. Wang, and T. J. Pinnavaia, App. Clay Sci., 15, 11, 1999.

8. Y. Komori, A. Matsumaru , T. Itagaki, Y. Sugahara, and K. Kuroda, Clay Sci., 47, 2000.

9. R. A. Vaia , D. J. Klaus , J. K. Edward , and E. P. Giannelis, Chem. Mater., 8, 2628, 1996.

10. J. M. Brown , D. Curliss , and R. A. Vaia, Chem. Mater., 12 , 3376, 2000.

11. Schollhorm, R. Physica, 99B, 89, 1980.

12. Parry, G. S. Physica, 105B, 261, 1981.

13. Lagaly, G. Phil. Trans. R. Soc. (Lond.) A, 315, 1984.

14. T. J. Pinnavia and G. W. Beall (eds.) Polymer-clay nanocomposties, USA, Wiley series in polymer sceience, 229, 2000.

15. M. S. Wang, and Pinnavia, Epoxy-Clay Nanocomposites, 127-149, 2000.

16. M. S. Wang, and Pinnavia. J., Chem. Mat., 6, 468, 1994.

17. Y. Komori, A. Matsumaru, T. Itagaki, , Y. Sugahara, and K. Kuroda, Clay Sci., 47, 2000.

18. United States Patent 04739007 Composite material and process for manufacturing same 1988-04-19

19. A. Usumi, M. Kawasumi, Y. Kojima, A. Okada, T. Kurauchi and O. Kamigaito, J. Mater. Res., 8, 1174, 1993.

20. A. Okada, M. Kawasumi, T. Kurauchi and O. Kamigaito, Pol. Prep, 28, 447, 1987.

21. M. Okamoto, S. Morita and T. Kokata, Polymers, 42, 2685, 2001.

22. O. Beker, L. Varley and G. Simon, 43, 4365. 2002.

23. D. Sekelik, E. Stepanov, D. Schiraldi, A. Hiltner and E. Baer, J. Pol. Sci.; Pol. Phys., 37, 847,1999.

24. T. Gopakumar, , J. Lee, M. Kontopoulou and J. Parent, 43, 5483. 2002.

25. Jin, Y., H. Park, S. Im and S. Kwak, Rapid Commun., 23, 135, 2002.

26. M. Okamoto, S. Morita, H. Taguchi, Y. Kim, T. Kataka and H. Tateyama, Polymers, 41, 3887, 2000.

27. Y. Feng and R.G. Nelson, In: Proceeding Nanocomposite, San Diego, CA, 2002.

28. E.P. Giannelis, Chem. Mater., 5, 1064, 1993.

29. Yoon, P., T. Fornes and D. Paul, Polymers, 43, 6727, 2002.

30. C. Davis, L. Mathias, J. Gilman, D. Schiraldi, J. Shields, P. Trulove, T. Sutto and H. Delong, J. Pol. Sci., Polymer Phys., 40, 2661, 2002. .

31. A. Usuki , M. Kato, A. Okada and T. Kurauchi, J. App. Pol. Sci., 63, 137-138, 1997.

32. P. Aranda, and E. Ruiz-Hitzky, Chem. Mater., 4, 1395, 1992.

33. K. Strawhecker, and E. Manias, Chem. Mater., 12: 2943, 2000.

34. H. Jeon, H. Jung, S. Lee and S. Hudson, Polymer Bull., 41, 107, 1998.

35. Wang, K., M. Choi, C. Koo, Y. Choi and I. Chung, Polymers, 42, 9819, 2001.

36. Jin, Y., H. Park, S. Im and S. Kwak, Rapid Commun., 23, 135, 2002.

37. Vaia RA, Jandt KD, Kramer EJ, and Giannelis EP, Chem. Mater., 8, 2628, 1996.

38. T. D. Ngo, M.-T. Ton-That, S.V. Hoa, and K.C. Cole. 69, 1831, 2009.

39. Unitika Ltd Hiromu Fuji, Katsumi Kuratani, Kazuyuki Wakamura, Masaaki Yamazaki, Polyamide resin composition, EP1022313 A1, Europe Patent Office, 26/07/2000.

40. Y. Kojima, A. Usuki, M. Kawasumi, A. Okada, Y. Fukushima, T. Kurauchi and O. Kamigaito,. J. Mat., 8, 1185, 1993.

41. Y. Kojima, A. Usuki, M. Kawasumi, A. Okada, T. Kurauchi and O. Kamigaito, J. App. Pol. Sci., 49, 1259, 1993.

42. E. Sancaktar, and J. Kuznicki, Inter. J. Adhesion Adhesives, 31, 286, 2011.

43. L.Wang, K. Wang, L.. Chen, Y. Zhang and C. He, Comp. A: App. Sci. Man., 37, 1890, 2006.

44. W. Ke, W. Lei, W. Jingshen, C. Ling,and C. He, Langmuir, 21, 3613, 2005.

45. P. B. Messersmith , E. P. Giannelis Chem. Mater., 6, 1719, 1994.

46. L. Jiankun, K. Yucai, Q. Zongneng, and Y. X. Su, J. Pol. Sci, Part B: Pol. Phy., 39, 115, 2001.

47. T. J. Pinnavaia, T. Lan , and P. D. Kaviratna, Chem. Mater., 7, 2144, 1995.

48. J. H. Park and S.C. Jana, Macromolecules, 36, 2758, 2003.

49. J. H. Park, Y. T. Lim, O. O. Park, Macromol. Rapid Commun. 22, 616, 2001.

50. P. V. Sanjeevkumar, M. Ashokkumar,B. Chandramohanreaddy, and G.

Ramachandrareddy, Intern. J. Nanomaterials. Biostructures. 200, 661, 1999.

51. H.T. Rana, R.K. Gupta, H.V.S. Gangarao and L.N. Sridhar, American Inst. Chem. Eng. J., 51, 3249, 2005.

52. N. Abacha, T. Sakai, K. Tsuda, and M. Kubouchi, Key Eng. Mat., 353, 2167, 2007.

53. C. Chenggang, M. Khobaib and D. Curliss, Progress Organic Coatings, 47, 376, 2003.

54. W. Keyoonwong, M. Kubouchi, T. Sakai and S. Aoki, in Proceedings of ISEEE09, 158, Rayong, Thailand, 2009.

55. M. Kubouchi, Y. Guo, N. Abacha and T. Sakia, in Proceedings of ICSAAM 2009, Tarbes, France, 2009.

56. D.H. Song, H.M. Lee, H.J. Choi, J. Phy Chem. Solids. 69, 1383, 2008.

57. W. Keyoonwong, Y. Guo, M.Kubouchi, S. Aoki, T. Sakai, Inter. J. Corrosion, 1, 2012.

58. T. Lan, T.J. Pinnavaia, Chem. Material, 6, 2216, 1994.

59. K. Saitoh, K. Ohashi, T. Oyama, A. Takahashi, J. Kadota, H. Hirano and K. Hasegawa, J. App. Pol. Sci., 122, 666, 2011.

60. X. Kornmann, H. Lindberg and L.A. Berglund, Polymer, 42, 4493, 2001.

61. X. Kornmann, L. A. Berglund, R. Thomann, R. Mulhaupt, J. Finter, Pol. Eng. Sci., 42, 1815, 2002.

62 K. Sterkya, H. Jacobsenb, I. Jakubowiczc, N. Yarahmadic, and T. Hjertbergd, Euro. Poly. J., 46, 1203, 2010.

63. K. Sterky, T. Hjertberg and H. Jacobsen, Pol. Degrad. Stab., 94, 1564, 2009.

64. T. P. Mohan, M. Ramesh Kumar, R. Velmurugan, J. Mat. Sci., 41, 5915, 2006

65. Z. Wang, T.J. Pinnavaia, Chem. Mat., 10, 1820, 1998.

66. I. Curtu and D. L. Motoc, Mat. Plas., 45, 366, 2008.

67. A. Esfandiari, H. Nazokdast, A. Rashidi and M. E. Yazdanshenas, J. App. Sci., 8, 545, 2008.

68. A. Esfandiari, Fib. Pol., 9, 48. 2008.

69. C. Shan, Z. Gu, L. Wang, P. Li, G. Song, Z. Gao, and X. Yang, J. App. Pol. Sci., 119, 1185, 2011.

70. K. Yano, A. Usuki and A. Okada, J. Pol. Sci. Part A: Pol. Chem., 35, 2289, 1997.

71. J. Yeha, H. Huanga,C.. Chena, W. Sua and Y. Yub, Surf. Coatings Tech., 200, 2753, 2006.

73. N. Abacha, M. Kubouchi, T. Sakai and K, Tsuda, J. App. Pol. Sci., 112, 1021, 2009.

74. A. Yasmin, J. Abot and I. Daniel, Scripta Materialia, 49, 81, 2003.

75. Y. Tian, H. Yu, S. Wu, G. Ji and J. Shen, J. Mat. Sci., 39, 4301, 2004.

76. Y. Zhanga, J. Leeb, H. Jangb, C. Nahb, Comp. Part B: Eng., 35, 133, 2004.

78 P. Pradyawong, W. Keyoonwong, S. Aoki and M. Kubouchi, in Proceedings of 17th Regional Symposium on Chem. Eng. RSCE-2010, pp.45-49, Bangkok, Thailand, 2010.

79. L. Goettler, K. Y. Lee, H Thakkar, Pol. Rev., 47, 291, 2007.

80. M. Zanetti, Macro. Mol. Mat. Eng., 279, 1, 2000.

81. D. R. Paul, L. M. Robeson, Polymer, 49, 3187, 2008.

82. O. Becker, R. J. Varley, G. P. Simon, Euro. Poly. J., 40, 87, 2004.

83. Z. Wang, T.Lan, T.J. Pinnavaia, Chem. Mat.,. 8, 2200, 1996.

84. C. Zilg, R. Mülhaupt, J. Finter, Macromol. Chem. Phys. 200, 661, 1999.

85. K. Wang, L. Chen, J. Wu, M. L. Toh, C. He, A. F. Yee, Macromol, 38, 788, 2005.

Acknowledgements

First of all, I would like to thank my supervisor Prof. Masatoshi Kubouchi. His constant devotion to teaching and research, his continuous support and comments have been key factors towards the completion of my doctor degree. His guidance has provided me a different view of approaching my research and has inspired me on my daily pursue to learning.

I would also like to express my upmost gratitude to Monbukagakusho (*MEXT*) Scholarship for granting me the opportunity to study and do research at Tokyo Institute of Technology.

Also, I would like to thankful to the National University Corporation Tokyo Institute of Technology, Center for Advanced Materials Analysis for XRD and TEM analysis.

For the members of Kubouchi laboratory I also give my heartfelt thanks for the assistance, support, and daily humor.

Last but not least, I would like to extend my deepest gratitude to my family in Thailand for their moral support and understanding to my current undertakings. Their persistence, support, and faith in me have allowed me to bring this project to fruition.

Questions and answers

1. Prof. Shioya: effect of viscosity on clay dispersion, weight of clay was constant. Regarding to Einstein's equation, total volume fraction (of clay suspension) should be the same before and after exfoliation. Why did the viscosity increase? Please explain.

Answer: Einstein's equation for viscosity of a dispersion of solid spheres

$$\eta' = \eta\,(1 + 2.5\varphi + \ldots) \quad \text{(Eq.1)}$$

where φ = Volume fraction of the dispersed phase

$\eta', \eta =$ Viscosities of the suspension and the solvent respectively

Ellipsoidal or similar shapes in which one of the axes is longer than the other (e.g. clay platelets) proposed by Simha (1940) [1] and Larson (1999) [2].

$$\eta' = \eta\,(1 + V\varphi) \quad \text{(Eq.2)}$$

For disc-sharped particles: $V = \frac{A}{tan^{-1}(A)}$

Where A= Aspect ratio (ratio of diameter (D) to thickness (t))

If % weight of fillers is constant, total volume fraction should be the same before and after mixing in case of fillers themselves are the same shapes and structure before and after mixing. However, in case of layered silicate nanofillers which are containing 2-10 sheets per gallery, the structures of nanofiller are not the same. Before mixing, nanofiller pack together as clay galleries. However, after mixing, nanofiller disperse randomly in the matrix as exfoliated structure. The effect of volume fraction on the viscosity behaves as having occupied the volume equal to that which would have been occupied (Fig.1). Therefore, exfoliated clay structure would be occupied volume much more than conventional and intercalated clay structure (Fig.2).

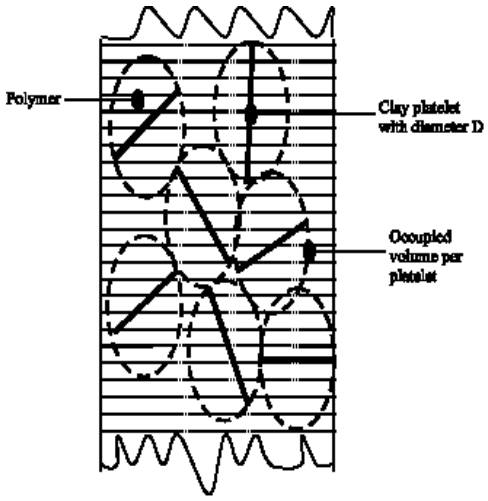

Fig.1 The morphology of a polymer-clay nanocomposite showing the increase in the occupied volume fraction of the filler due to its asymmetric nature

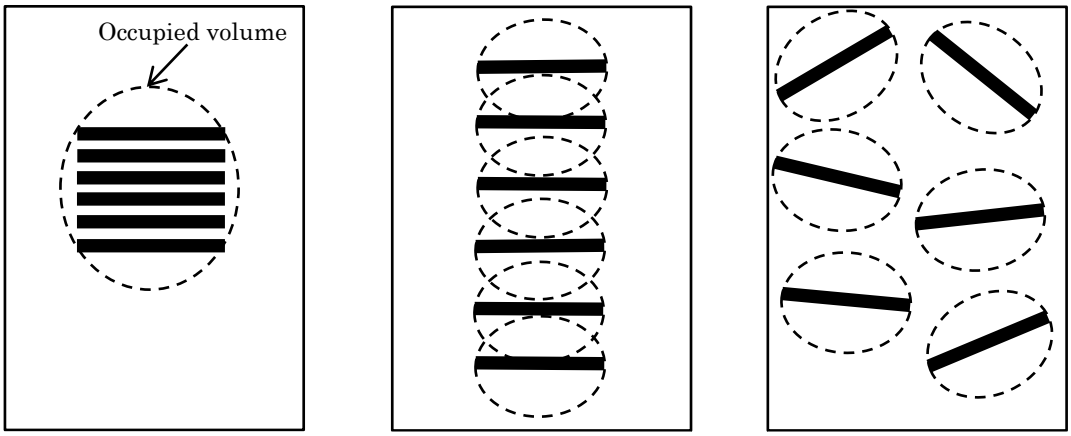

Fig.2 The morphology of polymer-clay nanocomposites in different clay structures.

2. Prof. Wiwat: please explain why organoclay and epoxy matrix could prevent diffusion.

Answer: Firstly, epoxy polymerization may occur with onium ions on clay layers, after that, reacts with initially amine organic agent and makes epoxy-network. They would obtain not only exfoliated clay structure in epoxy matrix but also, strong bonding

between organoclay and epoxy network. Especially exfoliated clay structure could be fixed more into polymeric matrix and occupied volume pre platelet compared to the other structures. These phenomena could affect to decrease polymer mobility and lead to lower weight uptake of sulfuric acid. Therefore, anti-corrosion performance would be better.

3. Prof. Otaguchi: flexural Strength, recommend at 60 min. Why?

Answer: The mixing duration that was recommended was considered not only flexural strength but also flexural modulus to keep high performance of the nanocomposites.

In case of flexural strength, it increased and kept stable from 60 to 240 mins mixing duration. In case of flexural modulus, it increased from 30 to 60 mins mixing duration, and decreased from 60 to 240 mins mixing duration. If considering to keep high both flexural strength and modulus, it would be at 60 mins.

4. Prof. Yoshikawa: what parameter is the important parameter in case of industrial scale?

Shear force from high speed mixing method is important. If so, the shear force should be considered instead of mixing speed, isn't it?

Answer: To scale up to industrial scale, shear force is one of the important mechanical parameters to achieve fully exfoliated clay structure of the nanocomposites.

Nevertheless, chemical reaction from exfoliators is noticeably one of the main keys for synthesis fully exfoliated clay structure of the nanocomposites too. As mentioned on Chapter 2, if it applied only mechanical, the fully exfoliated clay structure does not occur. It has to be applied combined mechanical and chemical methods.

Calculating shear force of recommended condition, D3+organoclay (after mixing)

$$\tau_{yx} = \mu \frac{dv_x}{dy} = \frac{F}{A}$$

$\mu = 4.377\ Pa \cdot s$
$dv_x = 24000\ rpm\ x\ 2\pi(0.0075\ m) = 18.84\ m/s$
$dy = 0.0025\ m$
$A = 2\pi(0.0075m) = 0.0471\ m^2$

So, shear force for recommended condition is about 1554 N

5. Associate Prof. Mori: Alignment of clay is mixed using high speed mixing method. Would it affect to XRD results?

Answer: It would not affect to XRD results because firstly, after mixing with high speed mixing homogenizer (step 1), it mixes with the vacuum mixer which mix without any direction for 10 minutes (step 2), and secondly, in this study, the clay loading is very low, 1 phr. If the clay loading is very high (more than 10 phr), the mixing direction could affect to alignment of clay. So there is no direction of clay alignment in the nanocomposites for these experimental conditions.

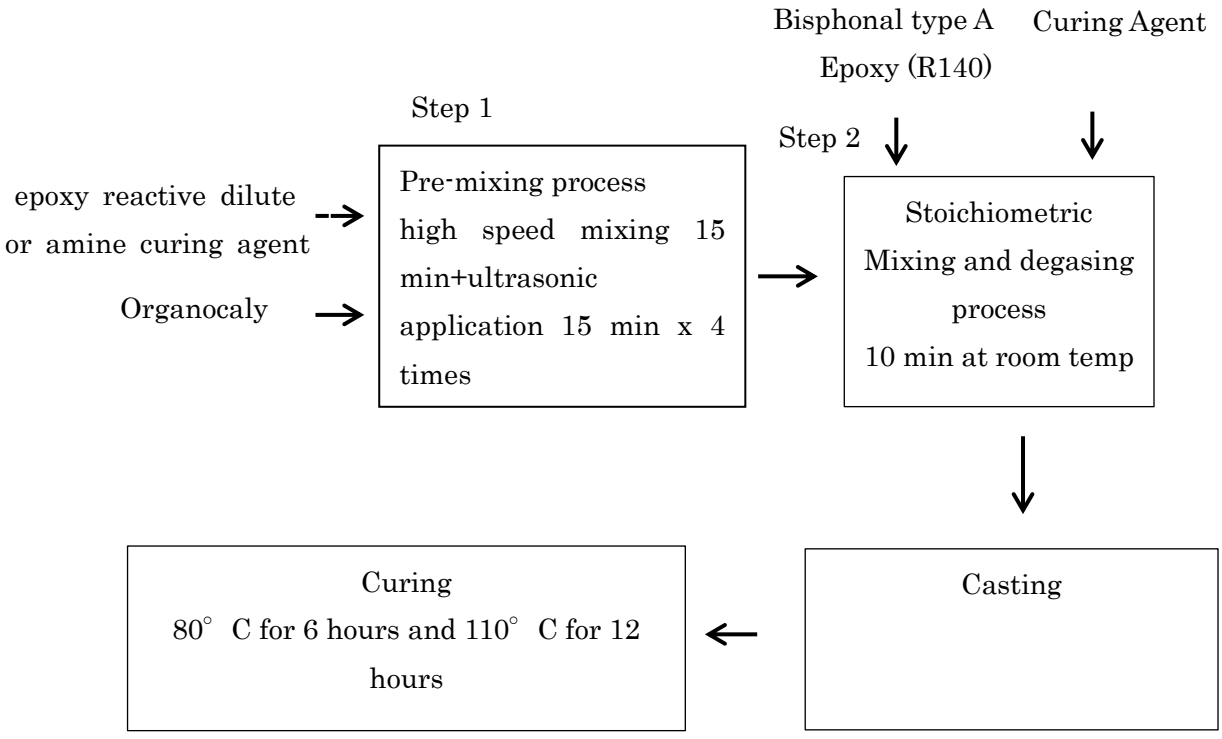

Fig. 4 Preparation procedure of epoxy/organoclay nanocomposites

6. Prof. Shioya: weight change is fickian diffusion but phenomena from EDS are non-fickian diffusion. Why?

Answer: If considering the results in details, % mass change penetration profiles obey to non-fickian as shown in Fig. 5 [3]. (However, in this study, % weight change data roughly plot to consider the tendency only.) Sulfuric ion from the acid solution increases the same to specific gravity. However, sulfur penetration depth is proportional to square root of time. Non-fickian behavior took place in this study because it occured not only diffusion but also chemical reaction between sulfuric ions and polymer chain which produced the salt. As these phenomena, the penetration of the solution has to penetrate thought the new path of sulfuric salt too.

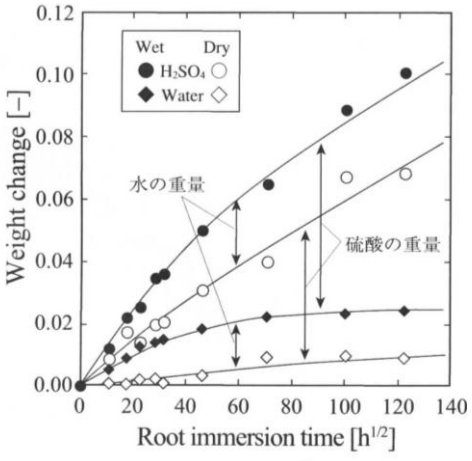

Fig. 5 Weight change of EP1 (Bisphenol A)

7. Prof. Yoshikawa: what is the condition of “hand mixing” for this experiment?

Answer: Hand mixing condition was 60 times per minute. Experimental mixing in

details, the clay suspension was mixed 15 minutes continuously, after that put it in the ultrasonic bath 15 minutes. And keep doing these mixing conditions for 4 time or equal 60 minutes.

8. Prof. Mori: Chapter 3 and 4, are experimental conditions the same? Especially, data for before mixing condition.

Answer: It is the same experimental conditions and I have added more data of "sample+clay (before mixing)" in Chapter 3 as following:

Table 1 Viscosities of samples

Sample	**Viscosity [Pa • s]**	**% Change of viscosity base on neat sample**	**% Change of viscosity base on sample before mixing**
Neat resin	12.82		
resin+clay (before mixing)	19.93	55.41	
resin+clay (after mixing)	22.36	74.40	12.22
E1	0.01		
E1+clay (before mixing)	0.03	222.02	
E1+clay (after mixing)	0.61	7305.32	2199.61
E2	0.03		
E2+clay (before mixing)	0.07	106.07	
E2+clay (after mixing)	0.24	590.75	235.20
E3	0.02		
E3+clay (before mixing)	0.05	116.42	
E3+clay (after mixing)	0.20	748.99	292.28
D1	0.05		
D1+clay (before mixing)	0.11	135.33	
D1+clay (after mixing)	0.07	47.90	-37.16
D2	0.39		
D2+clay (before mixing)	0.80	103.78	
D2+clay (after mixing)	4.38	1010.69	445.04

References

[1] Simha, R., 1940. The influence of brownian movement on the viscosity of solutions. J. Phys. Chem., 44: 25-25.

[2] Larson, R., 1999. The Structure and Rheology of Complex Fluids. 1st Edn., Oxford University Press, New York, pp: 280-281.